REFERENCES

Acharya, M & Escudier, MP 1985, 'Turbulent flow over mesh roughness', paper presented to Fifth International Symposium on Turbulent Shear Flows, New York.

Akinlade, OG, Bergstrom, DJ, Tachie, MF & Castillo, L 2004, 'Outer flow scaling of smooth and rough wall turbulent boundary layers', *Experiments in Fluids*, vol. 37, pp. 604-612.

Albrecht, H-E, Borys, M, Damaschke, N & Tropea, C 2003, *Laser doppler and phase doppler measurement techniques*, Springer.

Andrewartha, J 2005, *Tarraleah no.1 canal - hydraulic and structural performance*, GR-AM-504, Hydro Tasmania Energy, Hobart.

Andrewartha, J & Cribbin, N 2006, '"When the going gets rough, the rough stops flowing" Roughness issues in hydro tasmania water conveyance structures', paper presented to 12th Hydro Power Engineering Exchange, 22-27 October, Tasmania.

Andrewartha, J & Cribbin, N 2009, 'When the going gets rough, the rough stops flowing', *24th Biennial Conference of the Concrete Institute of Australia*, Sydney.

Andrewartha, J & Perkins, K 2009, *Test plate trials - an investigation of biofilm growth on various substrates based on upgrade options for hydroelectric canals*, University of Tasmania, Hobart.

Andrewartha, J, Sargison, J, Barton, A, Cribbin, N, Denne, A & Walker, G 2006, 'Roughness issues in hydro tasmania water conveyance structures', *Australasian Corrosion Association, Corrosion and Prevention Conference*, Hobart, Australia.

Andrewartha, J, Sargison, J, Henderson, A, Perkins, K & Walker, G 2008a, 'The effect of freshwater biofilms on skin friction drag', *16th International Association of Hydraulic Engineering International Symposium on Hydraulic Structures*, Nanjing, China, 1940-1945.

Andrewartha, J, Sargison, J & Perkins, K 2008b, 'The influence of freshwater biofilms on drag in hydroelectric power schemes', *WSEAS Transactions on Fluid Mechanics: SPECIAL ISSUE: Sustainable Energy and Environmental Fluid Mechanics*, vol. 3, no. 3, pp. 201-206.

Andrewartha, J, Wallis, M & van Bladeren, D 2007, *Tarraleah no.1 canal and mossy marsh siphon capacity assessment*, Hydro Tasmania Consulting, Hobart.

Antonia, RA & Krogstad, PA 2001, 'Turbulence structure in boundary layers over different types of surface roughness', *Fluid Dynamics Research*, vol. 28, pp. 139 - 157.

Antonia, RA & Luxton, RE 1971, 'The response of a turbulent boundary layer to a step change in surface roughness part 1. Smooth to rough', *Journal of Fluid Mechanics*, vol. 48, no. 4, pp. 721-761.

Arndt, REA & Ippen, AT 1970, 'Turbulence measurements in liquids using an improved total pressure probe', *Journal of Hydraulic Research*, vol. 8, no. 2, pp. 131-158.

Bakken, OM, Krogstad, PA, Ashrafian, A & Andersson, HI 2005, 'Reynolds number effects in the outer layer of the turbulent flow in a channel with rough walls', *Physics of Fluids*, vol. 17.

Bandyopadhyay, PR 1987, 'Rough-wall turbulent boundary layers in the transition regime', *Journal of Fluid Mechanics*, vol. 180, pp. 231-266.

Barton, A 2007, 'Friction, roughness and boundary layer characteristics of freshwater biofilms in hydraulic conduits', PhD thesis, University of Tasmania.

Barton, A, Brandner, P, Sargison, J & Walker, G 2007, 'A force balance to measure the total drag of biofilms on test plates', paper presented to 16th Australasian Fluid Mechanics Conference, Gold Coast, Australia.

Barton, A, Sargison, J, Osborn, J, Perkins, K & Hallegraeff, G 2010, 'Characterizing the roughness of freshwater biofilms using a photogrammetric methodology', *Biofouling*, vol. 26, no. 4, pp. 439-448.

Barton, A, Wallis, M, Sargison, J, Buia, A & Walker, G 2008, 'Hydraulic roughness of biofouled pipes, biofilm character, and measured improvements from cleaning', *Journal of Hydraulic Engineering*, vol. 134, no. 6, pp. 852-857.

Barton, AF & Sargison, JE 2004, *Tarraleah canal paint trials*, University of Tasmania, Hobart.

Baum, C, Simon, F, Meyer, W, Fleischer, L-G, Siebers, D, Kacza, J & Seeger, J 2003, 'Surface properties of the skin of the pilot whale *globicephala melas*', *Biofouling*, vol. 19, pp. 181-186.

Bendall, T 2005, 'Application of photogrammetric techniques to the mapping of biofouled surfaces', Honours thesis, University of Tasmania.

Bergstrom, DJ, Kotey, NA & Tachie, MF 2002, 'The effects of surface roughness on the mean velocity profile in a turbulent boundary layer', *Journal of Fluids Engineering*, vol. 124, pp. 664-670.

Biggs, BJF & Thomsen, HA 1995, 'Disturbance of stream periphyton by pertubations in shear stress - time to structural failure and differences in community resistance', *Journal of Phycology*, vol. 31, pp. 233-241.

Bland, CEG, Bayley, RW & Thomas, EV 1975, 'Some observations on the accumulation of slime in drainage pipes and the effects of these accumulations on the resistance to flow', *Public Health Engineering*, pp. 21-28.

Booij, R & Tukker, J 1994, '3-dimensional laser doppler measurements in a curved flume', *7th International Symposium on Applications of Laser Techniques to Fluid Mechanics*, Lisbon, Portugal, 28.25.21-28.25.28.

Bradshaw, P 1959, 'A simple method of determining skin friction from velocity profiles', *Journal of Aerospace Sciences*, vol. 26, p. 841.

Bradshaw, P 1971, *An introduction to turbulence and its measurement*, The commonwealth and international library thermodynamics and fluid mechanics series, Permagon Press Ltd.

Bradshaw, P 1987, 'Wall flows', in F Durst, BE Launder, JL Lumley, FW Schmidt & JH Whitelaw (eds), *Turbulent shear flows 5 - selected papers from the fifth international symposium on turbulent shear flows*, Springer-Verlag, New York, pp. 171-115.

Brady, RFJ & Aronson, CL 2003, 'Elastomeric fluorinated polyurethane coatings for nontoxic fouling control', *Biofouling*, vol. 19, pp. 59-62.

Brandner, PA, Clarke, DB & Walker, GJ 2004, 'Development of a fast response pressure probe for use in a cavitation tunnel', paper presented to 15th Australasian Fluid Mechanics Conference, The University of Sydney, Australia, 13-17 December.

Brett, TM 1980, 'Head-loss measurements on hydroelectric conduits', *ASCE J. Hydraulics Division*, vol. HY1, pp. 173- 190.

Brown, KC & Joubert, PN 1969, 'The measurement of skin friction in turbulent boundary layers with adverse pressure gradients', *Journal of Fluid Mechanics*, vol. 35, no. 4, pp. 737-757.

Brzek, B, Cal, RB, Johansson, G & Castillo, L 2007, 'Inner and outer scalings in rough surface zero pressure gradient turbulent boundary layers', *Physics of Fluids*, vol. 19, no. 6, pp. 065101: 065101-065117.

Buchave, P, George, WK & Lumley, JL 1979, 'The measurement of turbulence with the laser-doppler anemometer', *Annual Review of Fluid Mechanics*, vol. 11, pp. 443-503.

Callow, ME 1993, 'A review of fouling in freshwater', *Biofouling*, vol. 7, pp. 313-327.

Callow, ME 2000, 'Algal biofilms', in LV Evans. (ed.), *Biofilms : Recent advances in their study and control*, Harwood Academic, Australia.

Candries, M 2001, 'Drag, boundary-layer and roughness characteristics of marine surfaces coated with antifoulings', PhD thesis, University of Newcastle-Upon-Tyne.

Candries, M & Altar, M 2003, 'On the drag and roughness characteristics of antifoulings', *International Journal of Maritime Engineering*, pp. 35-60.

Candries, M & Altar, M 2005, 'Experimental investigation of the turbulent boundary layer of surfaces coated with marine antifoulings', *Journal of Fluids Engineering*, vol. 127, pp. 219-232.

Candries, M, Atlar, M, Mesbahi, E & Pazouki, K 2003, 'The measurement of the drag characteristics of tin-free self-polishing co-polymers and fouling release coatings user a rotor apparatus', *Biofouling*, vol. 19, pp. 27-36.

Carpenter, PW 2005, 'Biology-based drag reduction', paper presented to 2nd International Symposium on Seawater Drag Reduction, Busan, Korea 23-26 May.

Castro, I 2007, 'Rough-wall boundary layers: Mean flow universality', *Journal of Fluid Mechanics*, vol. 585, pp. 469-485.

Chanson, H 2000, 'Boundary shear stress measurements in undular flows: Application to standing wave bed forms', *Water Resources Research*, vol. 36, no. 10, pp. 3063-3076.

Characklis, WG 1973, 'Attached microbial growths - ii. Frictional resistance due to microbial slimes', *Water Research*, vol. 7.

Chue, SH 1975, 'Pressure probes for fluid measurements', *Progress in Aerospace Science*, vol. 16, no. 2, pp. 147-223.

Clauser, FH 1954, 'Turbulent boundary layers in adverse pressure gradients', *Journal of Aerospace Sciences*, vol. 21, pp. 91-108.

Coleman, H & Steele, W 1995, 'Engineering application of experimental uncertainty analysis', *AIAA Journal*, vol. 33, no. 10, pp. 1888-1895.

Coleman, HW, Hodge, BK & Taylor, RP 1984, 'A re-evaluation of schlichting's surface roughness experiment', *Journal of Fluids Engineering*, vol. 106, pp. 60-65.

Coles, D 1956, 'The law of the wake in the turbulent boundary layer', *Journal of Fluid Mechanics*, vol. 1, pp. 191-226.

Connelly, JS, Schultz, MP & Flack, KA 2006, 'Velocity-defect scaling for turbulent boundary layers with a range of relative roughness', *Experiments in Fluids*, vol. 40, pp. 188-195.

Dantec Dynamics 2006, *Bsa flow software version 4.10 installation and user's guide*, Denmark.

Dantec Dynamics 2009, *Laser doppler anemometry - measurement principles*.

DeGraaf, D & Eaton, J 2000, 'Reynolds-number scaling of the flat-plate boundary layer', *Journal of Fluid Mechanics*, vol. 422, pp. 319-346.

Deutsch, S, Fontaine, A, Moeny, M & Petrie, H 2005, 'Drag reduction with combined micro-bubble and polymer injection', paper presented to 2nd International Symposium on Seawater Drag Reduction, Busan, Korea, 23-26 May.

Dobretsov, S, Dahms, H-U & Qian, P-Y 2006, 'Inhibition of biofouling by marine microorganisms and their metabolites', *Biofouling*, vol. 22, no. 1, pp. 43-54.

Durst, F, Fischer, M, Jovanovic, J & Kikura, H 1998, 'Methods to set up and investigate low reynolds number, fully developed turbulent plane channel flows', *Journal of Fluids Engineering*, vol. 120, pp. 496-503.

Durst, F, Jovanovic, J & Sender, J 1995, 'Lda measurements in the near-wall region of a turbulent pipe flow', *Journal of Fluid Mechanics*, vol. 295, pp. 305-335.

Durst, F, Melling, A & Whitelaw, JH 1981, *Principles and practice of laser-doppler anemometry*, 2nd edn, Academic Press Inc., London.

Edwards, R 1987, 'Report on the special panel on statistical particle bias problems in laser anemometry', *Journal of Fluids Engineering*, vol. 109, pp. 89-93.

Figliola, R & Beasley, D 2000, *Theory and design for mechanical measurements*, 3rd edn, John Wiley & Sons.

Finelli, CM, Hart, DD & Fonseca, DM 1999, 'Evaluating the spatial resolution of an acoustic doppler velocimeter and the consequences for measuring near-bed flows', *Journal of Limnology and Oceanography*, vol. 44, no. 7, pp. 1793-1801.

Flack, KA, Schultz, MP & Connelly, JS 2007, 'Examination of a critical roughness height for outer layer similarity', *Physics of Fluids*, vol. 19.

Flack, KA, Schultz, MP & Shapiro, TA 2005, 'Experimental support of townsend's reynolds number similarity hypothesis on rough walls', *Physics of Fluids*, vol. 17.

Flemming, H-C, Wingender, J, Moritz, R, Borchard, W & Mayer, C 1999, 'Physico-chemical properties of biofilms - a short review', in CW Keevil (ed.), *Biofilms in the aquatic environment*, Royal Society of Chemistry, Cambridge.

Garcia, CM, Cantero, MI, Nino, Y & Garcica, MH 2004, 'Acoustic doppler velocimeters (adv) performance curves (apcs) sampling the flow turbulence', paper presented to World Water and Environment Resources Congress, Utah.

George, WK & Castillo, L 1997, 'Zero-pressure gradient turbulent boundary layer', *Applied Mechanics Review*, vol. 50, no. 11, pp. 689-729.

Gordon, L & Cox, J 2000, *Acoustic doppler velocimeter performance in a laboratory flume*, Nortek USA and National Sedimentation Laboratory Mississippi.

Granville, PS 1976, 'A modified law of the wake for turbulent shear layers', *Journal of Fluids Engineering*, vol. 98, pp. 578-580.

Hama, FR 1954, 'Boundary-layer characteristics for smooth and rough surfaces', *Transactions of the Society of Naval Architects and Marine Engineers*, vol. 62, pp. 333-351.

Haslbeck, EG & Bohlander, G 1992, 'Microbial biofilm effects on drag - lab and field', paper presented to Proceedings 1992 S.N.A.M.E. Ship Production Symposium.

Hinze, JO 1975, *Turbulence*, 2nd edn, Mcgraw-hill series in mechanical engineering, McGraw-Hill.

International Hydropower Association 2005, *The contribution of hydropower (factsheet)*, 2009, <http://www.hydropower.org/>.

Jimenez, J 2004, 'Turbulent flows over rough walls', *Annual Review of Fluid Mechanics*, vol. 36, pp. 173-196.

Johnson, P & Barlow, R 1989, 'Effect of measuring volume length on two-component laser velocimeter measurements in a turbulent boundary layer', *Experiments in Fluids*, vol. 8, pp. 137-144.

Kaftori, D, Hetsroni, G & Banergee, S 1995, 'Particle behaviour in the turbulent boundary layer. I. Motion, deposition, and entrainment', *Physics of Fluids*, vol. 5, pp. 1095-1106.

Karlsson, RI, Eriksson, J & Persson, J 1993, 'Ldv measurements in a plane wall jet in a large enclosure', *6th International Symposium on LDA*, Lisbon, Portugal, 311-332.

Keirsbulck, L, Labraga, L, Mazouz, A & Tournier, C 2002, 'Surface roughness effects on turbulent boundary layer structures', *Journal of Fluids Engineering*, vol. 124, pp. 127-135.

Kilroy, C 2004, *A new alien diatom, didymosphenia geminata (lyngby) schmidt: Its biology, distribution, effects and potential risks for new zealand fresh waters*, National Institute of Water and Atmospheric Research Ltd, Christchurch.

Klebanoff, P 1955, 'Characteristics of turbulence in a boundary layer with zero pressure gradient', *NACA Report 1247*.

Krogstad, PA, Andersson, HI, Bakken, OM & Ashrafian, A 2005, 'An experimental and numerical study of channel flow with rough walls', *Journal of Fluid Mechanics*, vol. 530, pp. 327-352.

Krogstad, PA & Antonia, RA 1999, 'Surface roughness effects in turbulent boundary layers', *Experiments in Fluids*, vol. 27, pp. 450-460.

Krogstad, PA, Antonia, RA & Browne, LWB 1992, 'Comparison between rough- and smooth-wall turbulent boundary layers', *Journal of Fluid Mechanics*, vol. 245, pp. 599-617.

Kunkel, GJ, Allen, JJ & Smits, AJ 2007, 'Further support for townsend's reynolds number similarity hypothesis in high reynolds number rough-wall pipe flow', *Physics of Fluids*, vol. 19, no. 5.

Leonardi, S, Orlandi, P & Antonia, RA 2007, 'Properties of d- and k-type roughness in a turbulent channel flow', *Physics of Fluids*, vol. 19, no. 12.

Lewandowski, Z & Stoodley, P 1995, 'Flow induced vibrations, drag force, and pressure drop in conduits covered with biofilm', *Water Science and Technology*, vol. 32, no. 8, pp. 19-26.

Lewkowicz, A & Das, D 1985, 'Turbulent boundary layers on rough surfaces with and without a pliable overlayer: A simulation of marine fouling', *International Shipbuilding Progress, Marine Technology Monthly*, vol. 32, pp. 174-186.

Lewthwaite, J, Molland, A & Thomas, K 1985, 'An investigation into the variation of ship skin frictional resistance with fouling', *Transactions RINA*, vol. 127, pp. 269-284.

Ligrani, PM & Moffat, RJ 1986, 'Structure of transitionally rough and fully rough turbulent boundary layers', *Journal of Fluid Mechanics*, vol. 162, pp. 69-98.

Loeb, GI, Laster, D & Gracik, T 1984, 'The influence of microbial films on hydrodynamic drag of rotating discs', in JD Costlow & R Tipper (eds), *Marine biodeterioration: An interdisciplinary study*, Naval Institute Press, Annapolis, MD, pp. 88-94.

Lohrmann, A, Cabrera, R & Kraus, NC 1994, 'Acoustic-doppler velocimeter (adv) for laboratory use', paper presented to Fundamentals and Advancements in Hydraulic Measurements and Experimentation, Buffalo, New York.

Lu, SS & Willmarth, WW 1973, 'Measurements of the structure of the reynolds stress in a turbulent boundary layer', *Journal of Fluid Mechanics*, vol. 60, no. 3, pp. 481-511.

Macintosh, J & Isaacs, L 1992, 'Rpt - the roving preston tube', *11th Australasian Fluid Mechanics Conference*, University of Tasmania, Hobart, Australia, 1049-1052.

McEntee, W 1915, 'Variation of frictional resistance of ships with condition of wetted surface', *Transactions of the Society of Naval Architects and Marine Engineers*, vol. 23, pp. 37-42.

McFie, H 1956, *Algae and moss in canals*, Hydro-Electric Commission, Hobart, Tasmania.

McFie, H 1973, 'Biological, chemical and related engineering problems in large storage lakes of tasmania', in WC Ackermann, White, G.F. and Worthington, E.B. (ed.), *Man-made lakes: Their problems and environmental effects*, American Geophysical Union, Washington, D.C., vol. 17, pp. 56-62.

McFie, H 1976, 'Power storage lakes: Biological depositions and energy losses in tasmania', paper presented to 47th ANZAAS Congress, Hobart.

McKeon, B, Li, J, Morrison, J & Smits, AJ 2003, 'Pitot probe corrections in fully developed turbulent pipe flow', *Measurement Science and Technology*, vol. 14, pp. 1449-1458.

McLaughlin, DK & Tiederman, WG 1973, 'Biasing correction for individual realisation of laser anemometer measurements in turbulent flows', *The Physics of Fluids*, vol. 16, no. 12, pp. 2082-2088.

Mehta, RD & Bradshaw, P 1979, 'Design rules for small low speed wind tunnels', *The Aeronautical Journal of the Royal Aeronautical Society*, pp. 443-449.

Minkus, AJ 1954, 'Deterioration of the hydraulic capacity of pipelines', *New England Water Works Association*, vol. LXVIII, no. 1, pp. 1-10.

Montes, S 1998, *Hydraulics of open channel flow*, ASCE Press, New York, USA.

Nair, KVK, Satpathy, KK & Venugopalan, VP 1997, 'Biofouling control: Current methods and new approaches with emphasis on power plant cooling systems', in R Nagabhushanam & M Thompson (eds), *Fouling organisms of the indian ocean, biology and control technology*, A.A. Balkema, Rotterdam, pp. 159-189.

Nakagawa, H & Nezu, I 1981, 'Structure of space-time correlations of bursting phenomena in an open-channel flow', *Journal of Fluid Mechanics*, vol. 104, pp. 1-43.

Nash, JF 1965, ' Turbulent boundary layer behaviour and the auxiliary equation', *AGARDograph 97*, pp. 245-279.

Nezu, I 2005, 'Open-channel flow turbulence and its research prospect in the 21st century', *Journal of Hydraulic Engineering*, vol. 131, no. 4, pp. 229-246.

Nezu, I & Nakagawa, H 1993, *Turbulence in open-channel flows*, Iahr monograph series, Balkema Publishers, Rotterdam, Netherlands.

Nikora, VI & Goring, DG 1998, 'Adv measurements of turbulence: Can we improve their interpretation', *Journal of Hydraulic Engineering*, vol. 124, no. 6, pp. 630-634.

Nikuradse, J 1933, 'Law of flow in rough pipes (translation of "Stomungsgesetze in rahen rohren")', *NACA Report 1292*.

Olivieri, A, Jacob, B, Cancello, A, van Oostrum, P, Campana, E & Piva, R 2005, 'The effect of microbubbles on a flat plate turbulent boundary layer', paper presented to 2nd International Symposium on Seawater Drag Reduction, Busan, Korea 23-26 May.

Osborn, J, Bae, Y-S, Grenness, M, Sargison, J, Barton, A, Sprent, A, Walker, G & Bendall, T 2005, 'Mapping surface biofilms to improve the efficiency of water conveyance', *Spatial Sciences Congress: Spatial Intelligence, Innovation and Praxis: The National Biennial Conference of the Spatial Sciences Institute*, Spatial Sciences Institute, Melbourne, 406-415.

Ozaki, Y, Kawaguchi, T, Takeda, Y, Hishida, K & Maeda, M 2002, 'High time resolution ultrasonic velocity profiler', *Experimental Thermal and Fluid Science*, vol. 26, pp. 253-258.

Patel, V 1965, 'Calibration of the preston tube and limitations of its use in pressure gradients', *Journal of Fluid Mechanics*, vol. 23, no. 1, pp. 185-208.

Patel, VC 1998, 'Perspective: Flow at high reynolds number and over rough surfaces - achilles heel of cfd', *Journal of Fluids Engineering*, vol. 120, pp. 434-444.

Perkins, K 2009a, Test plate fouling reports to J Andrewartha.

Perkins, K 2009b, *Trials of alternative cleaning treatments involving the application of heat in tarraleah no.1 canal*, School of Plant Science, University of Tasmania, Hobart.

Perkins, K, Hallegraeff, G & Sargison, J 2009, 'Diatom fouling problems in a tasmanian hydro canal, including the description of *gomphonema tarraleahae* sp. Nov.' *Diatom Research*, vol. 24, no. 2, pp. 377-391.

Perkins, KJ 2005, 'Diatom fouling of tasmanian hydro canals', Honours thesis, University of Tasmania.

Perkins, KJ 2006, Water tunnel temperature control to JE Sargison.

Perry, AE & Joubert, PN 1963, 'Rough-wall boundary layers in adverse pressure gradients', *Journal of Fluid Mechanics*, vol. 17, pp. 193-211.

Perry, AE & Li, JD 1990, 'Experimental support for the attached-eddy hypothesis in zero-pressure-gradient turbulent boundary layers', *Journal of Fluid Mechanics*, vol. 218, pp. 405-438.

Perry, AE, Schofield, WH & Joubert, PN 1969, 'Rough wall turbulent boundary layers', *Journal of Fluid Mechanics*, vol. 37, no. 2, pp. 383-413.

Peterson, C 2007, 'Ecology of non-marine algae: Streams', in P McCarthy & A Orchard (eds), *Algae of australia: Introduction*, CSIRO Publishing, pp. 434-458.

Picologlou, BF, Zelver, N & Charaklis, WG 1980, 'Biofilm growth and hydraulic performance', *ASCE J. Hydraulics Division*, vol. HY5, pp. 733-747.

Poggi, D, Porporato, A & Ridolfi, L 2002, 'An experimental contribution to near-wall measurements by means of a special laser doppler anemometry technique', *Experiments in Fluids*, vol. 32, pp. 366-375.

Precht, E, Janssen, F & Huettel, M 2006, 'Near-bottom performance of the acoustic doppler velocimeter (adv) - a comparative study', *Aquatic Ecology*, vol. 40, pp. 481-492.

Preston, JH 1954, 'The determination of turbulent skin friction by means of pitot tubes', *Journal of the Royal Aeronautical Society*, vol. 58, pp. 109-121.

Preston, JH 1957, 'The minimum number for a turbulent boundary layer and the selection of a transition device', *Journal of Fluid Mechanics*, vol. 3, no. 4, pp. 373-384.

Raupach, MR, Antonia, RA & Rajagopalan, S 1991, 'Rough-wall turbulent boundary layers', *Applied Mechanics Review*, vol. 44, no. 1, pp. 1-25.

Ridgway, SH & Carder, DA 1993, 'Features of dolphin skin with potential hydrodynamic importance', *IEEE engineering in medicine and biology*, pp. 83-88.

Rigby, G, Hallegraeff, G & Taylor, A 2004, 'Ballast water heating offers a superior treatment option', *Journal of Marine Environmental Engineering*, vol. 7, pp. 217-230.

Sargison, J, Barton, A, Walker, G & Brandner, P 2009, 'Design and calibration of a water tunnel for skin friction research', *Australian Journal of Mechanical Engineering*, vol. 7, no. 2, pp. 1-14.

Schetz, JA 1993, *Boundary layer analysis*, Prentice-Hall Inc., New Jersey.

Schlichting, H 1955, *Boundary layer theory*, Permagon Press Ltd, London.

Schubauer, GB 1954, 'Turbulent process as observed in boundary layer and pipe', *Journal of Applied Physics*, vol. 25, no. 2, pp. 188-196.

Schultz, MP 1998, 'The effect of biofilms on turbulent boundary layer structure', PhD thesis, Florida Institute of Technology.

Schultz, MP 2000, 'Turbulent boundary layers on surfaces covered with filamentous algae', *Journal of Fluids Engineering*, vol. 122, pp. 357-363.

Schultz, MP 2004, 'Frictional resistance of antifouling coatings systems', *Journal of Fluids Engineering*, vol. 126, pp. 1039-1047.

Schultz, MP & Flack, KA 2005, 'Outer layer similarity in fully rough turbulent boundary layers', *Experiments in Fluids*, vol. 38, pp. 328-340.

Schultz, MP & Flack, KA 2007, 'The rough-wall turbulent boundary layer from the hydraulically smooth to the fully rough regime', *Journal of Fluid Mechanics*, vol. 580, pp. 381-405.

Schultz, MP & Flack, KA 2009, 'Turbulent boundary layers on a systematically varied rough wall', *Physics of Fluids*, vol. 21, pp. 015104: 015101-015109.

Schultz, MP & Swain, GW 1999, 'The effect of biofilms on turbulent boundary layers', *Journal of Fluids Engineering*, vol. 121, pp. 44-51.

Schultz, MP & Swain, GW 2000, 'The influence of biofilms on skin friction drag', *Biofouling*, vol. 15, no. 1-3, pp. 129-139.

Shockling, MA, Allen, JJ & Smits, AJ 2006, 'Roughness effects in turbulent pipe flow', *Journal of Fluid Mechanics*, vol. 564, pp. 267-285.

Sletfjerding, E, Gudmundsson, J & Sjoen, K 1998, 'Flow experiments with high pressure natural gas in coated and plain pipes: Comparison of transport capacity', paper presented to PSIG 30th Annual Meeting, Denver, Colorado, October 28-30, 1998.

Spalding, DB 1961, 'A single formula for the "Law of the wall"', *Journal of Applied Mechanics*, vol. 28, pp. 455-458.

Stoodley, P, Boyle, J, Cunningham, AB, Dodds, I, Lappin-Scott, HM & Lewandowski, Z 1999, 'Biofilm structure and influence on biofouling under laminar and turbulent flows', in CW Keevil (ed.), *Biofilms in the aquatic environment*, Royal Society of Chemistry, Cambridge.

Stoodley, P, Lewandowski, Z, Boyle, JD & Lapin-Scott, HM 1998, 'Oscillation characteristics of biofilm streamers in turbulent flowing water as related to drag and pressure drop', *Biotechnology and Bioengineering*, vol. 57, no. 5, pp. 536-544.

Swain, GW, Herpe, S, Ralston, E & Tribou, M 2006, 'Short-term testing of antifouling surfaces: The importance of colour', *Biofouling*, vol. 22, no. 6, pp. 425-429.

Tachie, MF 2000, 'Open channel turbulent boundary layers and wall jets on rough surfaces', PhD thesis, University of Saskatchewan.

Tachie, MF, Bergstrom, DJ & Balachandar, R 2000, 'Rough wall turbulent boundary layers in shallow open channel flows', *Journal of Fluids Engineering*, vol. 122, pp. 533-541.

Tachie, MF, Bergstrom, DJ & Balachandar, R 2004, 'Roughness effects on the mixing properties in open channel turbulent boundary layers', *Journal of Fluids Engineering*, vol. 126, pp. 1025 - 1032.

Takeda, Y 1995, 'Instantaneous velocity profile measurement by ultrasonic doppler method', *JSME International Journal Series B Fluids and Thermal Engineering*, vol. 38, no. 1, pp. 8-16.

Takeda, Y 1999, 'Ultrasonic doppler method for velocity profile measurement in fluid dynamics and fluid engineering', *Experiments in Fluids*, vol. 26, pp. 177-178.

Townsend, A 1976, *The structure of turbulent shear flow*, Cambridge monographs on mechanics and applied mathematics, Cambridge University Press.

Townsin, RL 2003, 'The ship hull fouling penalty', *Biofouling*, vol. 19, pp. 9-15.

U.S. Army Corps of Engineers *Hec-ras user's manual*.

Voulgaris, G & Trowbridge, JH 1998, 'Evaluation of the acoustic doppler velocimeter (adv) for turbulence measurements', *Journal of Atmospheric and Oceanic Technology*, vol. 15, pp. 272-288.

Wallace, JM, Eckelmann, H & Brodkey, RS 1972, 'The wall region in turbulent shear flow', *Journal of Fluid Mechanics*, vol. 54, no. 1, pp. 39-48.

Watanabe, S, Nagamatsu, N, Yokoo, K & Kawakami, Y 1969, 'The augmentation in frictional resistance due to slime', *Journal Kansai Soc Nav Arch*, vol. 131, pp. 45-51.

Wetherbee, R, Lind, JL, Burke, J & Quatrano, RS 1998, 'The first kiss: Establishment and control of initial adhesion by raphid diatoms', *Journal of Phycology*, vol. 34, pp. 9-15.

White, FM 1991, *Viscous fluid flow*, 2nd edn, McGraw-Hill.

White, RJ & Chamberlain, AHL 1982, 'Attachment of epiphytic freshwater diatoms', *Microscopy*, vol. 34, pp. 470-476.

Whitehouse, D 2002, *Surfaces and their measurement*, Hermes Penton Science, UK.

Whitton, B, Ellwood, N & Kawecka, B 2009, 'Biology of the freshwater diatom *didymosphenia*: A review', *Hydrobiologia*, vol. 630, pp. 1-37.

Wilderer, PA, Cunningham, A & Schindler, U 1995, 'Hydrodynamics and shear stress: Report from the discussion session', paper presented to Water Science and Technology - Selected Proceedings of the IAWQ International Conference and Workshop on Biofilm Structure, Growth and Dynamics, Noordwikerhout, The Netherlands.

Winter, KG 1977, 'An outline of the techniques available for the measurement of skin friction in turbulent boundary layers', *Progress in Aerospace Science*, vol. 18, pp. 1-57.

Wu, Y & Christensen, KT 2007, 'Outer-layer similarity in the presence of a practical rough-wall topography', *Physics of Fluids*, vol. 19, no. 8.

Zhang, Z & Eisele, K 1995, 'Off-axis alignment of an lda-probe and the effect of astigmatism on measurements', *Experiments in Fluids*, vol. 19, pp. 89-94.

Zhang, Z & Eisele, K 1998a, 'Further considerations of the astigmatism error associated with off-axis alignment of an lda-probe', *Experiments in Fluids*, vol. 24, pp. 83-89.

Zhang, Z & Eisele, K 1998b, 'On the overestimation of the flow turbulence due to fringe distortion in lda measurement volumes', *Experiments in Fluids*, vol. 25, pp. 371-374.

APPENDICES

A SUPPORTING DATA FOR CHAPTER 7

A1 Roughness Data from Photogrammetry Measurements

Table A.1 Average roughness parameters and statistical information for RP1 (clean) (see Table 4.2 for definitions)

Window	Roughness Parameters [mm]					Statistical moments				Peak Count
	R_a	R_q	R_p	R_v	R_t	1st (mean)	2nd (variance)	3rd (skewness)	4th (kurtosis)	
A	0.26	0.33	0.92	-0.81	1.73	0.93	0.21	0.34	0.13	15
C	0.36	0.39	1.14	-1.07	2.21	1.07	0.20	0.10	-0.04	15
E	0.28	0.34	0.98	-0.84	1.82	0.84	0.12	0.22	0.21	18

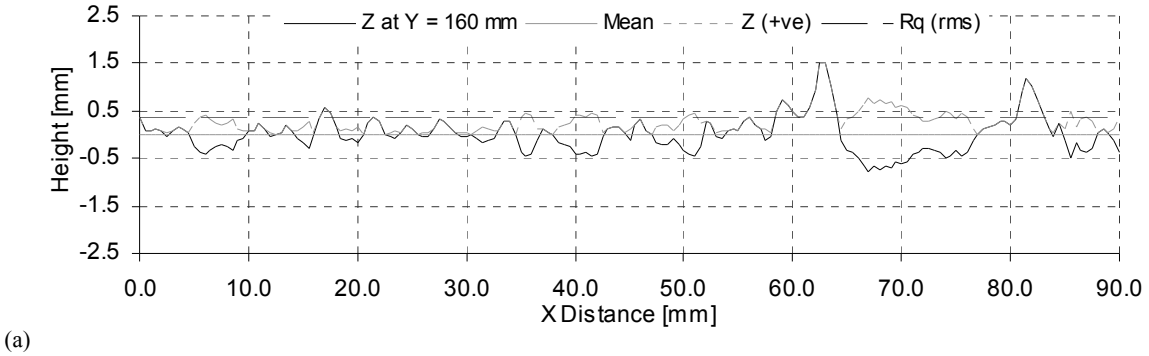

(a)

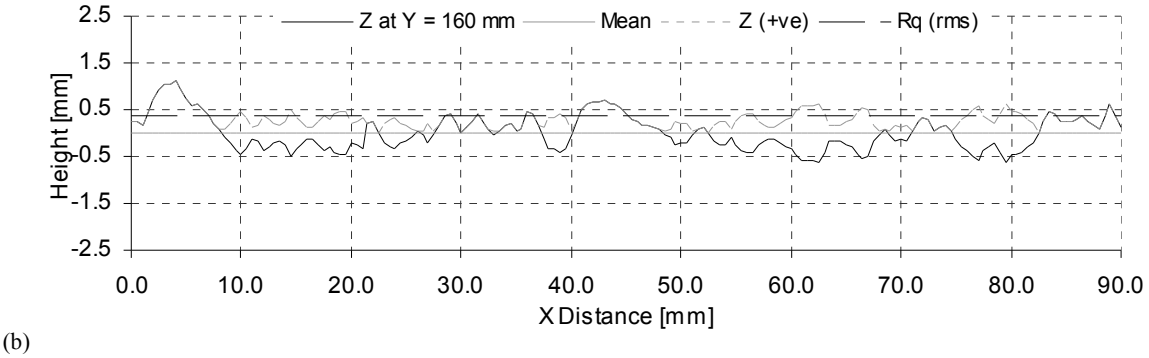

(b)

Figure A.1 Cross sections at Y = 160 mm for RP1 (clean): (a) window A; (b) window E

Table A.2 Average roughness parameters and statistical information for RP1 F1 (see Table 4.2 for definitions)

Window	Roughness Parameters [mm]					Statistical moments				Peak Count
	R_a	R_q	R_p	R_v	R_t	1st (mean)	2nd (variance)	3rd (skewness)	4th (kurtosis)	
A	0.70	0.83	1.60	-1.72	3.31	1.72	0.71	-0.04	-0.80	7
C	0.68	0.81	1.67	-1.68	3.35	1.68	0.69	-0.07	-0.60	9
E	0.37	0.45	1.13	-0.97	2.10	0.97	0.21	0.27	-0.22	11

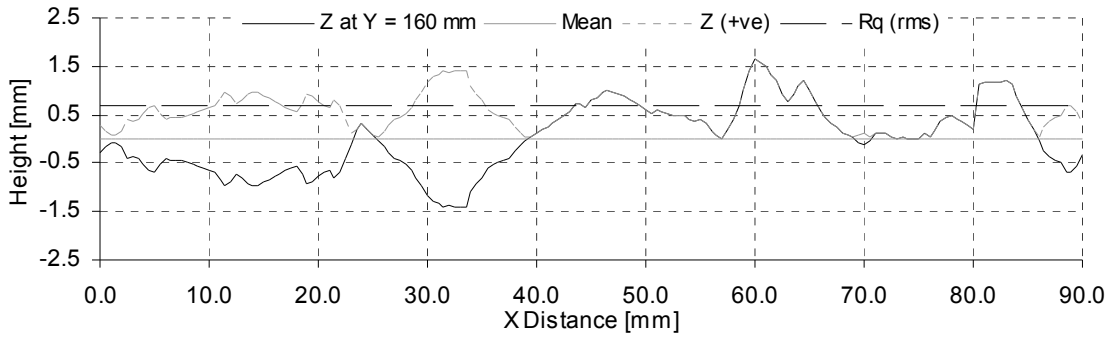

(a)

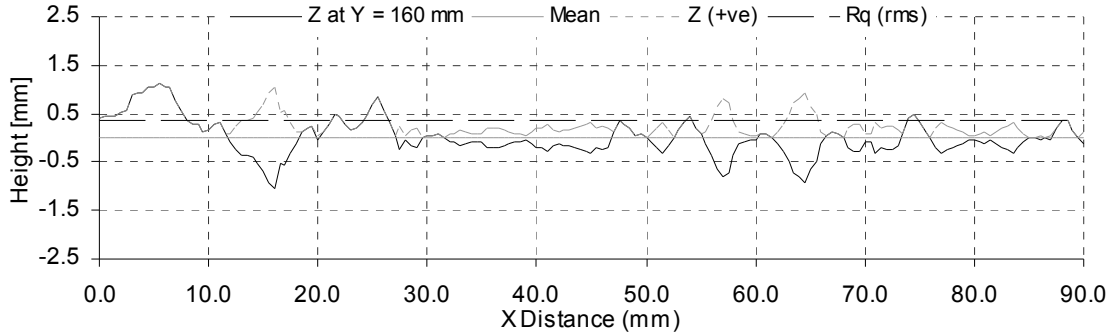

(b)

Figure A.2 Cross sections at Y = 160 mm for RP1 F1: (a) window A; (b)window E

Table A.3 Average roughness parameters and statistical information for SP1 F2 (see Table 4.2 for definitions)

Window	Roughness Parameters [mm]					Statistical moments				Peak Count
	R_a	R_q	R_p	R_v	R_t	1st (mean)	2nd (variance)	3rd (skewness)	4th (kurtosis)	
A	0.39	0.45	1.28	-0.76	2.04	0.76	0.24	0.74	0.02	10
C	0.36	0.43	1.11	-0.51	1.62	0.51	0.19	0.93	-0.02	7
E	0.05	0.06	0.30	-0.14	0.44	0.14	0.00	1.32	4.88	21

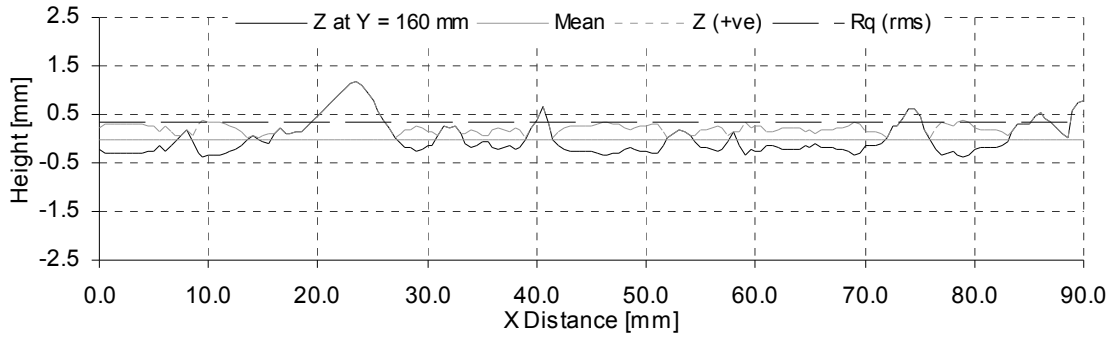

(a)

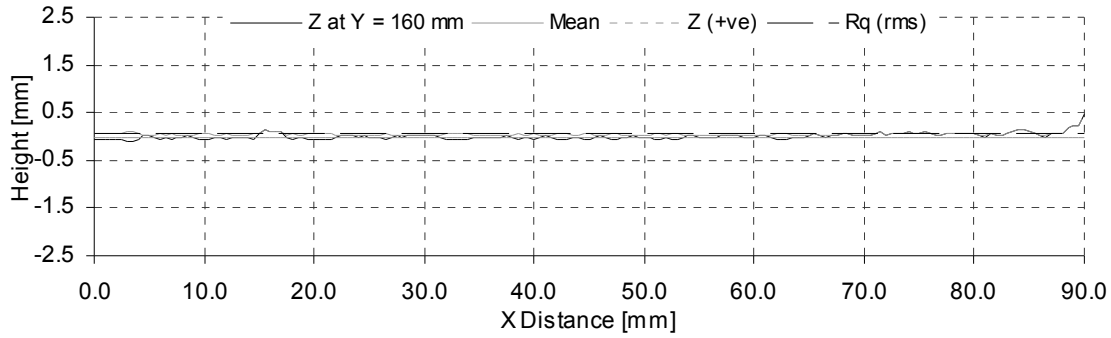

(b)

Figure A.3 Cross sections at Y = 160 mm for SP1 F2: (a) window A; (b) window E

Table A.4 Average roughness parameters and statistical information for SP2 F3 (see Table 4.2 for definitions)

Window	Roughness Parameters [mm]					Statistical moments				Peak Count
	R_a	R_q	R_p	R_v	R_t	1st (mean)	2nd (variance)	3rd (skewness)	4th (kurtosis)	
A	0.02	0.03	0.10	-0.07	0.17	0.17	0.01	0.06	-0.23	19
C	0.02	0.03	0.09	-0.07	0.16	0.26	0.02	0.12	-1.10	22
E	0.02	0.03	0.11	-0.13	0.24	0.13	0.00	-0.16	3.05	22

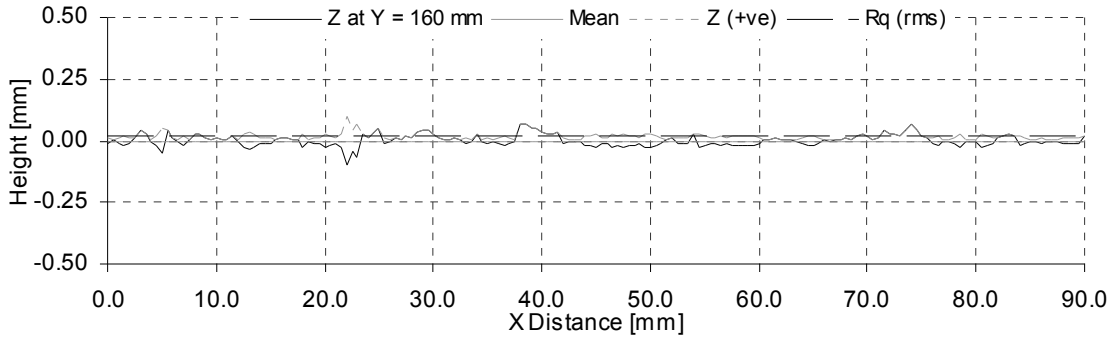

(a)

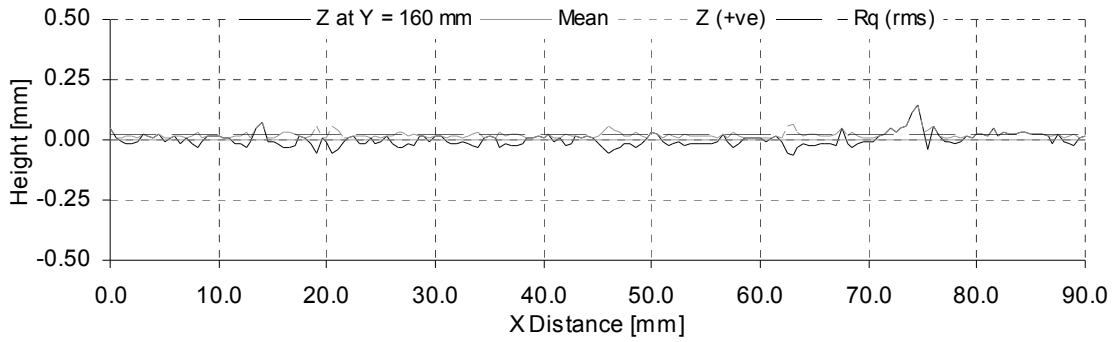

(b)

Figure A.4 Cross sections at Y = 160 mm for SP2 F3: (a) window A; (b) window E

Table A.5 Average roughness parameters and statistical information for RP1 F4 (see Table 4.2 for definitions)

Window	Roughness Parameters [mm]					Statistical moments				Peak Count
	R_a	R_q	R_p	R_v	R_t	1st (mean)	2nd (variance)	3rd (skewness)	4th (kurtosis)	
A	0.30	0.37	1.06	-0.81	1.87	0.81	0.14	0.29	0.11	13
C	0.35	0.42	1.06	-0.88	1.94	0.88	0.19	0.14	-0.37	12
E	0.31	0.39	1.03	-0.77	1.79	0.85	0.19	0.32	-0.06	12

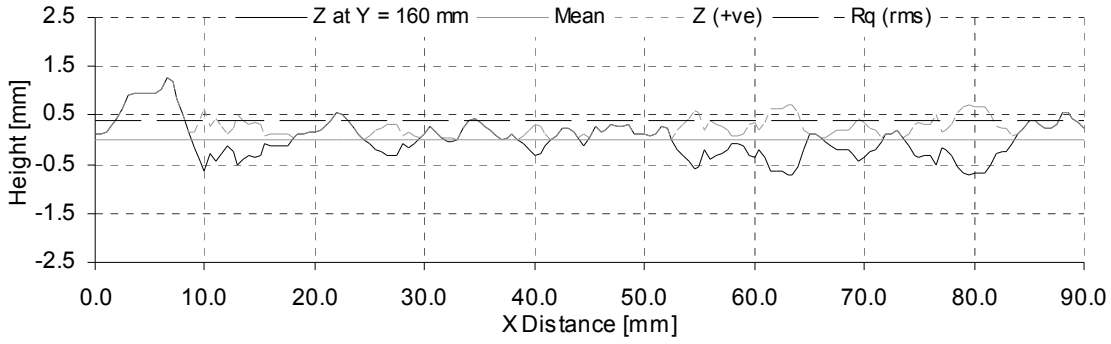

(a)

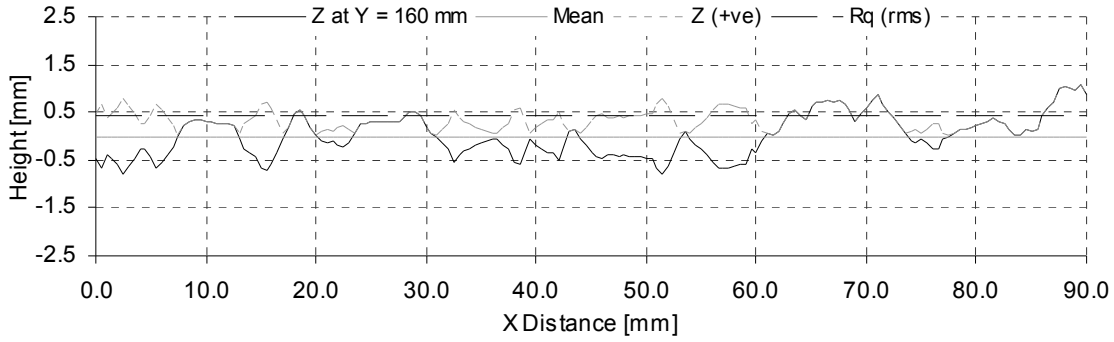

(b)

Figure A.5 Cross sections at Y = 160 mm for RP1 F4: (a) window A; (b) window E

Table A.6 Average roughness parameters and statistical information for RP2 Clean (see Table 4.2 for definitions)

Window	Roughness Parameters [mm]					Statistical moments				Peak Count
	R_a	R_q	R_p	R_v	R_t	1st (mean)	2nd (variance)	3rd (skewness)	4th (kurtosis)	
A	0.45	0.57	1.37	-1.22	2.59	1.22	0.33	0.21	-0.15	8
B	0.43	0.53	1.45	-1.19	2.63	1.19	0.30	0.39	0.60	11
D	0.37	0.46	1.30	-1.06	2.36	1.06	0.22	0.22	0.18	10
E	0.35	0.45	1.25	-0.99	2.24	0.99	0.20	0.29	0.41	13

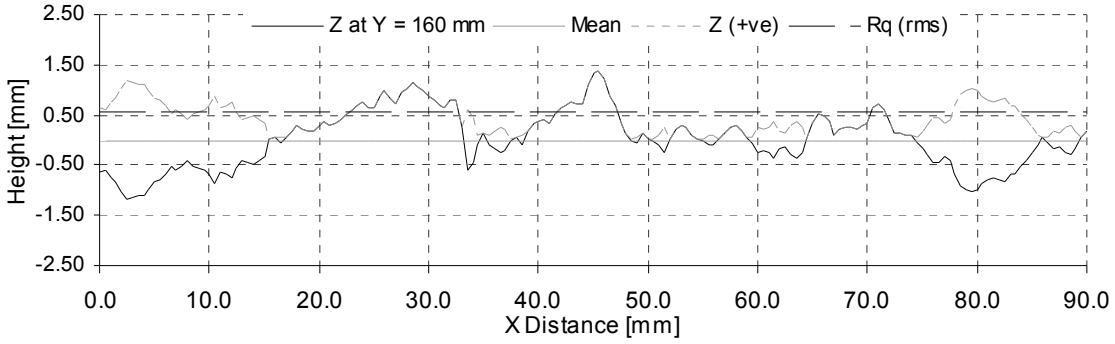

(a)

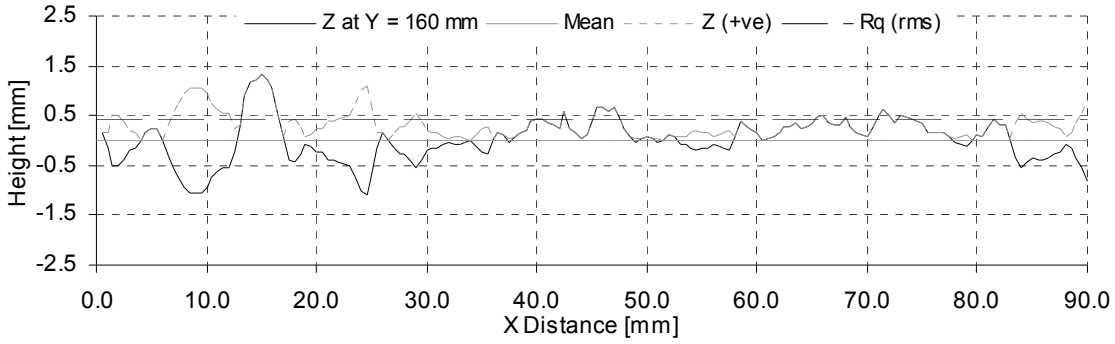

(b)

Figure A.6 Cross sections at Y = 160 mm for RP2 Clean: (a) window A; (b) window E

Table A.7 Average roughness parameters and statistical information for RP2 F5 (see Table 4.2 for definitions)

Window	Roughness Parameters [mm]					Statistical moments				Peak Count
	R_a	R_q	R_p	R_v	R_t	1st (mean)	2nd (variance)	3rd (skewness)	4th (kurtosis)	
A	0.45	0.56	1.34	-1.33	2.67	1.33	0.33	-0.12	0.19	6
B	0.35	0.45	1.17	-1.17	2.34	1.17	0.22	-0.05	0.14	7
D	0.35	0.44	1.28	-1.01	2.29	1.01	0.21	0.33	0.24	10
E	0.31	0.39	1.07	-0.97	2.04	0.97	0.16	0.06	0.06	11

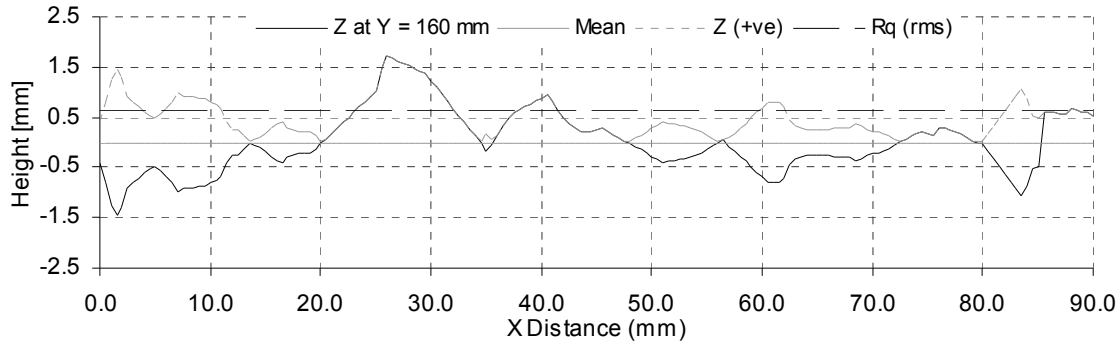

(a)

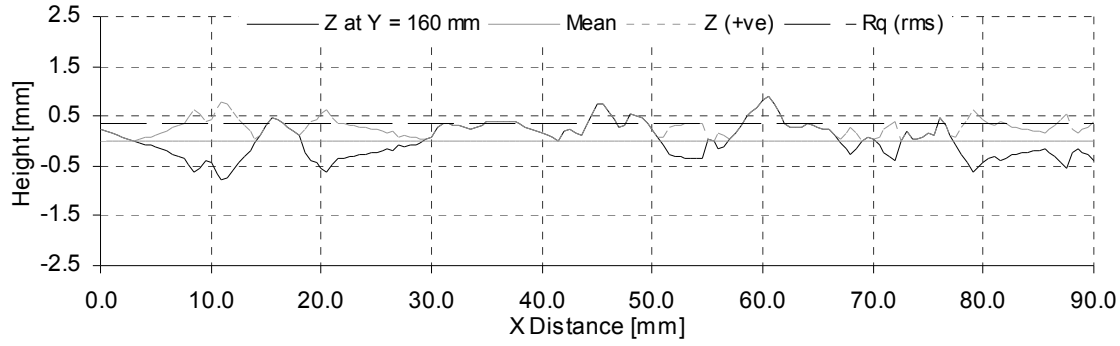

(b)

Figure A.7 Cross sections at Y = 160 mm for RP2 F5: (a) window A; (b) window E

Table A.8 Average roughness parameters and statistical information for SP1 F6 (see Table 4.2 for definitions)

Window	Roughness Parameters [mm]					Statistical moments				Peak Count
	R_a	R_q	R_p	R_v	R_t	1st (mean)	2nd (variance)	3rd (skewness)	4th (kurtosis)	
A	0.38	0.48	1.31	-0.94	2.25	0.94	0.24	0.41	-0.06	10
B	0.37	0.45	1.06	-0.90	1.95	0.90	0.21	0.30	-0.42	11
D	0.03	0.04	0.12	-0.12	0.24	0.21	0.01	0.02	-0.51	23
E	0.02	0.03	0.10	-0.10	0.19	0.10	0.00	0.19	0.76	26

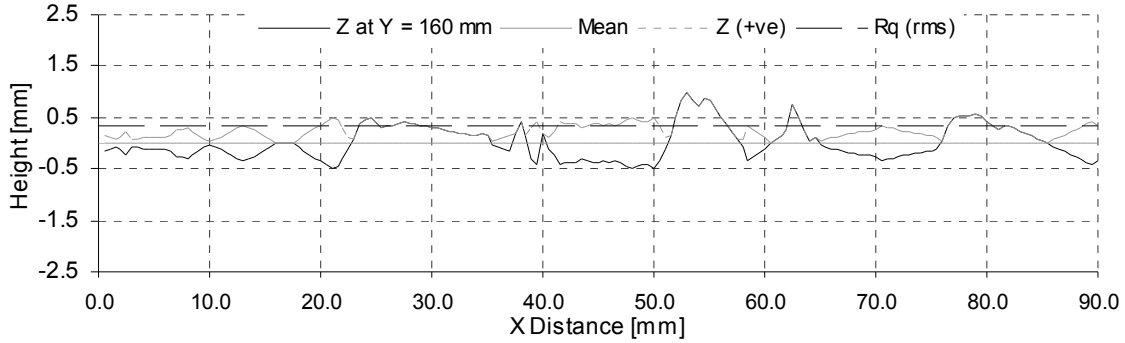

(a)

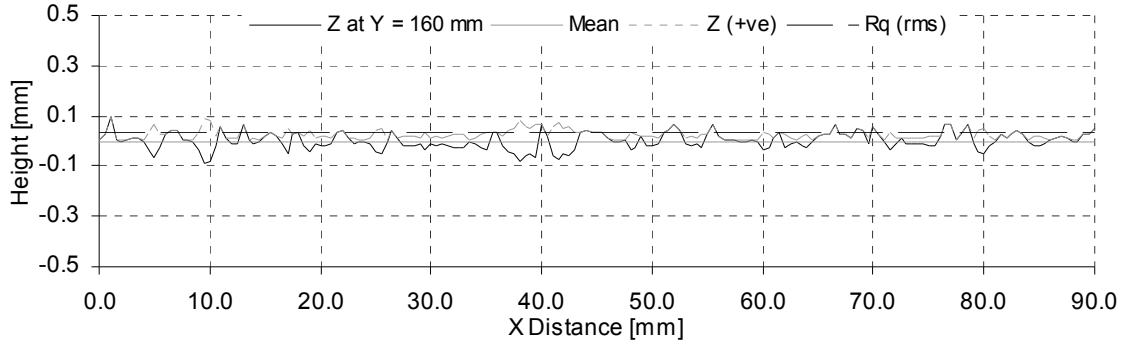

(b)

Figure A.8 Cross sections at Y = 160 mm for SP1 F6: (a) window A; (b) window E

A2 Tabulated Boundary Layer Profile Data

Table A.9 Boundary layer characteristics for SP Lab (LDV set up in one-dimension)

x [mm]	U [m/s]	T [deg C]	Re_l	Re_θ	δ [mm]	δ^* [mm]	θ [mm]	H	u^* [m/s]	c_f	Π	ε [mm]	k_s [mm]	Re_k	Δu^+
100	1.01	14.71	8.77E+05	2310	29.83	3.39	2.63	1.29	0.046	0.004135	-0.05	0.00	-	<5	0.00
100	1.25	14.79	1.09E+06	2880	32.74	3.33	2.64	1.26	0.056	0.003976	-0.11	0.02	-	<5	0.00
100	1.75	15.36	1.55E+06	4070	38.27	3.26	2.62	1.24	0.076	0.003766	-0.22	0.01	-	<5	0.00
100	2.00	15.37	1.76E+06	4730	42.35	3.30	2.67	1.23	0.085	0.003643	-0.26	0.01	-	<5	0.00
250	1.01	14.70	8.76E+05	2490	34.45	3.70	2.84	1.31	0.044	0.003890	0.00	0.00	-	<5	0.00
250	1.26	15.04	1.10E+06	3080	32.25	3.57	2.79	1.28	0.054	0.003675	0.05	0.04	-	<5	0.00
250	1.75	14.79	1.52E+06	4190	31.41	3.44	2.75	1.25	0.073	0.003499	0.05	0.05	-	<5	0.00
250	2.00	15.23	1.76E+06	4790	34.30	3.41	2.72	1.26	0.082	0.003394	0.00	0.01	-	<5	0.00
500	1.01	14.88	8.77E+05	2570	28.03	3.80	2.92	1.30	0.043	0.003698	0.24	0.09	-	<5	0.00
500	1.25	15.04	1.09E+06	3150	29.00	3.70	2.87	1.29	0.052	0.003517	0.24	0.05	-	<5	0.00
500	1.75	15.31	1.54E+06	4410	28.91	3.61	2.85	1.27	0.071	0.003298	0.24	0.05	-	<5	0.00
500	2.00	14.88	1.75E+06	5060	32.31	3.64	2.89	1.26	0.080	0.003217	0.18	0.09	-	<5	0.00
750	1.00	14.74	8.69E+05	2800	31.31	4.27	3.21	1.33	0.042	0.003579	0.28	0.01	-	<5	0.00
750	1.25	15.16	1.10E+06	3570	34.42	4.24	3.24	1.31	0.051	0.003388	0.23	0.02	-	<5	0.00
750	1.75	15.01	1.53E+06	4840	32.91	4.06	3.15	1.29	0.070	0.003213	0.26	0.04	-	<5	0.00
750	2.01	15.22	1.77E+06	5750	34.20	4.16	3.24	1.28	0.079	0.003118	0.25	0.01	-	<5	0.00
850	1.00	15.18	8.82E+05	2930	31.63	4.38	3.31	1.32	0.042	0.003543	0.29	0.02	-	<5	0.00
850	1.25	14.82	1.09E+06	3480	31.33	4.19	3.18	1.32	0.052	0.003417	0.29	0.02	-	<5	0.00
850	1.75	15.29	1.54E+06	5020	35.20	4.17	3.25	1.28	0.070	0.003200	0.22	0.04	-	<5	0.00
850	2.00	15.07	1.75E+06	5550	32.22	4.06	3.16	1.29	0.079	0.003129	0.29	0.04	-	<5	0.00

Table A.10 Boundary layer characteristics for SP Lab (LDV set up in two-dimensions)

x [mm]	U [m/s]	T [deg C]	Re_l	Re_θ	δ [mm]	δ^* [mm]	θ [mm]	H	u^* [m/s]	c_f	Π	ε [mm]	k_s [mm]	Re_k	Δu^+
850	1.04	15.06	9.10E+05	2710	29.54	3.74	2.97	1.26	0.044	0.003601	0.31	0.72	-	<5	0.00
850	1.27	14.95	1.11E+06	3330	30.25	3.74	2.98	1.26	0.053	0.003422	0.32	0.71	-	<5	0.00
850	1.74	14.79	1.51E+06	4360	30.88	3.58	2.88	1.24	0.070	0.003213	0.31	0.73	-	<5	0.00
850	1.99	14.99	1.74E+06	4980	31.23	3.52	2.85	1.24	0.079	0.003163	0.28	0.70	-	<5	0.00

Table A.11 Boundary layer characteristics for RP Lab (LDV set up in one-dimension)

x [mm]	U [m/s]	T [deg C]	Re_l	Re_θ	δ [mm]	δ^* [mm]	θ [mm]	H	u^* [m/s]	c_f	Π	ε [mm]	k_s [mm]	Re_k	Δu^+
98.5	1.01	15.21	8.86E+05	2530	32.94	3.86	2.84	1.36	0.061	0.007266	0.11	0.95	1.71	92	7.52
98.5	1.25	14.76	1.09E+06	3150	34.75	3.90	2.89	1.35	0.075	0.007222	0.08	0.95	1.74	114	8.06
98.5	1.75	15.25	1.54E+06	4380	30.83	3.84	2.84	1.36	0.102	0.006882	0.17	0.86	1.53	138	8.52
98.5	2.00	15.17	1.76E+06	5000	33.38	3.83	2.84	1.35	0.117	0.006843	0.12	0.87	1.51	156	8.81
251.5	1.01	14.69	8.75E+05	2790	31.09	4.38	3.18	1.38	0.058	0.006613	0.26	0.86	1.47	74	7.00
251.5	1.25	15.11	1.09E+06	3440	29.89	4.35	3.14	1.39	0.073	0.006766	0.28	0.87	1.61	103	7.80
251.5	1.75	15.24	1.54E+06	4850	29.63	4.34	3.14	1.38	0.099	0.006353	0.30	0.73	1.36	118	8.14
251.5	2.00	14.95	1.75E+06	5550	34.50	4.35	3.17	1.37	0.111	0.006129	0.21	0.69	1.22	119	8.14
751.3	1.01	14.68	8.77E+05	3880	33.63	6.59	4.41	1.49	0.062	0.007454	0.44	0.66	3.24	174	9.08
751.3	1.25	15.08	1.10E+06	4790	33.24	6.59	4.36	1.51	0.076	0.007427	0.45	0.60	3.28	219	9.65
751.3	1.75	14.97	1.53E+06	6730	33.18	6.61	4.39	1.51	0.105	0.007255	0.47	0.60	3.12	288	10.31
751.3	2.00	15.30	1.76E+06	7820	34.15	6.63	4.42	1.50	0.119	0.007151	0.46	0.60	3.03	321	10.57
853.2	1.00	-	-	-	-	-	-	-	-	-	-	-	-	-	-
853.2	1.26	15.24	1.11E+06	5100	35.81	6.73	4.57	1.47	0.076	0.007203	0.43	0.88	3.04	203	9.46
853.2	1.74	15.16	1.53E+06	7000	34.74	6.72	4.55	1.48	0.103	0.007005	0.47	0.82	2.86	260	10.06
853.2	1.99	14.89	1.74E+06	7910	33.87	6.71	4.53	1.48	0.117	0.006920	0.49	0.75	2.75	283	10.28

Table A.12 Boundary layer characteristics for RP Lab (LDV set up in two-dimensions)

x [mm]	U [m/s]	T [deg C]	Re_l	Re_θ	δ [mm]	δ^* [mm]	θ [mm]	H	u^* [m/s]	c_f	Π	ε [mm]	k_s [mm]	Re_k	Δu^+
850	1.01	15.17	8.84E+05	3910	33.08	6.56	4.41	1.49	0.056	0.006309	0.50	0.36	1.91	95	7.65
850	1.26	14.82	1.10E+06	4910	33.67	6.64	4.46	1.49	0.071	0.006251	0.50	0.32	1.93	119	8.20
850	1.75	14.82	1.52E+06	6740	32.91	6.64	4.42	1.50	0.098	0.006266	0.52	0.28	1.99	170	9.06
850	2.01	14.85	1.75E+06	7690	32.80	6.55	4.38	1.50	0.112	0.006264	0.51	0.31	1.98	195	9.38

Table A.13 Boundary layer characteristics for RP1 F1 (LDV set up in one-dimension)

x [mm]	U [m/s]	T [deg C]	Re_l	Re_θ	δ [mm]	δ^* [mm]	θ [mm]	H	u^* [m/s]	c_f	Π	ε [mm]	k_s [mm]	Re_k	Δu^+
499	1.00	14.87	8.76E+05	3440	30.67	5.85	3.91	1.49	0.066	0.008739	0.40	1.06	4.61	268	10.12
499	1.25	15.09	1.10E+06	4260	31.47	5.81	3.86	1.51	0.083	0.008696	0.38	0.99	4.52	329	10.63
499	1.75	14.92	1.53E+06	6170	32.43	6.00	4.02	1.49	0.110	0.007936	0.40	0.84	3.68	356	10.82
499	2.00	15.27	1.76E+06	7060	33.85	5.96	4.00	1.49	0.130	0.008492	0.35	1.04	4.42	508	11.69
850	1.01	14.89	8.81E+05	4070	35.24	6.82	4.60	1.48	0.067	0.008737	0.39	1.32	5.18	303	10.43
850	1.25	14.92	1.09E+06	5040	35.84	6.89	4.60	1.50	0.080	0.008261	0.41	1.08	4.61	325	10.61
850	1.76	15.17	1.54E+06	7410	37.73	7.19	4.79	1.50	0.115	0.008582	0.39	1.16	5.37	545	11.86
850	2.00	15.23	1.76E+06	8390	35.93	7.16	4.75	1.51	0.131	0.008664	0.43	1.22	5.53	642	12.26

Table A.14 Boundary layer characteristics for SP1 F2 (LDV set up in one-dimension)

x [mm]	U [m/s]	T [deg C]	Re_l	Re_θ	δ [mm]	δ^* [mm]	θ [mm]	H	u^* [m/s]	c_f	Π	ε [mm]	k_s [mm]	Re_k	Δu^+
500.5	1.01	14.95	8.78E+05	2860	29.86	4.44	3.25	1.37	0.049	0.004776	0.34	0.16	0.63	27	3.82
500.5	1.26	15.01	1.10E+06	3580	29.83	4.46	3.24	1.37	0.063	0.005017	0.35	0.20	0.69	38	5.01
500.5	1.75	15.07	1.54E+06	5110	32.03	4.58	3.32	1.38	0.089	0.005227	0.32	0.24	0.75	59	6.43
500.5	1.99	15.12	1.75E+06	5890	32.96	4.64	3.36	1.38	0.102	0.005217	0.31	0.28	0.77	69	6.82
850	1.01	15.00	8.86E+05	3330	33.19	5.07	3.75	1.35	0.050	0.004917	0.39	0.59	0.76	33	4.56
850	1.25	14.97	1.10E+06	4190	34.22	5.19	3.81	1.36	0.064	0.005271	0.38	0.78	0.89	50	5.92
850	1.75	15.26	1.54E+06	5960	34.97	5.25	3.85	1.36	0.089	0.005143	0.38	0.72	0.81	64	6.62
850	2.00	14.99	1.75E+06	6740	34.09	5.29	3.85	1.38	0.100	0.005067	0.42	0.60	0.78	69	6.83

Table A.15 Boundary layer characteristics for SP2 F3 using Bradshaw's Method (LDV set up in one-dimension)

x [mm]	U [m/s]	T [deg C]	Re_l	Re_θ	δ [mm]	δ^* [mm]	θ [mm]	H	u^* [m/s]	c_f	Π	ε [mm]	k_s [mm]	Re_k	Δu^+
500	1.00	14.76	8.72E+05	2810	31.85	4.22	3.21	1.32	0.042	0.003529	0.30	0.07	-	<5	0.00
500	1.25	15.10	1.10E+06	3390	29.10	4.07	3.07	1.32	0.051	0.003310	0.41	0.05	-	<5	0.00
500	1.75	14.88	1.53E+06	4680	29.85	4.03	3.06	1.32	0.067	0.002953	0.50	0.05	-	<5	0.00
500	2.00	15.43	1.77E+06	5620	31.40	4.11	3.16	1.30	0.076	0.002866	0.51	0.11	-	<5	0.00
854	1.01	15.28	8.87E+05	3090	32.48	4.59	3.48	1.32	0.041	0.003347	0.43	0.17	-	<5	0.00
854	1.25	15.09	1.10E+06	3840	32.84	4.60	3.48	1.32	0.050	0.003161	0.47	0.12	-	<5	0.00
854	1.75	14.83	1.53E+06	5410	33.62	4.65	3.54	1.31	0.066	0.002870	0.56	0.09	-	<5	0.00
854	1.98	15.14	1.74E+06	6080	32.49	4.57	3.48	1.31	0.074	0.002768	0.62	0.10	-	<5	0.00

Table A.16 Boundary layer characteristics for SP2 F3 using Perry and Li's Method (LDV set up in one-dimension)

x [mm]	U [m/s]	T [deg C]	Re_l	Re_θ	δ [mm]	δ^* [mm]	θ [mm]	H	u^* [m/s]	c_f	Π	ε [mm]	k_s [mm]	Re_k	Δu^+
500	1.00	14.76	8.72E+05	2810	31.85	4.22	3.21	1.32	0.044	0.003782	0.21	0.01	0.16	6.01	0.55
500	1.25	15.10	1.10E+06	3390	29.10	4.07	3.07	1.32	0.053	0.003571	0.32	0.01	0.14	6.33	0.65
500	1.75	14.88	1.53E+06	4680	29.85	4.03	3.06	1.32	0.075	0.003674	0.28	0.00	0.13	8.8	1.77
500	2.00	15.43	1.77E+06	5620	31.40	4.11	3.16	1.30	0.080	0.003169	0.40	0.05	0.08	5.95	0.84
854	1.01	15.28	8.87E+05	3090	32.48	4.59	3.48	1.32	0.041	0.003294	0.42	0.03	-	<5	-0.25
854	1.25	15.09	1.10E+06	3840	32.84	4.60	3.48	1.32	0.051	0.003257	0.40	0.02	-	<5	0.07
854	1.75	14.83	1.53E+06	5410	33.62	4.65	3.54	1.31	0.068	0.003006	0.46	0.00	-	<5	0.21
854	1.98	15.14	1.74E+06	6080	32.49	4.57	3.48	1.31	0.079	0.003167	0.45	0.04	0.09	6.59	1.09

Table A.17 Boundary layer characteristics for RP1 F4 (LDV set up in one-dimension)

x [mm]	U [m/s]	T [deg C]	Re_l	Re_θ	δ [mm]	δ^* [mm]	θ [mm]	H	u^* [m/s]	c_f	Π	ε [mm]	k_s [mm]	Re_k	Δu^+
249	1.01	15.27	8.92E+05	3000	31.91	5.04	3.35	1.51	0.066	0.008530	0.23	0.41	3.45	202	9.48
249	1.26	14.78	1.09E+06	3690	31.03	5.04	3.36	1.50	0.084	0.008958	0.23	0.55	4.08	300	10.41
249	1.75	15.09	1.53E+06	5150	31.75	4.97	3.35	1.48	0.116	0.008839	0.23	0.51	4.06	415	11.20
249	1.99	15.02	1.75E+06	5760	31.91	4.97	3.29	1.51	0.134	0.009018	0.23	0.56	4.31	507	11.69
850	1.01	15.25	8.89E+05	4280	35.38	7.18	4.79	1.50	0.061	0.007319	0.47	0.74	3.31	178	9.14
850	1.25	14.76	1.09E+06	5150	36.63	7.06	4.71	1.50	0.075	0.007184	0.45	0.73	3.14	206	9.49
850	1.75	15.15	1.54E+06	7340	35.56	7.15	4.76	1.50	0.105	0.007187	0.48	0.64	3.26	301	10.42
850	2.00	15.08	1.76E+06	8460	36.86	7.20	4.80	1.50	0.121	0.007296	0.46	0.82	3.47	369	10.91

Table A.18 Boundary layer characteristics for RP2 F5 (LDV set up in two-dimensions)

x [mm]	U [m/s]	T [deg C]	Re_l	Re_θ	δ [mm]	δ^* [mm]	θ [mm]	H	u^* [m/s]	c_f	Π	ε [mm]	k_s [mm]	Re_k	Δu^+
843	1.03	14.64	8.92E+05	3690	32.37	5.93	4.12	1.44	0.058	0.006385	0.46	0.72	1.84	93	7.55
843	1.25	14.61	1.08E+06	4500	31.87	5.99	4.14	1.45	0.075	0.007131	0.46	1.04	2.66	172	9.06
843	1.75	15.17	1.54E+06	6420	32.35	6.07	4.16	1.46	0.110	0.007898	0.43	1.37	3.61	350	10.79
843	2.02	15.04	1.77E+06	7370	32.17	6.01	4.15	1.45	0.120	0.007029	0.46	1.15	2.59	273	10.18

Table A.19 Boundary layer characteristics for SP1 F6 using Bradshaw's Method (LDV set up in two-dimensions)

x [mm]	U [m/s]	T [deg C]	Re_l	Re_θ	δ [mm]	δ^* [mm]	θ [mm]	H	u^* [m/s]	c_f	Π	ε [mm]	k_s [mm]	Re_k	Δu^+
843	1.04	14.75	9.05E+05	2900	30.36	4.11	3.19	1.29	0.043	0.003485	0.35	0.39	-	<5	0.00
843	1.26	15.00	1.11E+06	3500	30.91	4.01	3.15	1.27	0.052	0.003323	0.37	0.50	-	<5	0.00
843	1.74	14.92	1.52E+06	4710	31.04	3.92	3.09	1.27	0.068	0.003087	0.42	0.50	-	<5	0.00
843	1.99	15.00	1.74E+06	5470	31.02	4.02	3.13	1.29	0.077	0.003000	0.43	0.23	-	<5	0.00

Table A.20 Boundary layer characteristics for SP1 F6 using Perry and Li's Method (LDV set up in two-dimensions)

x [mm]	U [m/s]	T [deg C]	Re_l	Re_θ	δ [mm]	δ^* [mm]	θ [mm]	H	u^* [m/s]	c_f	Π	ε [mm]	k_s [mm]	Re_k	Δu^+
843	1.04	14.75	9.05E+05	2900	30.36	4.11	3.19	1.29	0.039	0.002795	0.48	0.14	-	<5	0.00
843	1.26	15.00	1.11E+06	3500	30.91	4.01	3.15	1.27	0.048	0.002854	0.46	0.35	-	<5	0.00
843	1.74	14.92	1.52E+06	4710	31.04	3.92	3.09	1.27	0.066	0.002893	0.44	0.42	-	<5	0.00
843	1.99	15.00	1.74E+06	5470	31.02	4.02	3.13	1.29	0.074	0.002790	0.46	0.14	-	<5	0.00

A3 Boundary Layer Profiles in Inner Coordinates

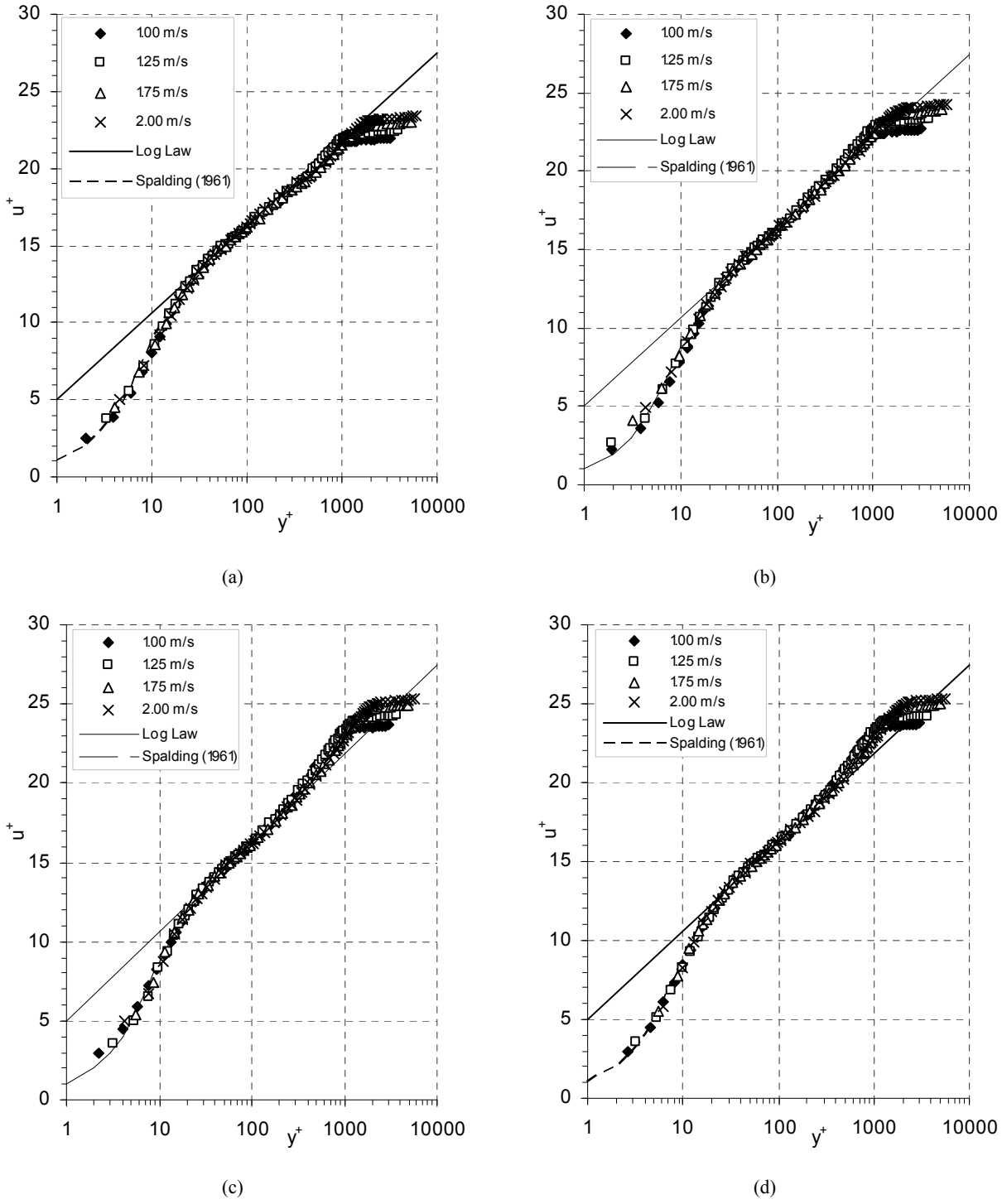

Figure A.9 SP Lab one-dimensional boundary layer profiles, normalised by u, at: (a) x = 100 mm; (b) x = 250 mm; (c) x = 750 mm; (d) x = 850 mm*

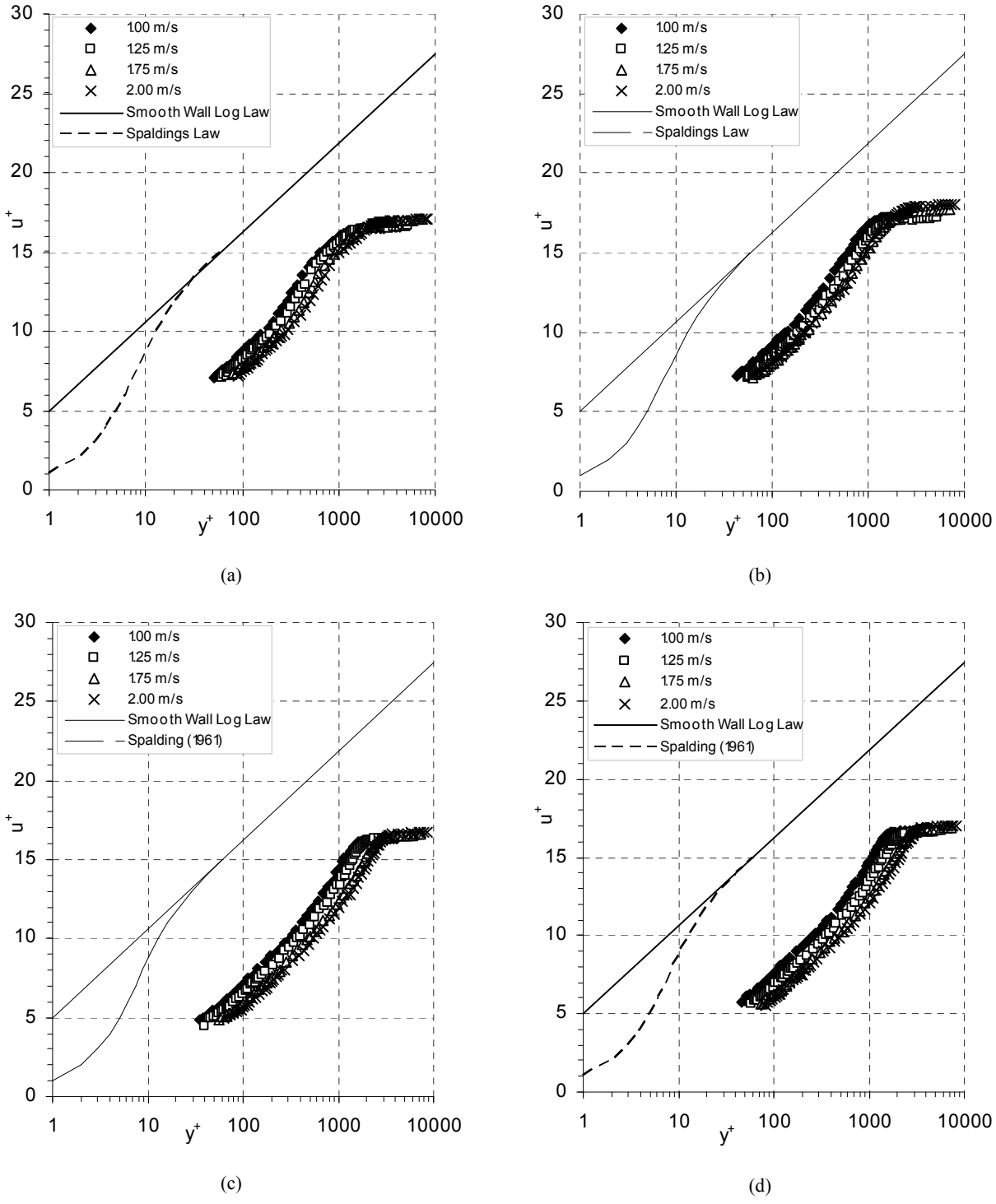

Figure A.10 RP Lab one-dimensional boundary layer profiles, normalised by u, at: (a) x = 100 mm; (b) x = 250 mm; (c) x = 750 mm; (d) x = 850 mm*

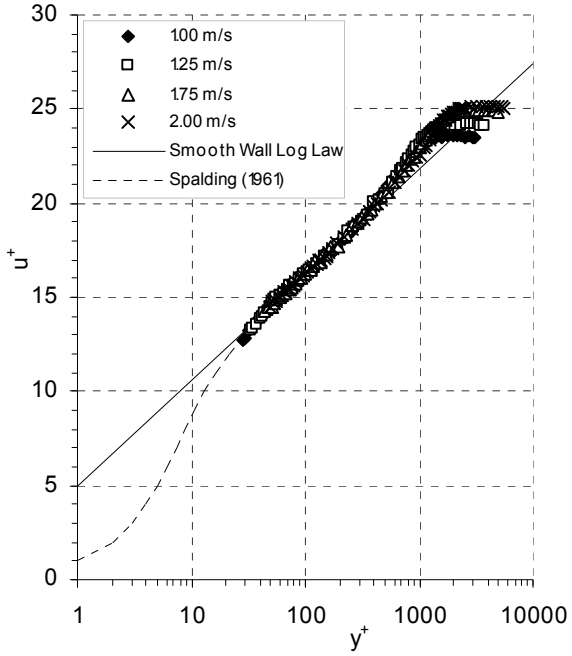

Figure A.11 SP Lab two-dimensional boundary layer profile, normalised by u, at x = 850 mm*

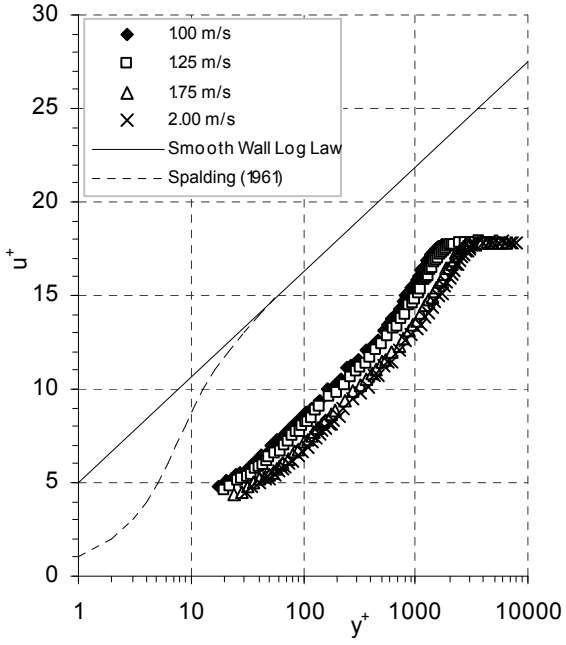

Figure A.12 RP Lab two-dimensional boundary layer profiles, normalised by u, at x = 850 mm*

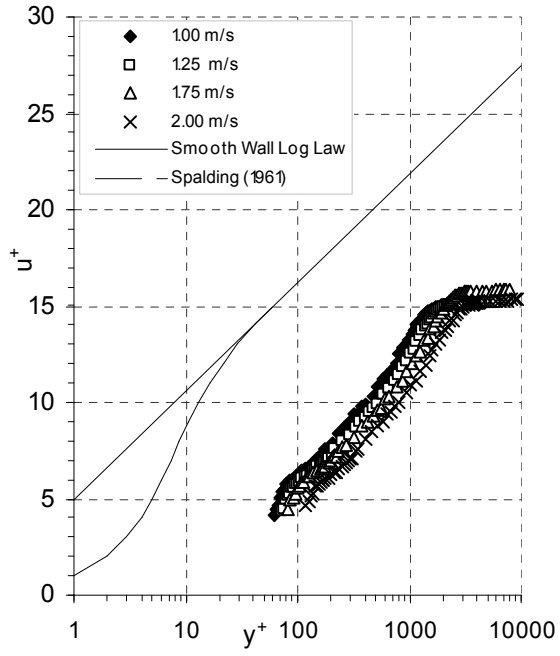

(a)

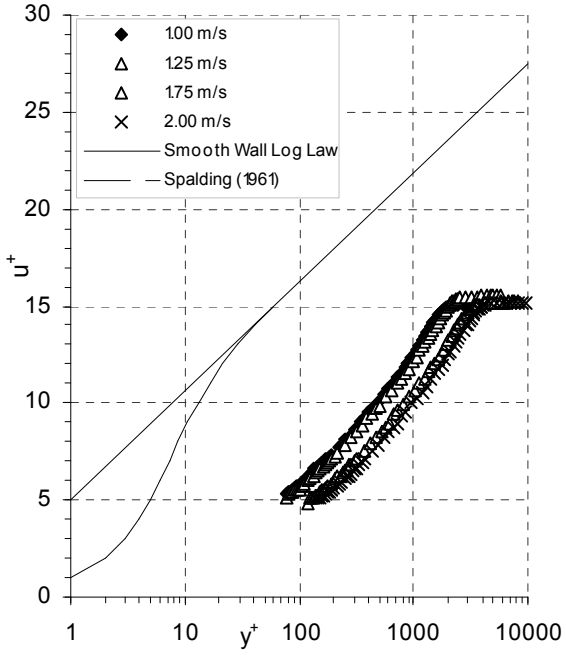

(b)

Figure A.13 One-dimensional RP1 F1 boundary layer profiles, normalised by u, at: (a) x = 500 mm; (b) x = 850 mm*

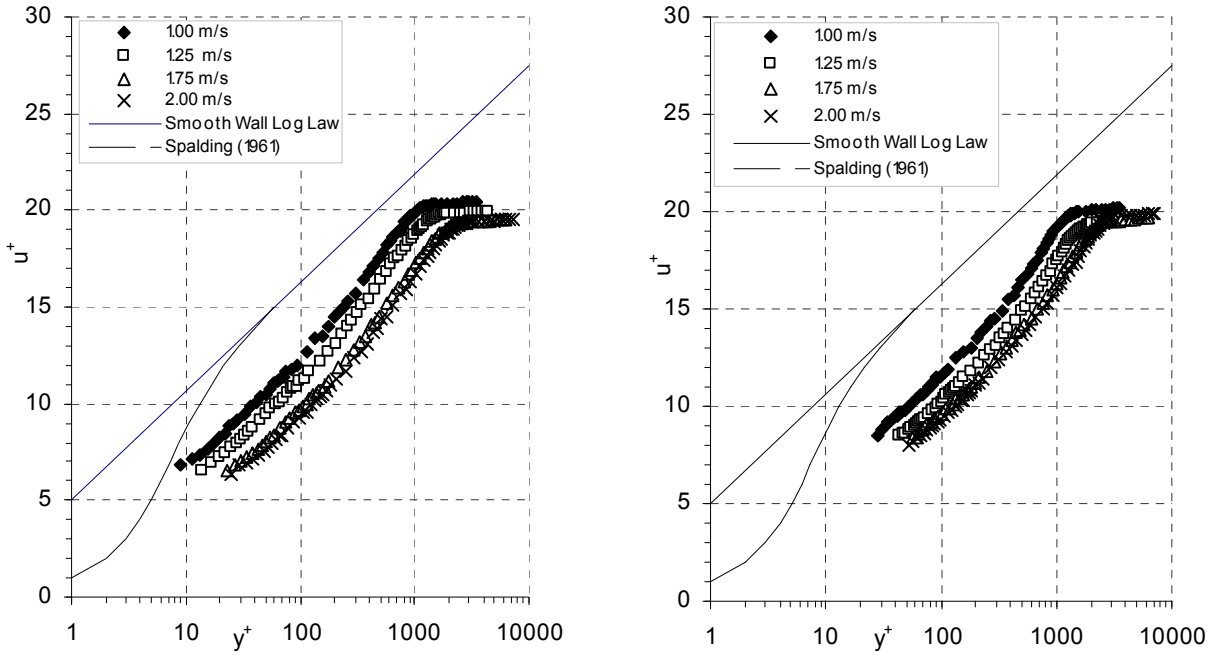

(a) (b)

Figure A.14 SP1 F2 one-dimensional boundary layer profiles, normalised by u, at: (a) x = 500 mm; (b) x = 850 mm*

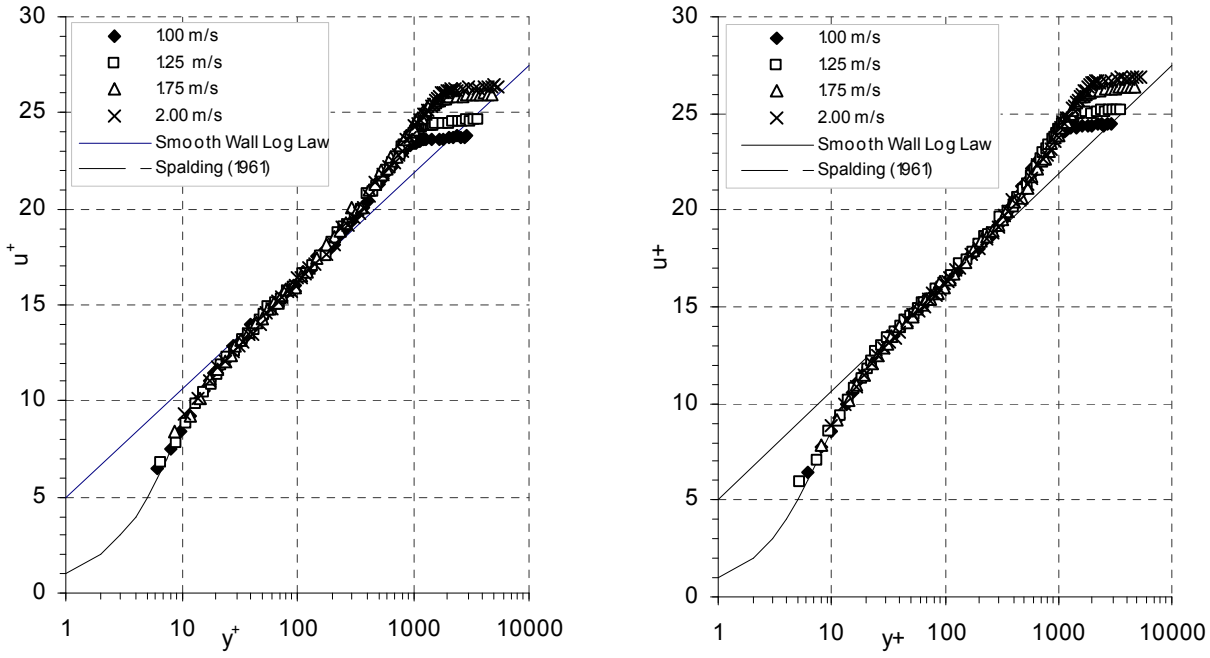

(a) (b)

Figure A.15 SP2 F3 one-dimensional boundary layer profiles using Bradshaw's Method, normalised by u, at: (a) x = 500 mm; (b) x = 850 mm*

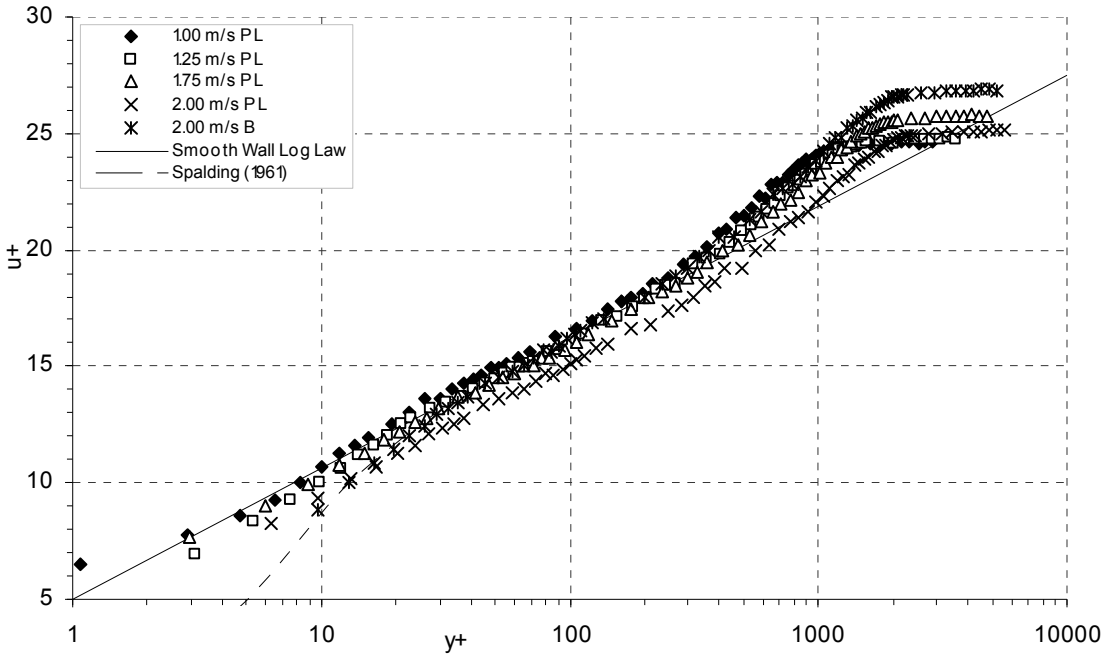

Figure A.16 SP2 F3 boundary layer profiles at x = 850 mm analysed using Perry and Li's Method (PL), compared with Bradshaw's Method (B) at U = 2.00 m/s

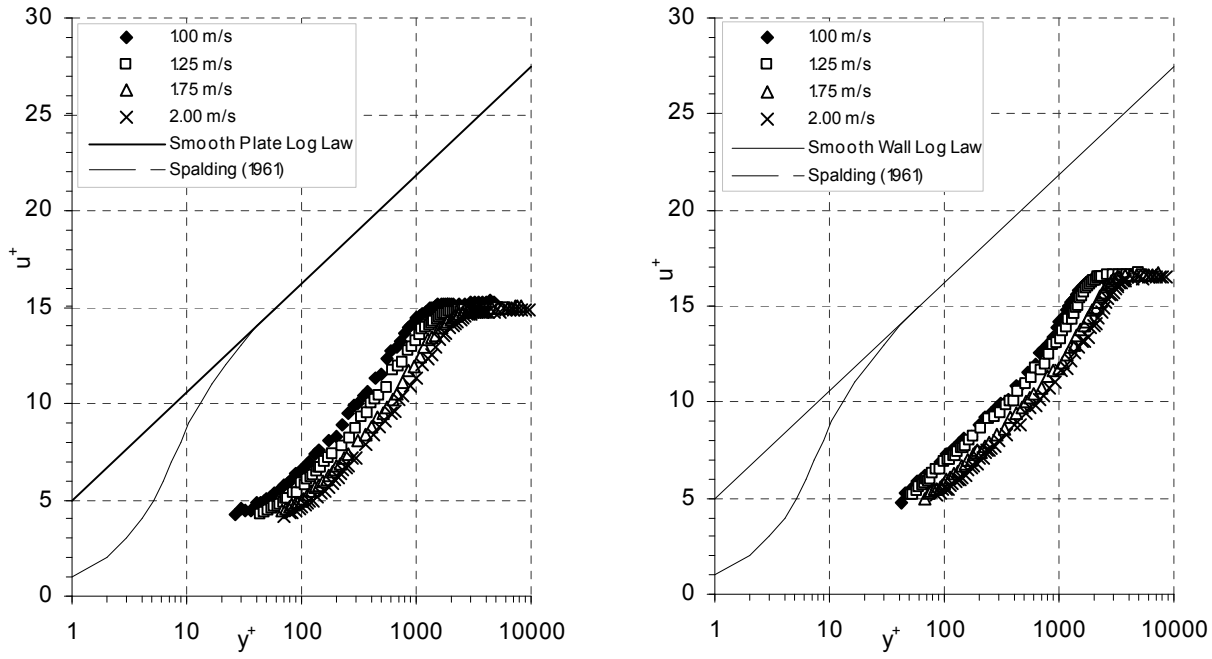

(a) (b)

Figure A.17 RP1 F4 boundary layer profiles, normalised by u, at: (a) x = 250 mm; (b) x = 850 mm*

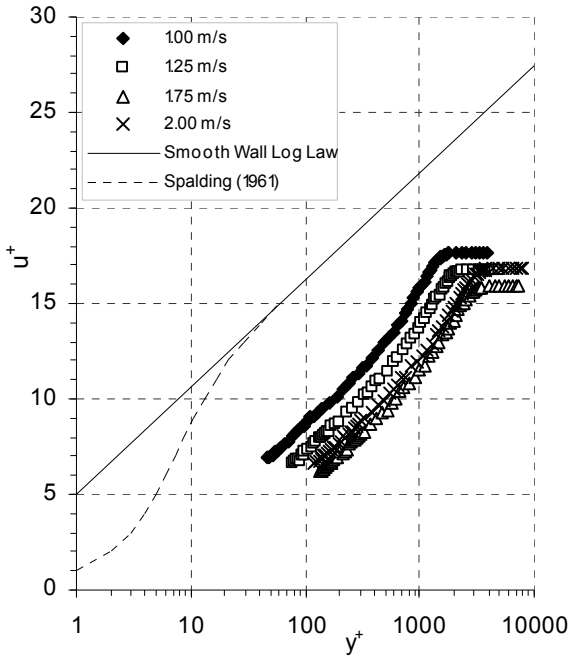

Figure A.18 RP2 F5 boundary layer profiles, normalised by u, at x = 850 mm*

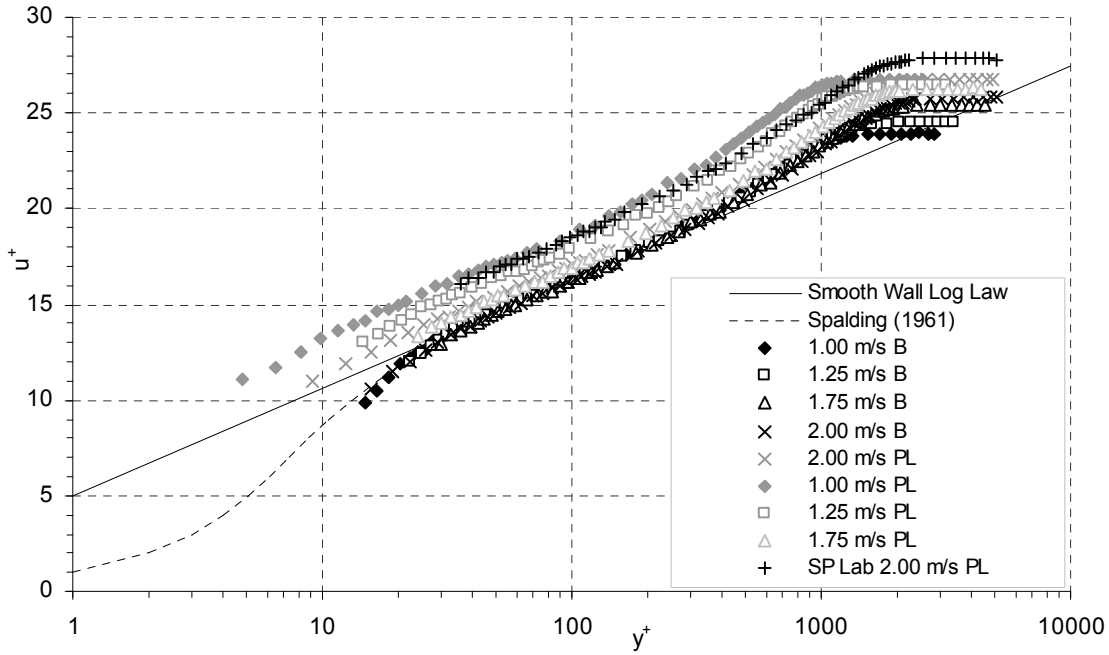

Figure A.19 SP1 F6 boundary layer profiles, normalised by u, from both Bradshaw's (B) and Perry and Li's (PL) Methods at x = 850 mm*

A4 Boundary Layer Profiles in Outer Coordinates

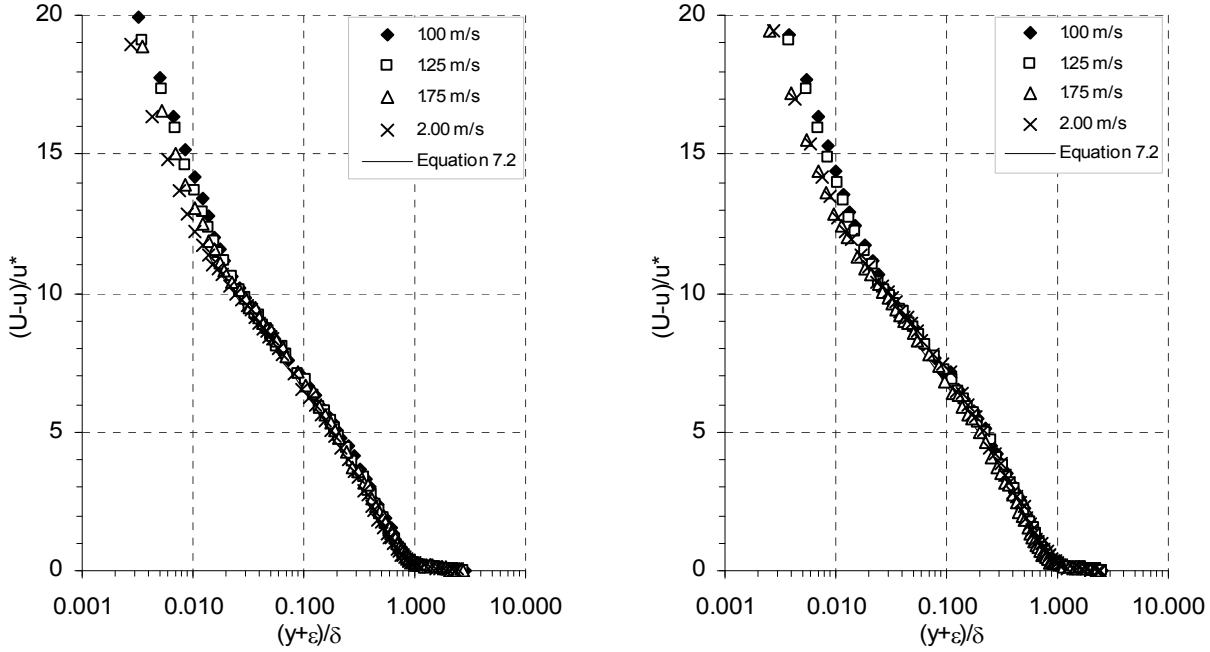

(a) (b)

Figure A.20 SP Lab velocity defect profiles at: (a) x = 500 mm; (b) x =850 mm

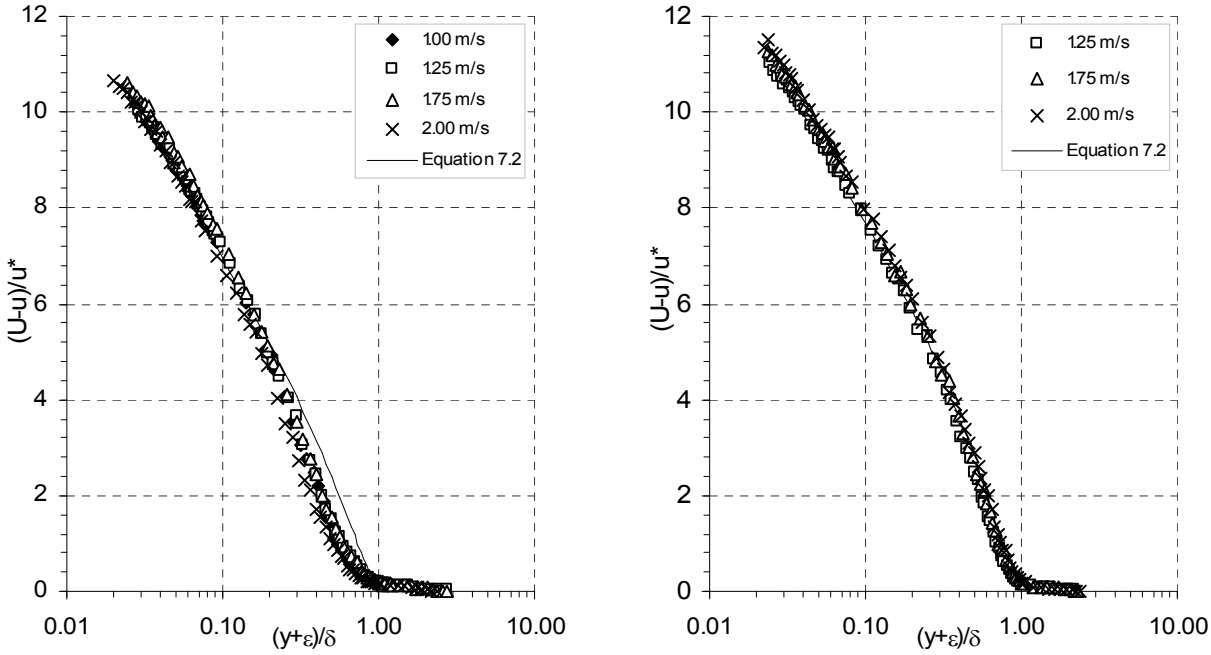

(a) (b)

Figure A.21 RP Lab velocity defect profiles at: (a) x = 250 mm; (b) x = 850 mm

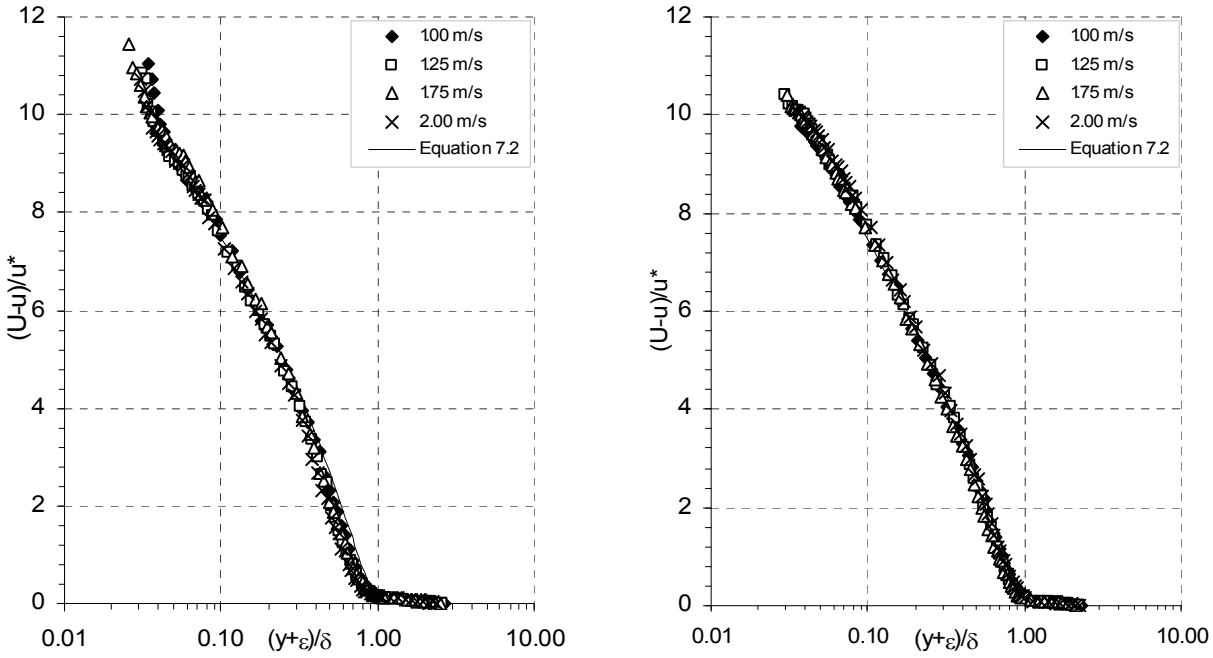

(a) (b)

Figure A.22 RP1 F1 velocity defect profiles at: (a) x = 500 mm; (b) x = 850 mm

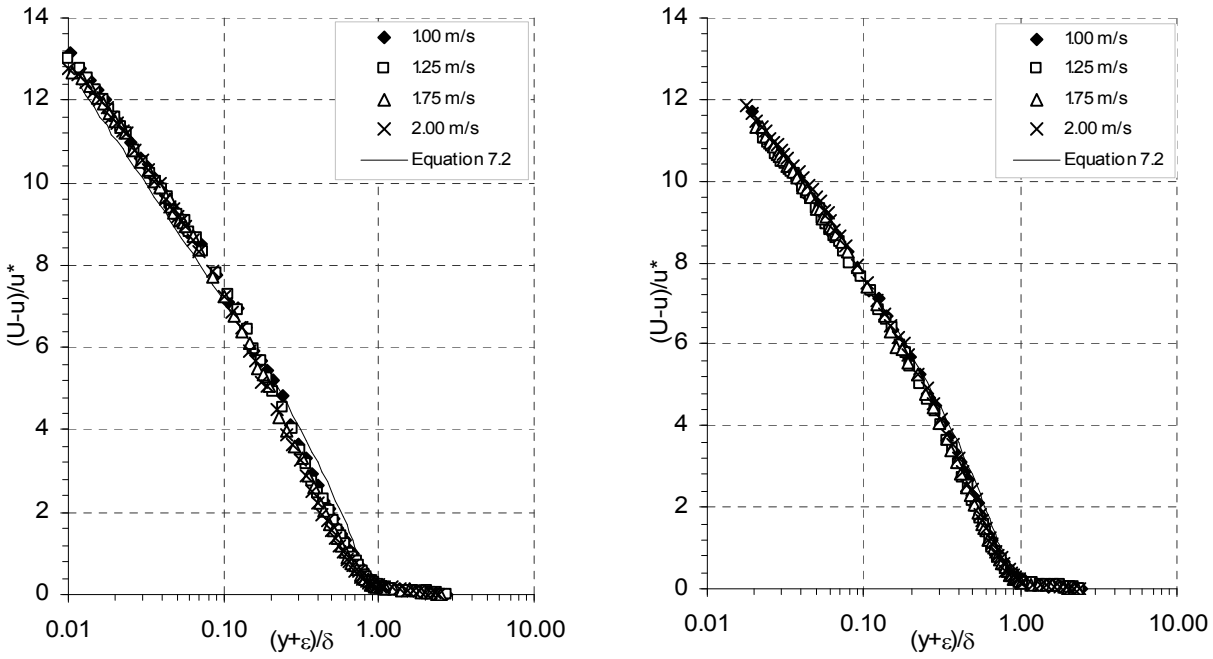

(a) (b)

Figure A.23 SP1 F2 velocity defect profiles at: (a) x = 500 mm; (b) x = 850 mm

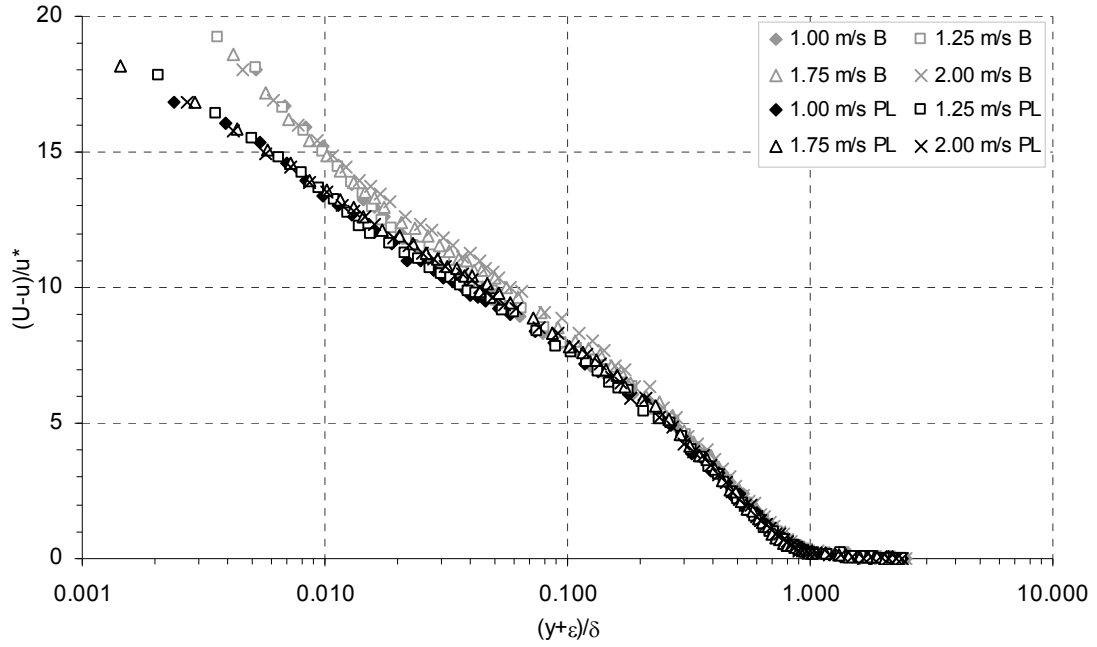

Figure A.24 SP2 F3 velocity defect profiles at x = 850 mm using different analysis methods: Bradshaw's Method (B); Perry and Li's Method (PL)

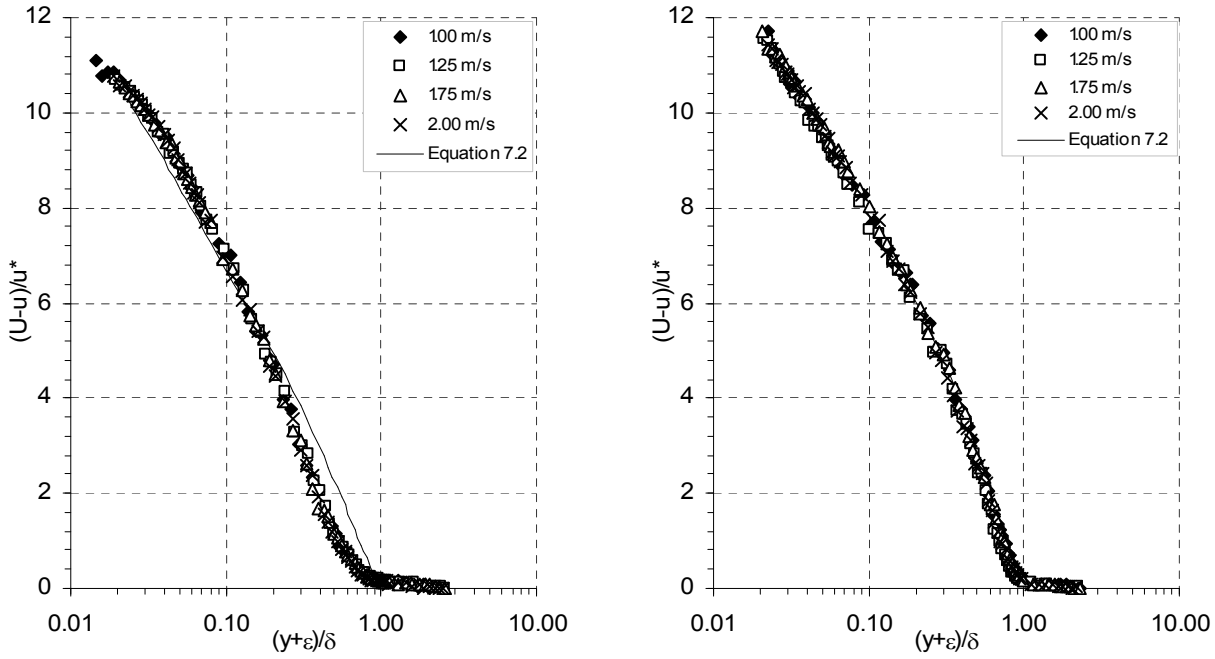

(a) (b)

Figure A.25 RP1 F4 velocity defect profiles at: (a) x = 250 mm; (b) x = 850 mm

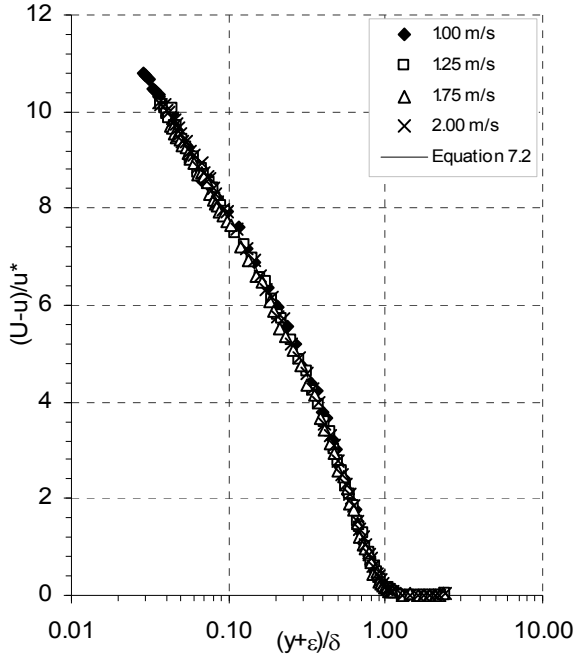

Figure A.26 RP2 F5 velocity defect profiles at x = 850 mm

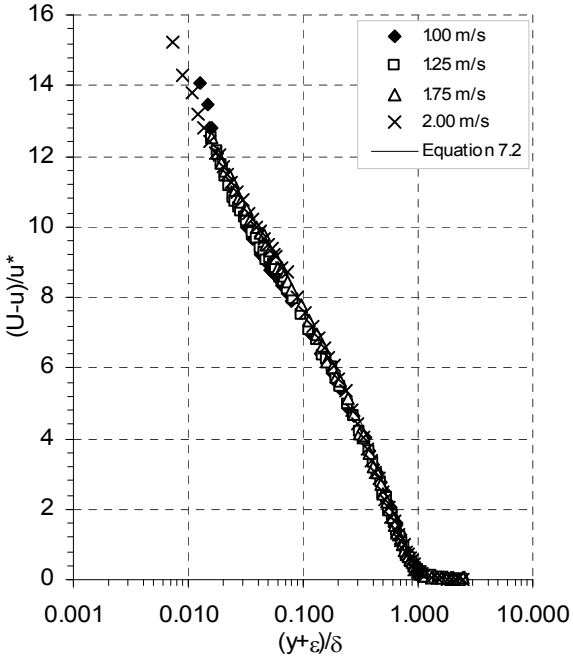

Figure A.27 SP1 F6 velocity defect profiles at x = 850 mm

A5 Roughness Plots

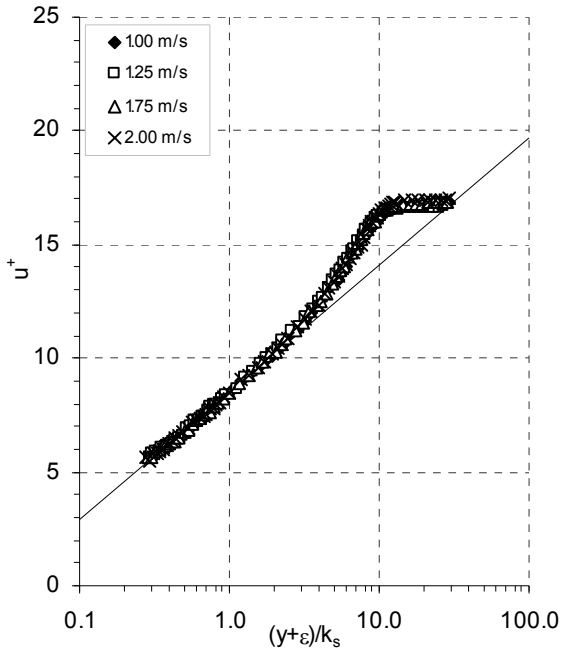

Figure A.28 RP Lab boundary layer profiles scaled using k_s at x = 850 mm

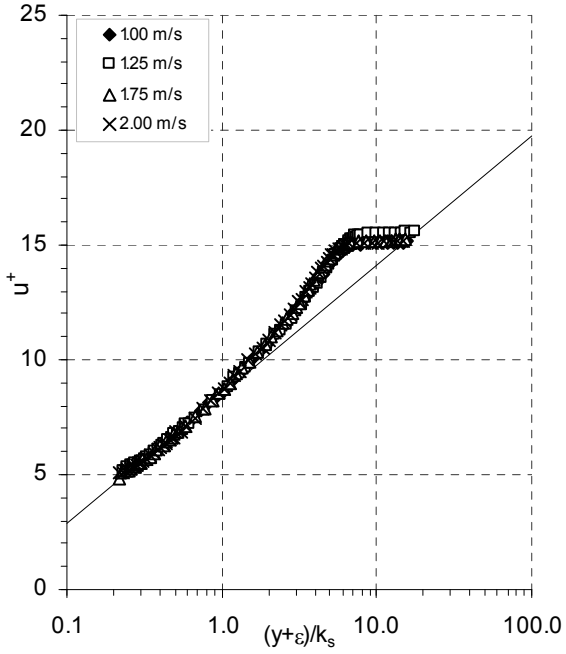

Figure A.29 RP1 F1 boundary layer profiles scaled using k_s at x = 850 mm

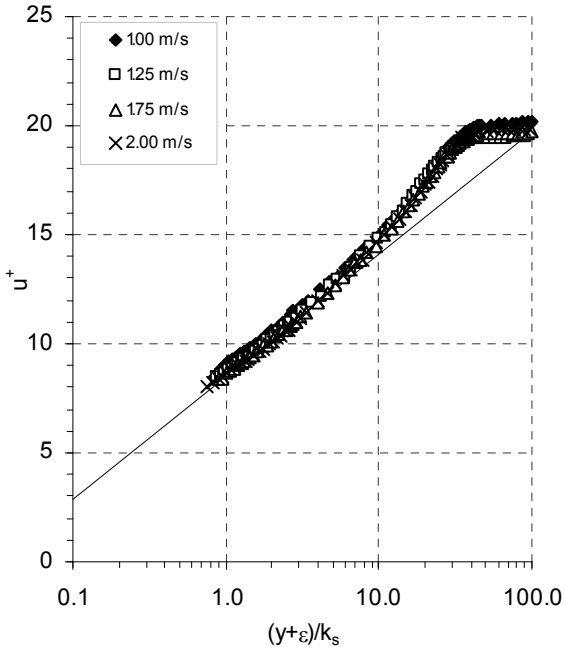

Figure A.30 SP1 F2 boundary layer profiles scaled using k_s at x = 850 mm

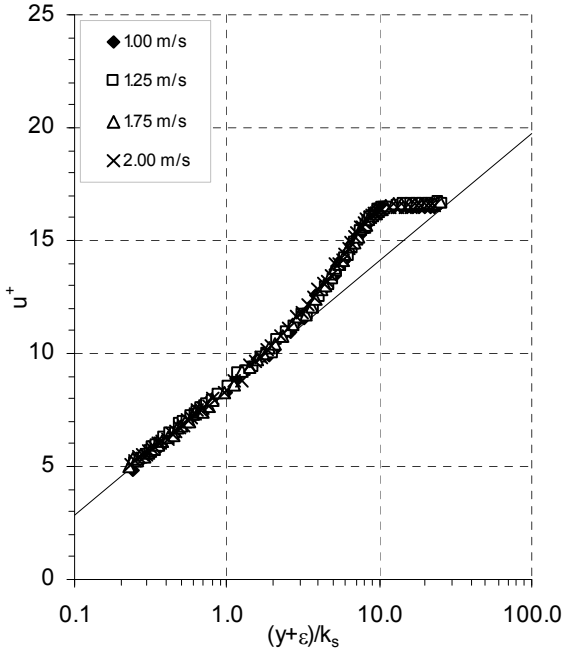

Figure A.31 RP1 F4 boundary layer profiles scaled using k_s at x = 850 mm

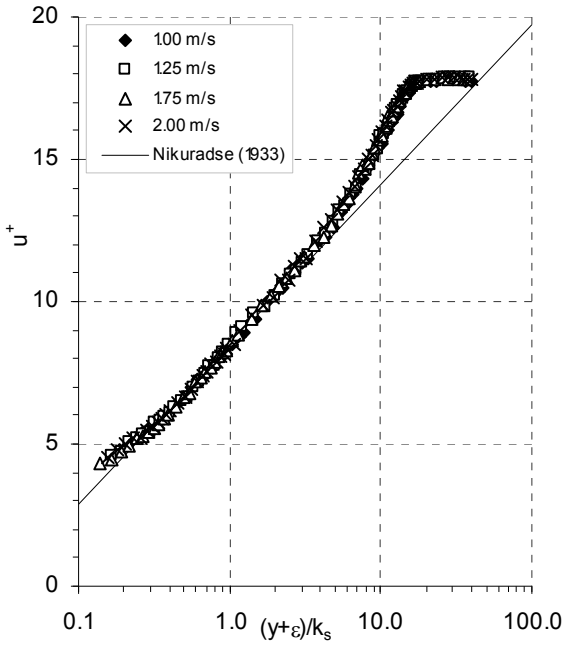

Figure A.32 RP Lab boundary layer profiles scaled using k_s at x = 850 mm

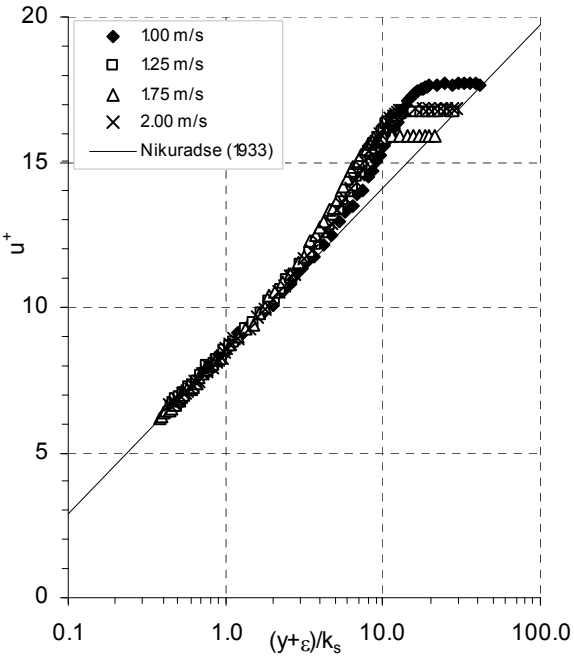

Figure A.33 RP2 F5 boundary layer profiles scaled using k_s at x = 850 mm

A6 Turbulence Intensity

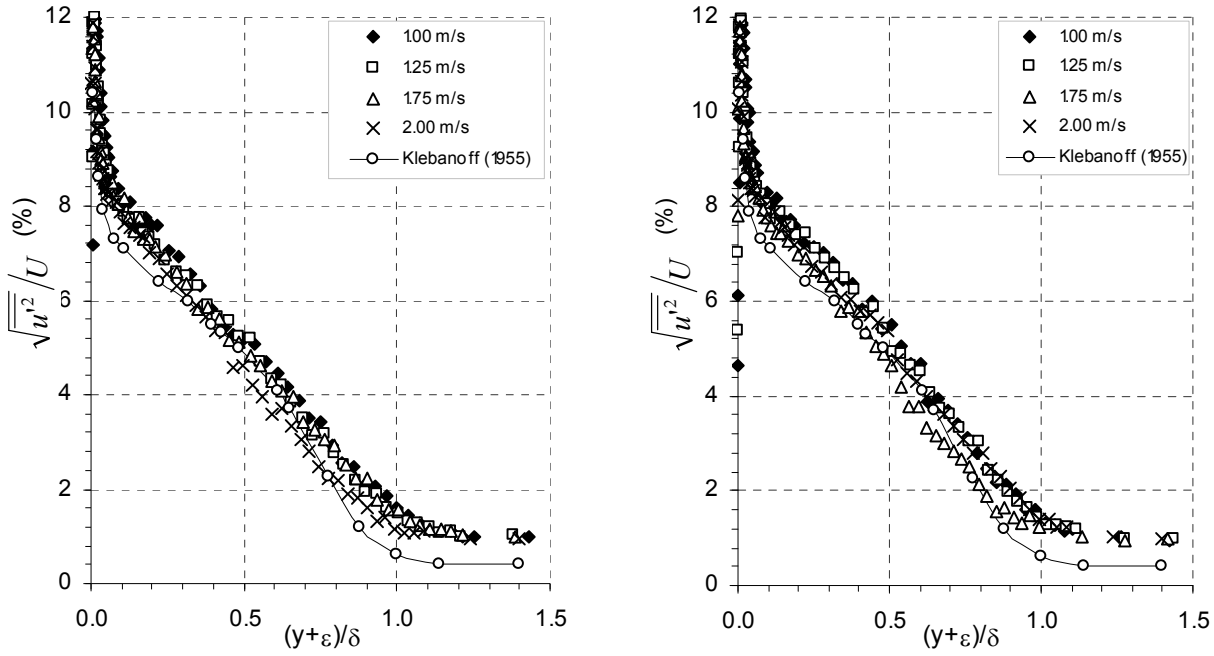

Figure A.34 SP Lab one-dimensional turbulence intensity profiles at: (a) x = 500 mm; (b) x = 850 mm

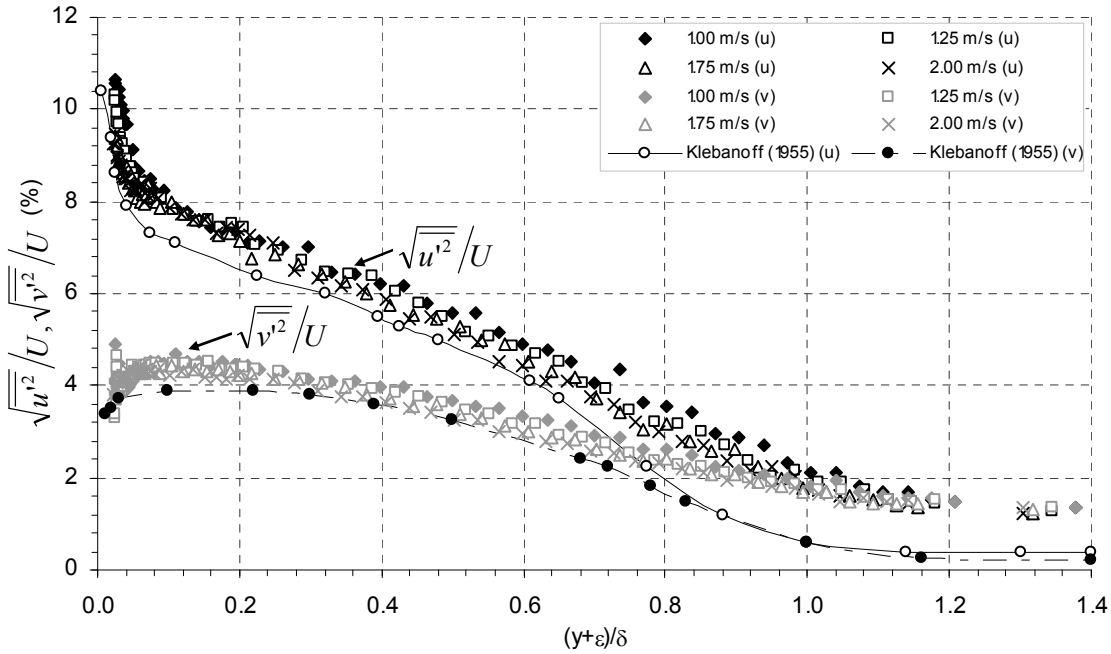

Figure A.35 SP Lab two-dimensional turbulence intensity profiles at x = 850 mm scaled using U

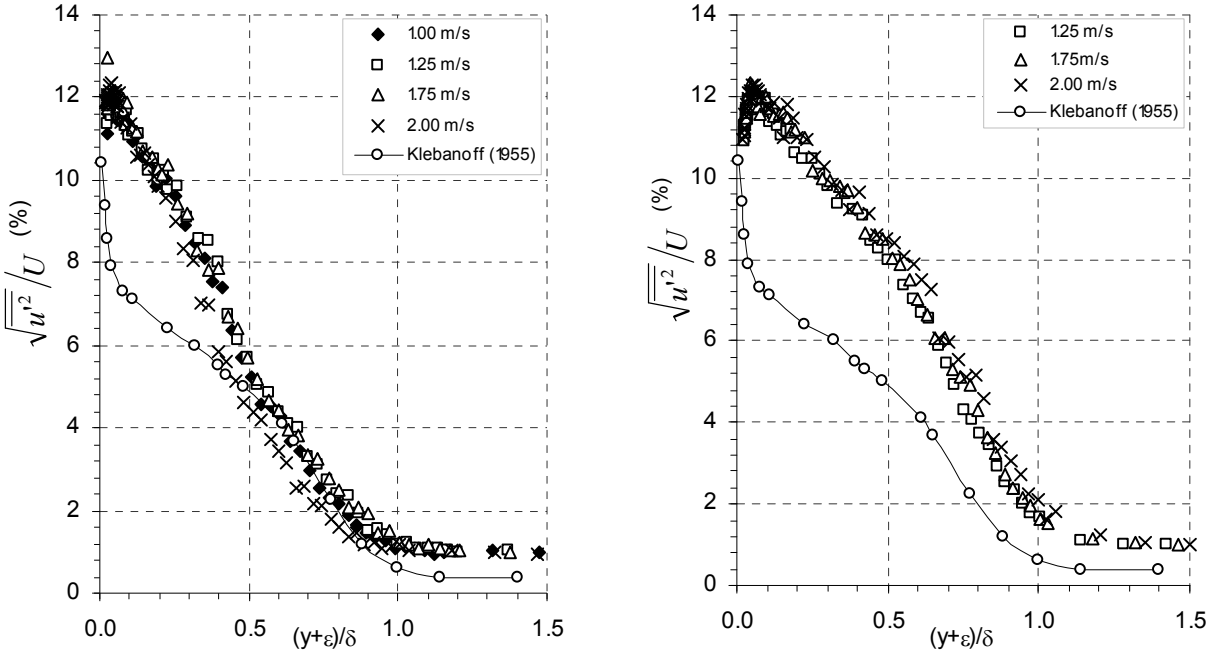

Figure A.36 RP Lab one-dimensional turbulence intensity profiles at: (a) x = 250 mm; (b) x = 850 mm

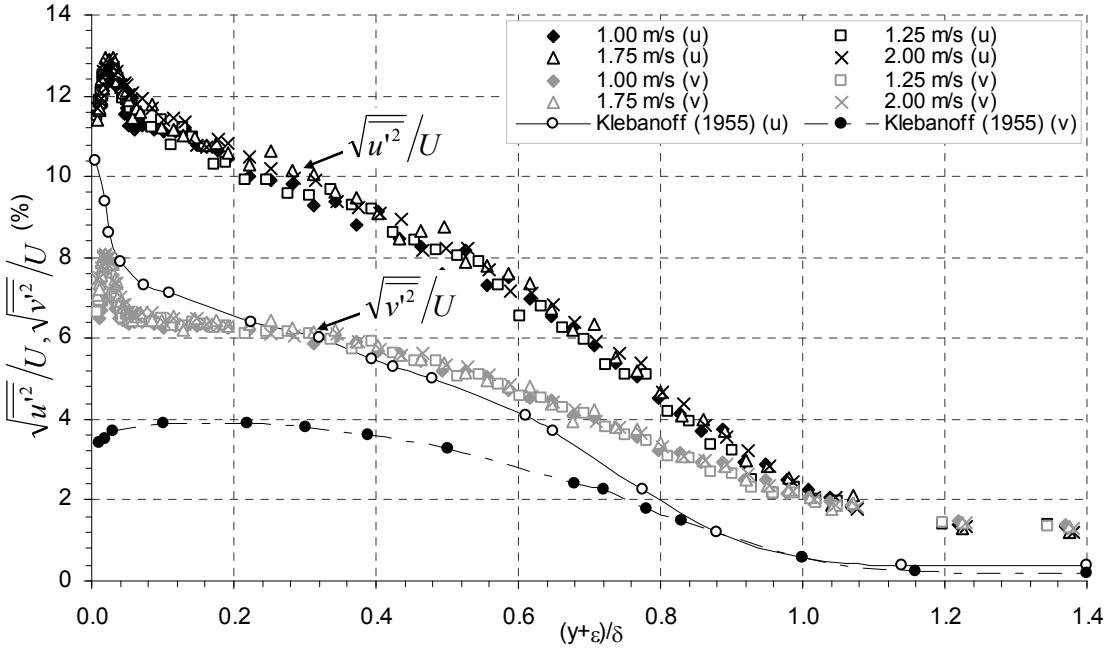

Figure A.37 RP Lab two-dimensional turbulence intensity profiles at x = 850 mm, scaled using U

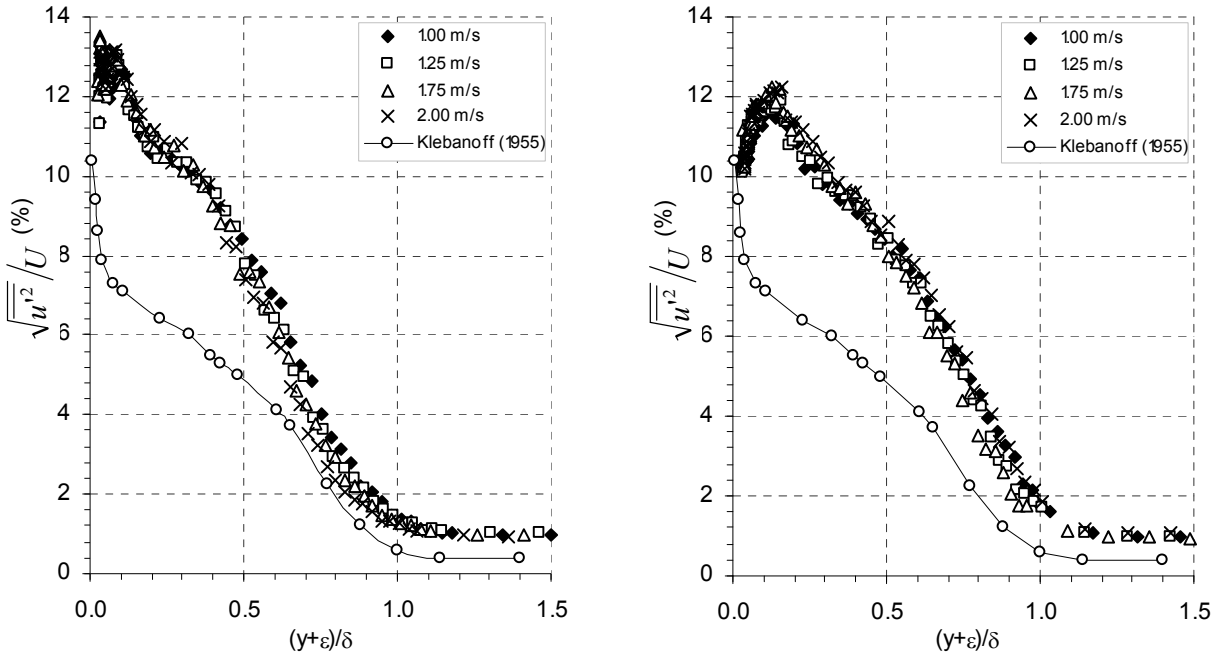

Figure A.38 RP1 F1 turbulence intensity profiles at: (a) x = 500 mm; (b) x = 850 mm

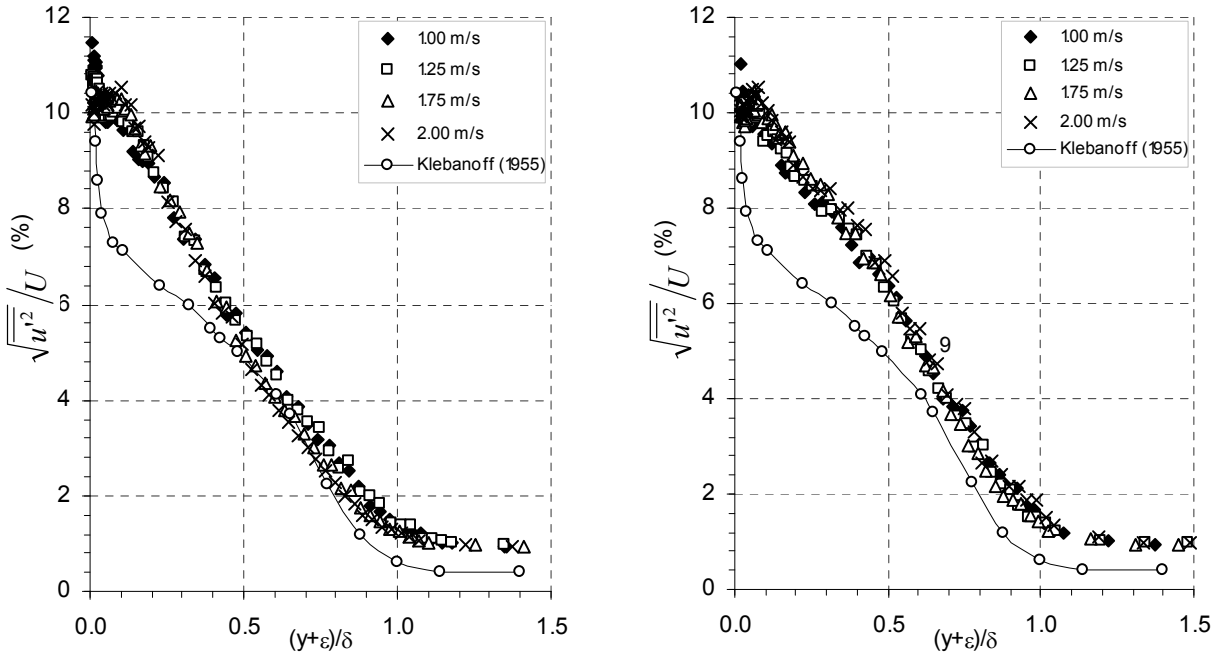

Figure A.39 SP1 F2 turbulence intensity profiles at: (a) x = 500 mm; (b) x = 850 mm

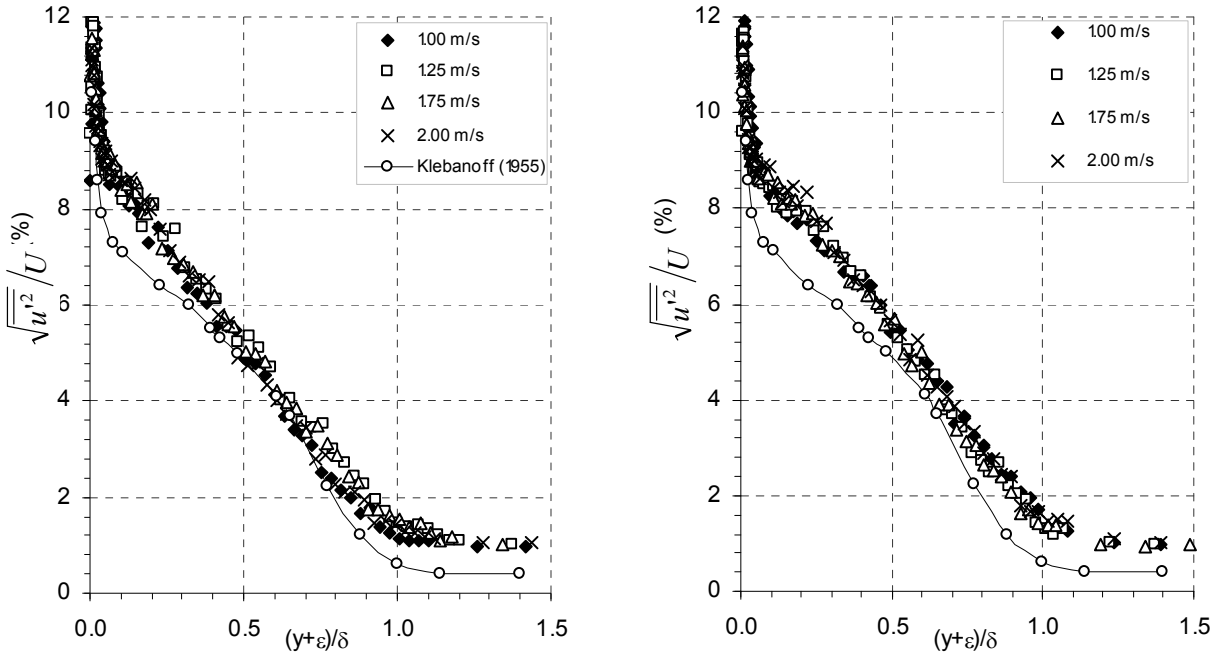

(a) (b)

Figure A.40 SP2 F3 turbulence intensity profiles, scaled using Bradshaw's Method, at: (a) x = 500 mm; (b) x = 850 mm

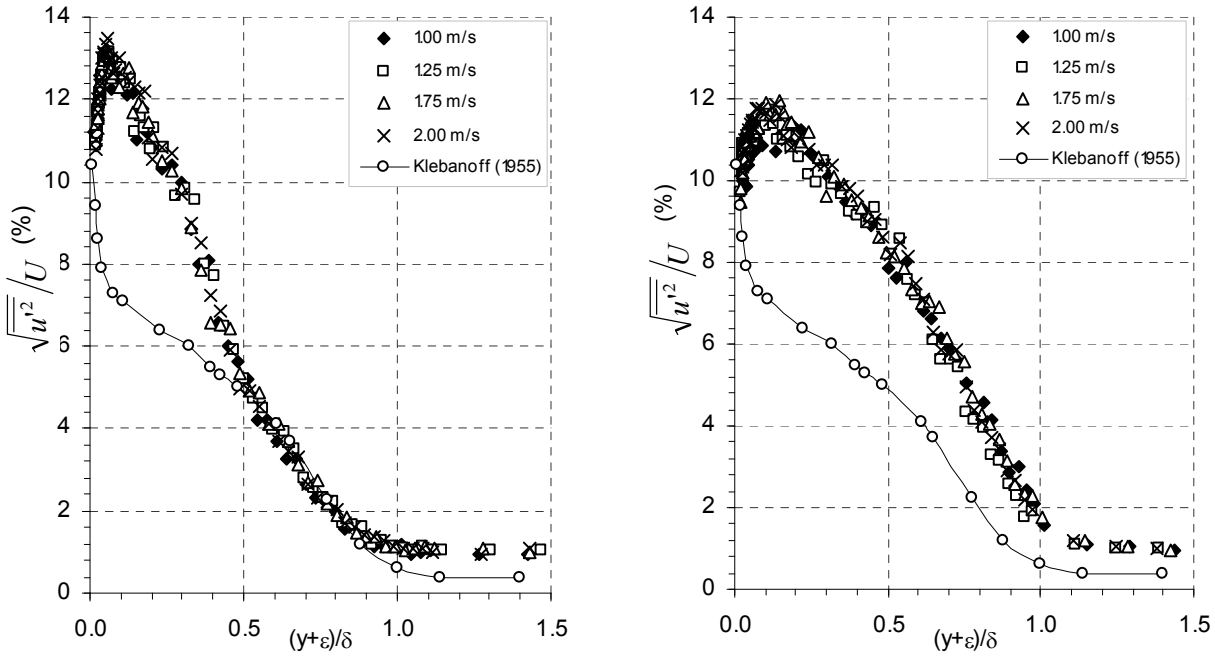

(a) (b)

Figure A.41 RP1 F4 turbulence intensity profiles at: (a) x = 250 mm; (b) x = 850 mm

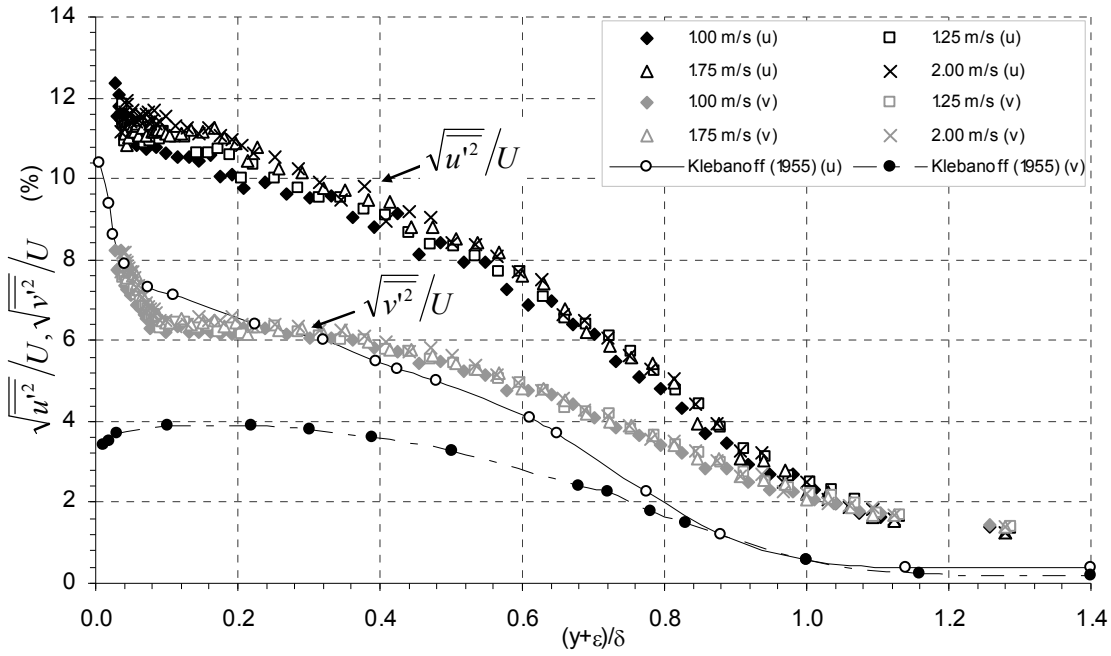

Figure A.42 RP2 F5 two-dimensional turbulence intensity profiles at x = 850 mm scaled using U

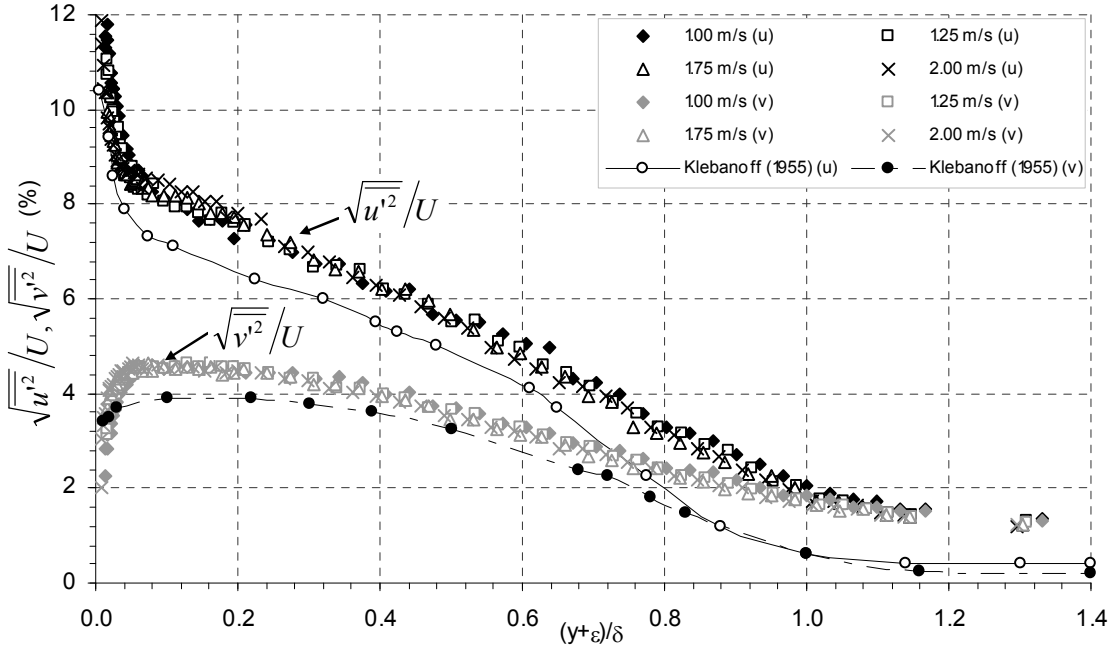

Figure A.43 SP1 F6 two-dimensional turbulence intensity profiles at x = 850 mm scaled using U

A7 Reynolds Normal Stresses

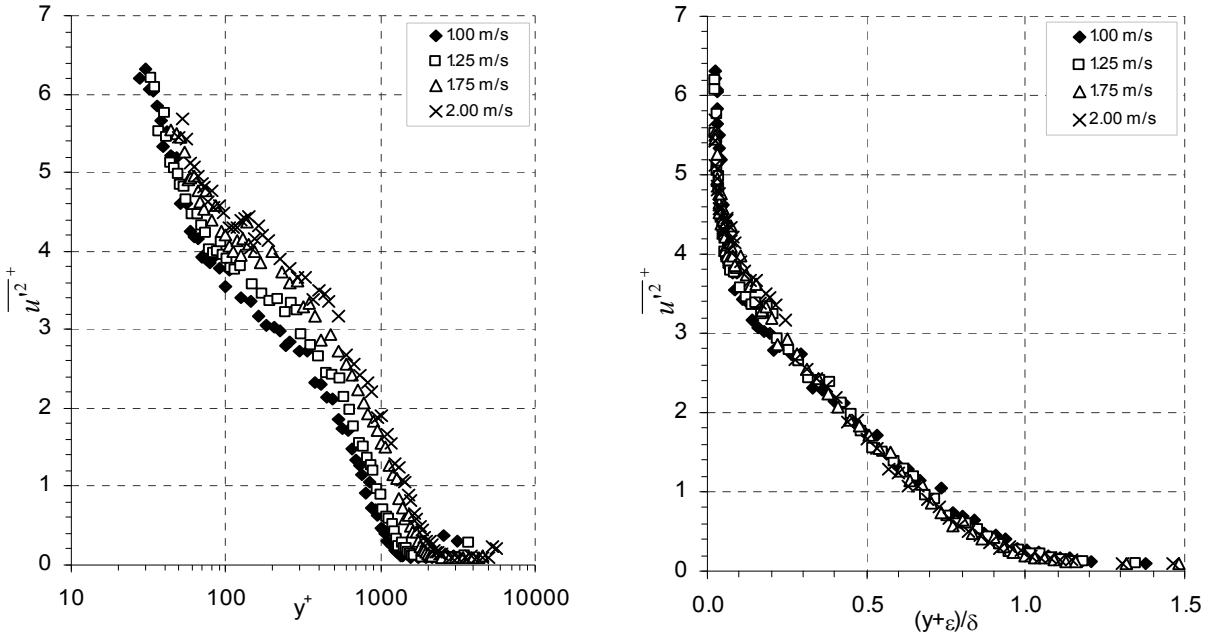

Figure A.44 SP Lab normalised streamwise Reynolds normal stress at x = 850 mm: (a) in inner variables; (b) in outer variables

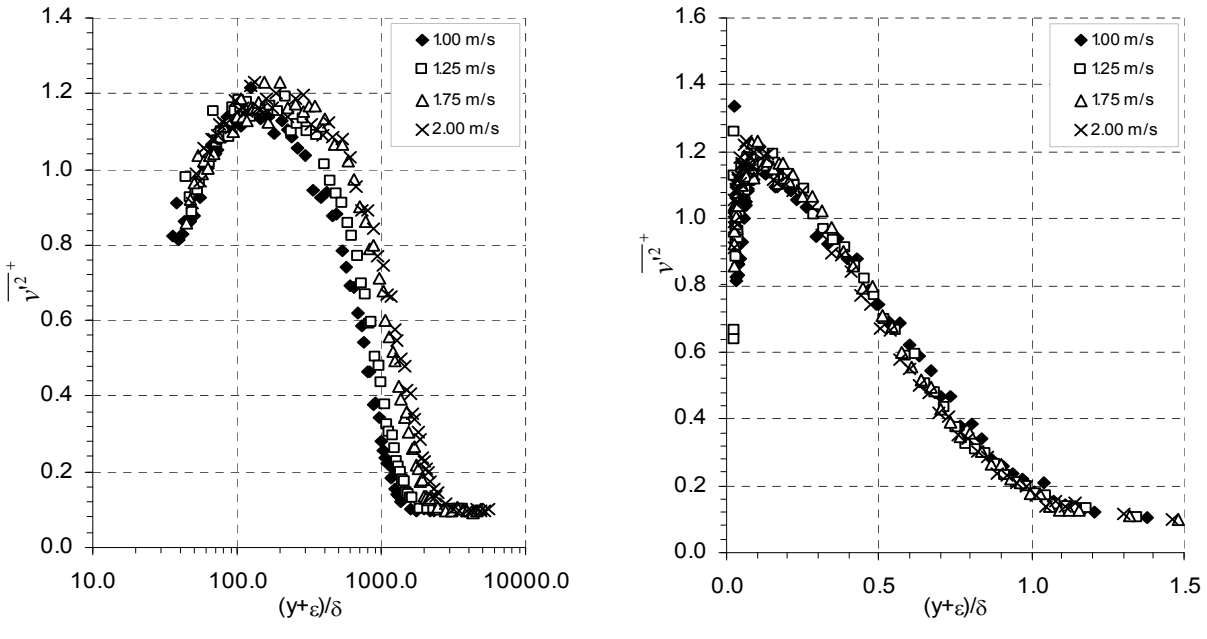

Figure A.45 SP Lab normalised wall-normal Reynolds normal stress at x = 850 mm: (a) in inner variables; (b) in outer variables

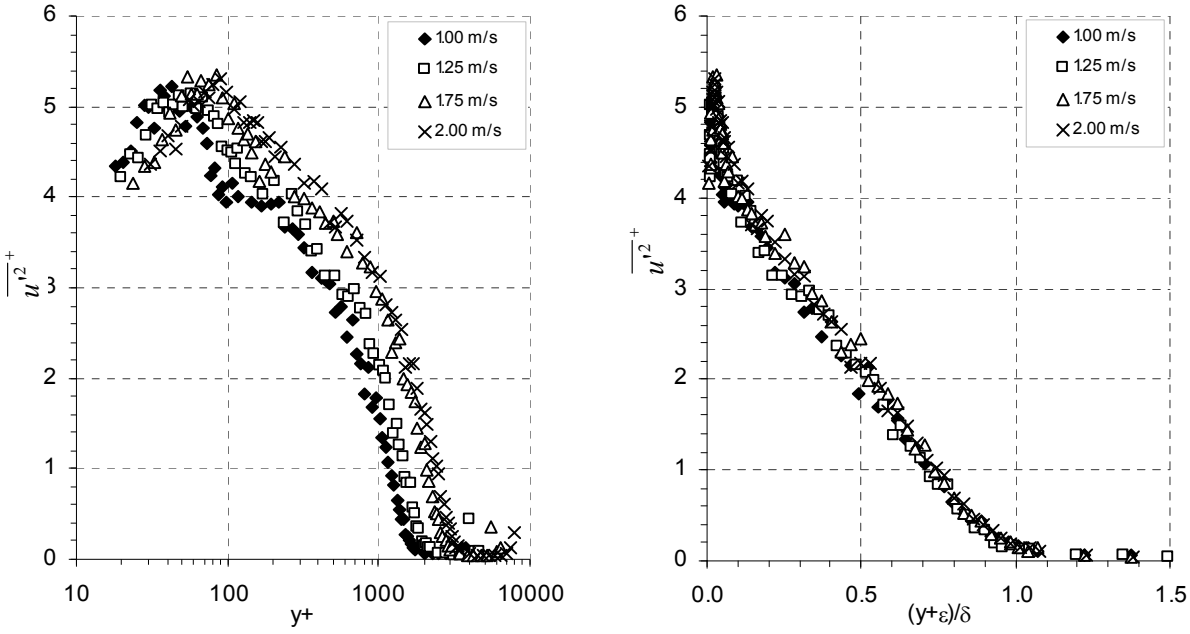

(a) (b)

Figure A.46 RP Lab normalised streamwise Reynolds normal stress at x = 850 mm: (a) in inner variables; (b) in outer variables

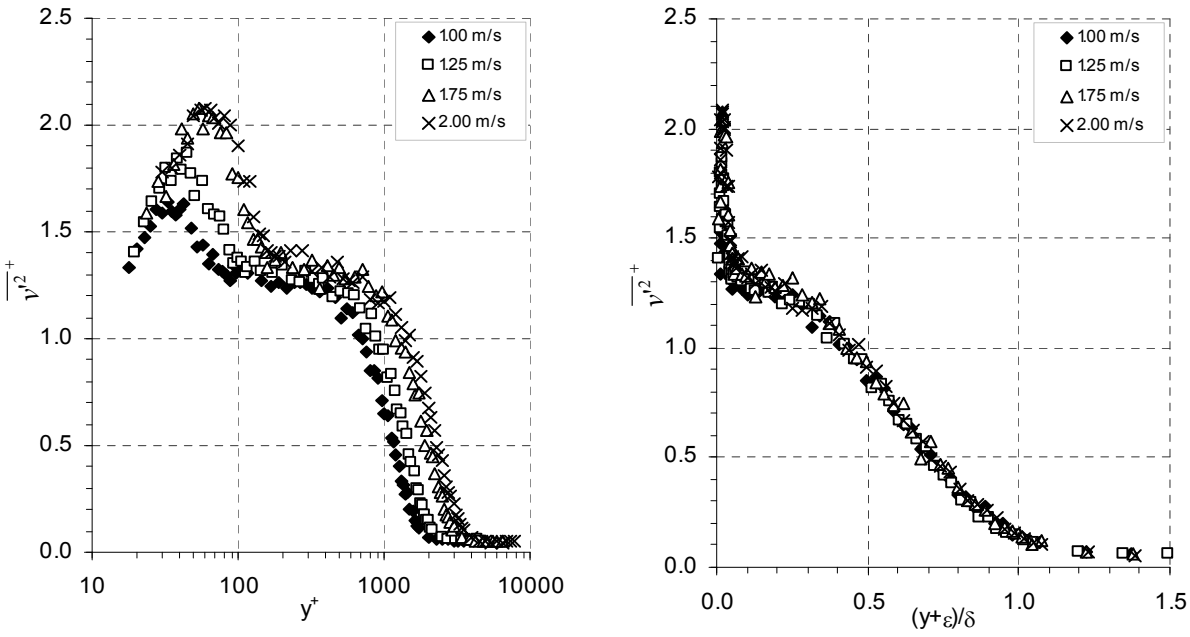

(a) (b)

Figure A.47 RP Lab normalised wall-normal Reynolds normal stress at x = 850 mm: (a) in inner variables; (b) in outer variables

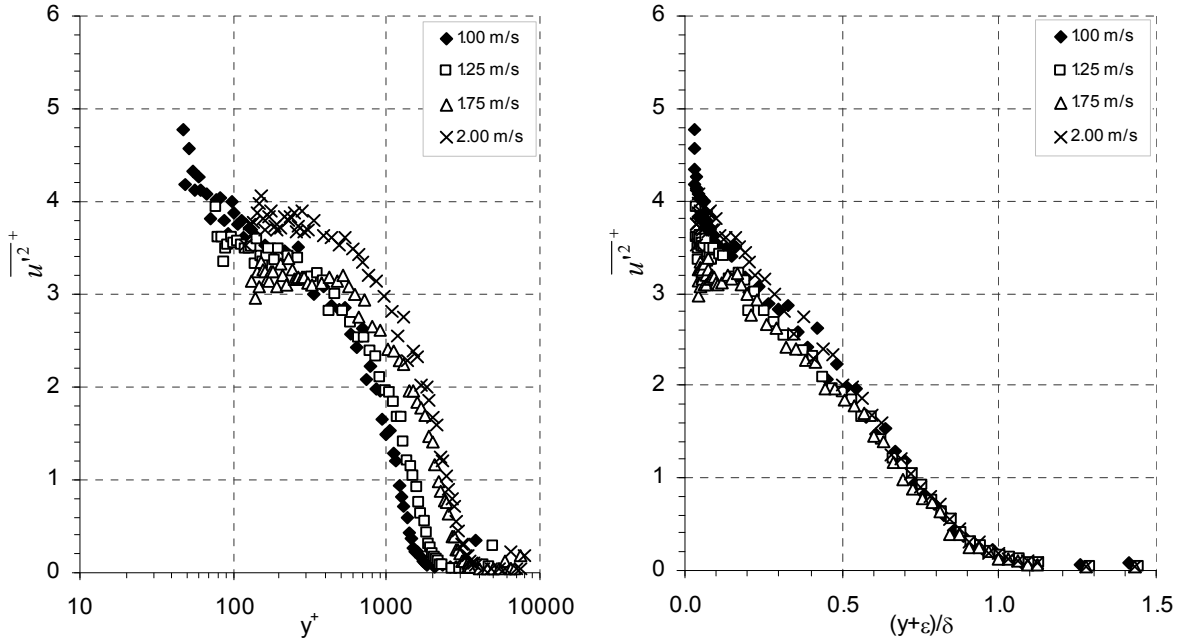

(a) (b)

Figure A.48 RP2 F5 normalised streamwise Reynolds normal stress at x = 850 mm: (a) in inner variables; (b) in outer variables

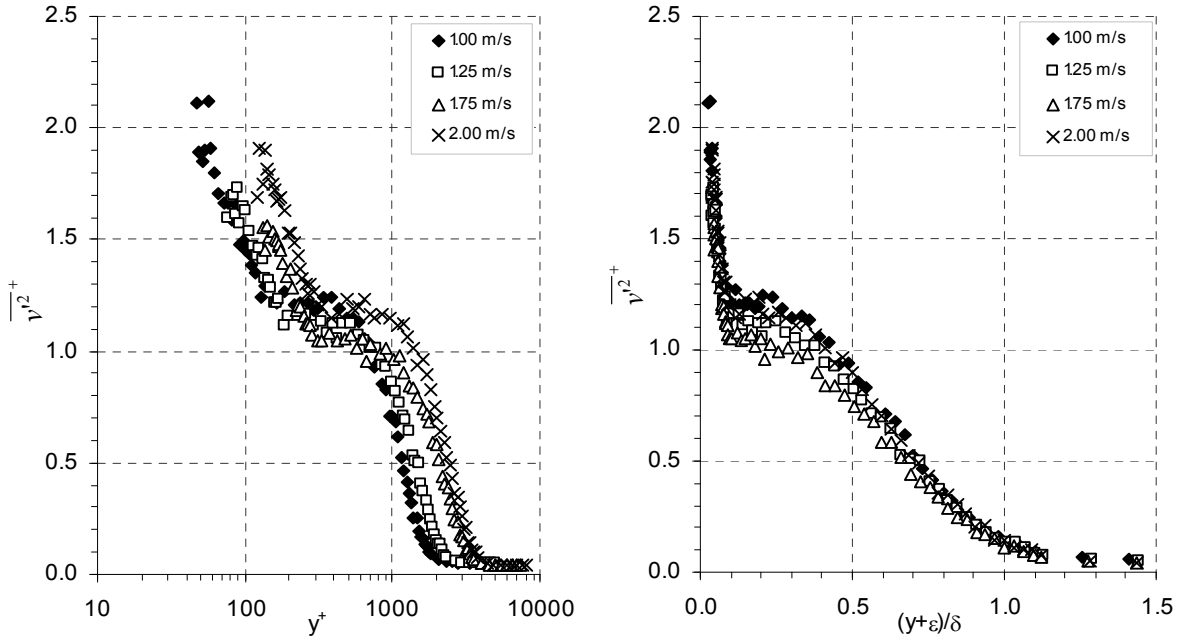

(a) (b)

Figure A.49 RP2 F5 normalised wall-normal Reynolds normal stress at x = 850 mm: (a) in inner variables; (b) in outer variables

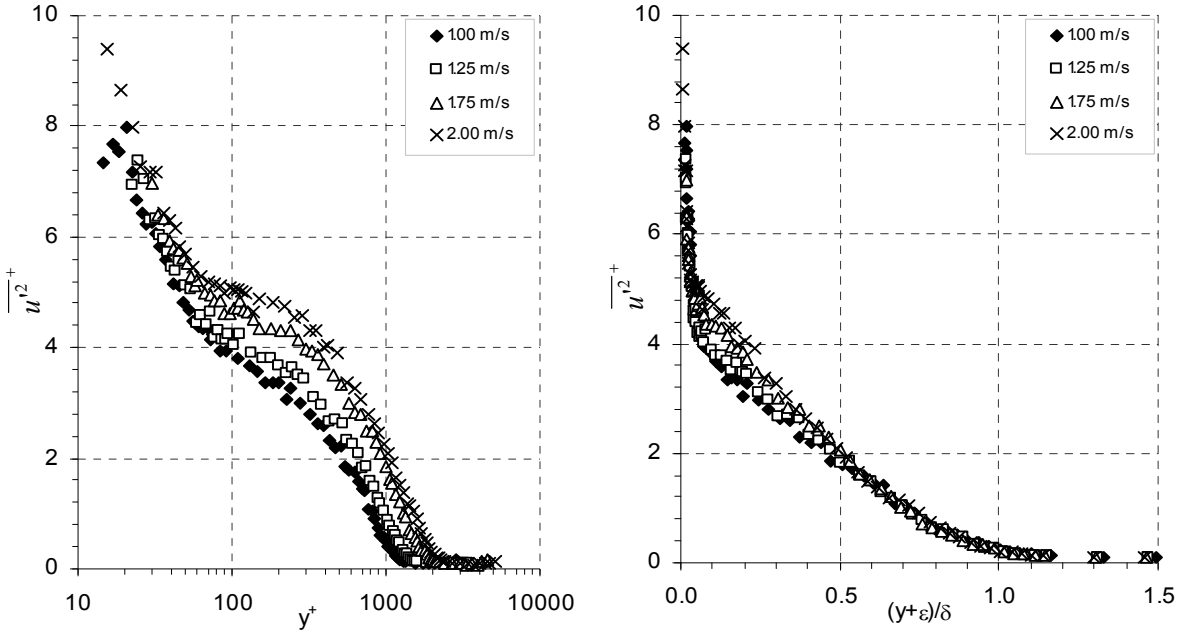

(a) (b)

Figure A.50 SP1 F6 normalised streamwise Reynolds normal stress at x = 850 mm: (a) in inner variables; (b) in outer variables

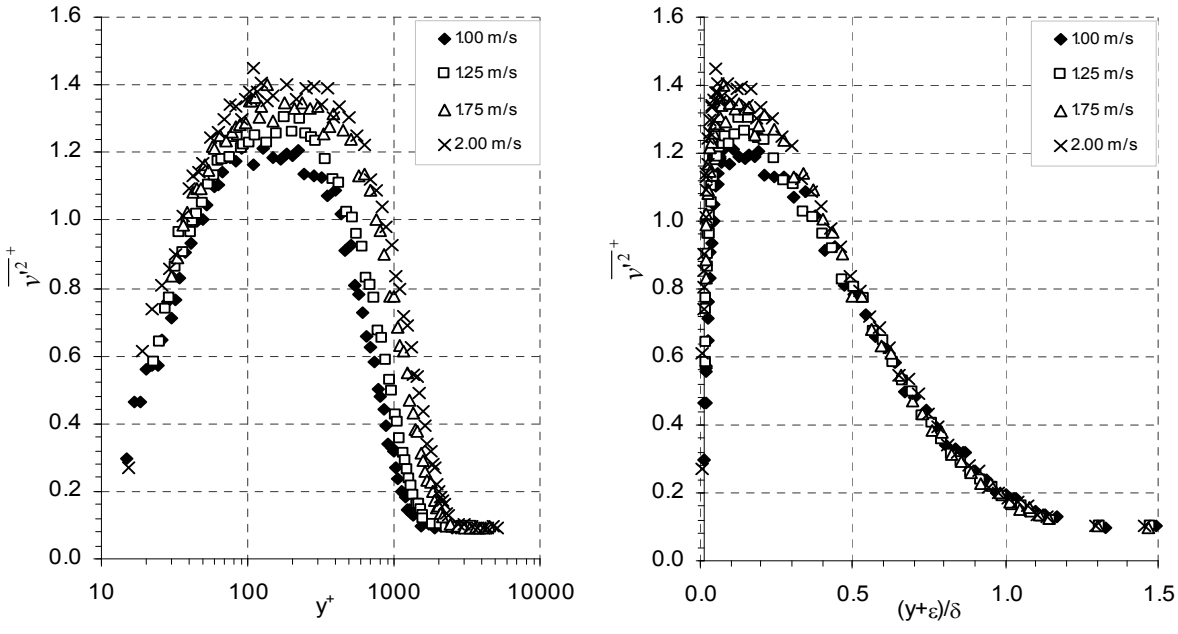

(a) (b)

Figure A.51 SP1 F6 normalised wall-normal Reynolds normal stress at x = 850 mm: (a) in inner variables; (b) in outer variables

A8 Reynolds Shear Stress

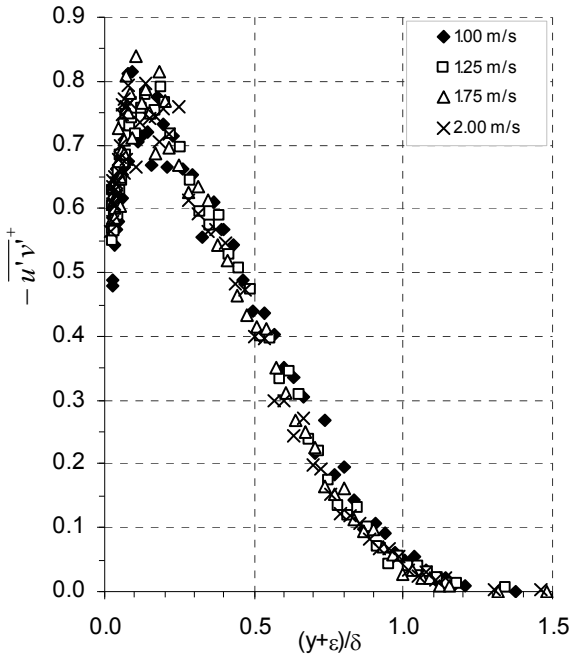

Figure A.52 SP Lab normalised Reynolds shear stress at x = 850 mm

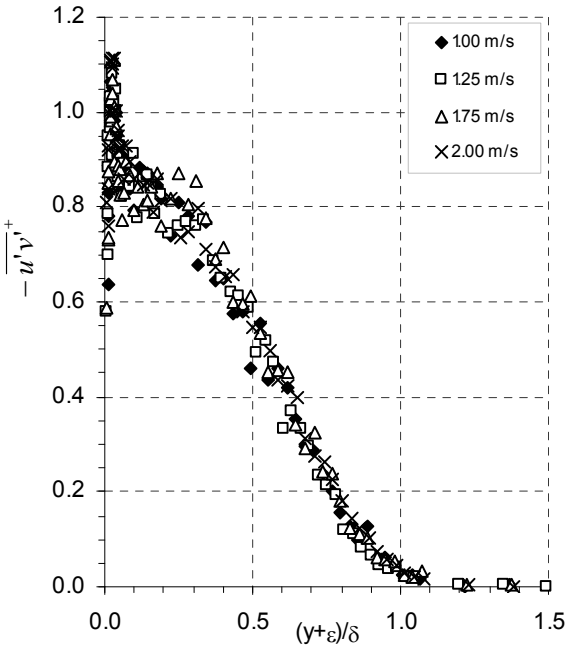

Figure A.53 RP Lab normalised Reynolds shear stress at x = 850 mm

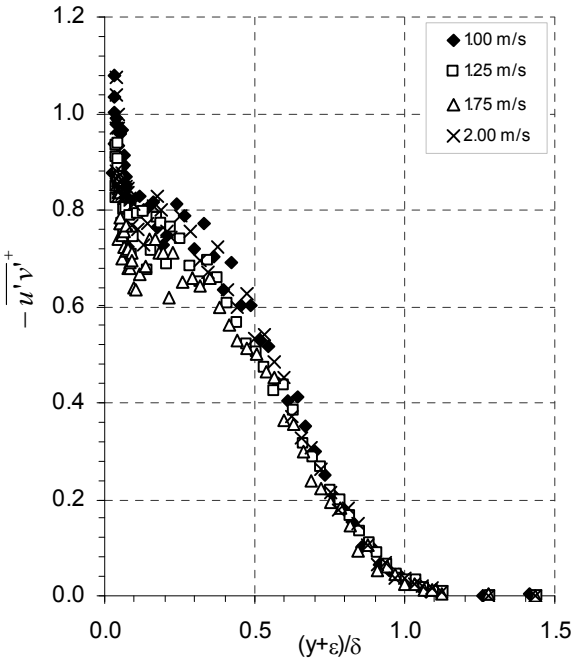

Figure A.54 RP2 F5 normalised Reynolds shear stress at x = 850 mm

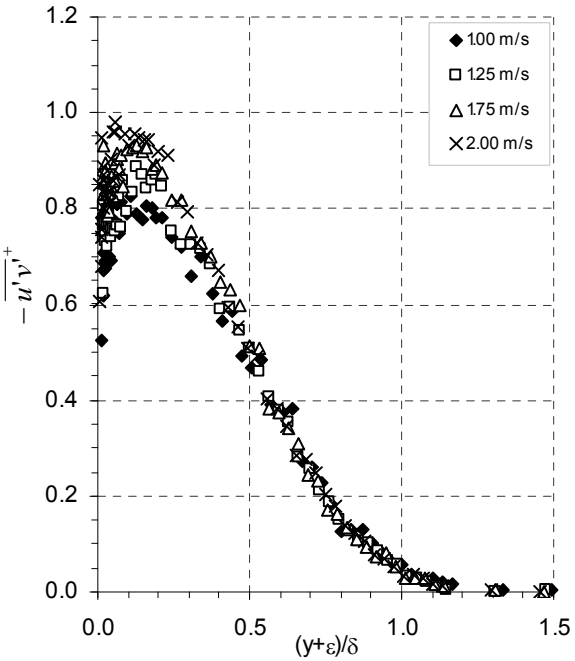

Figure A.55 SP1 F6 normalised Reynolds shear stress at x = 850 mm

A9 Quadrant Analysis

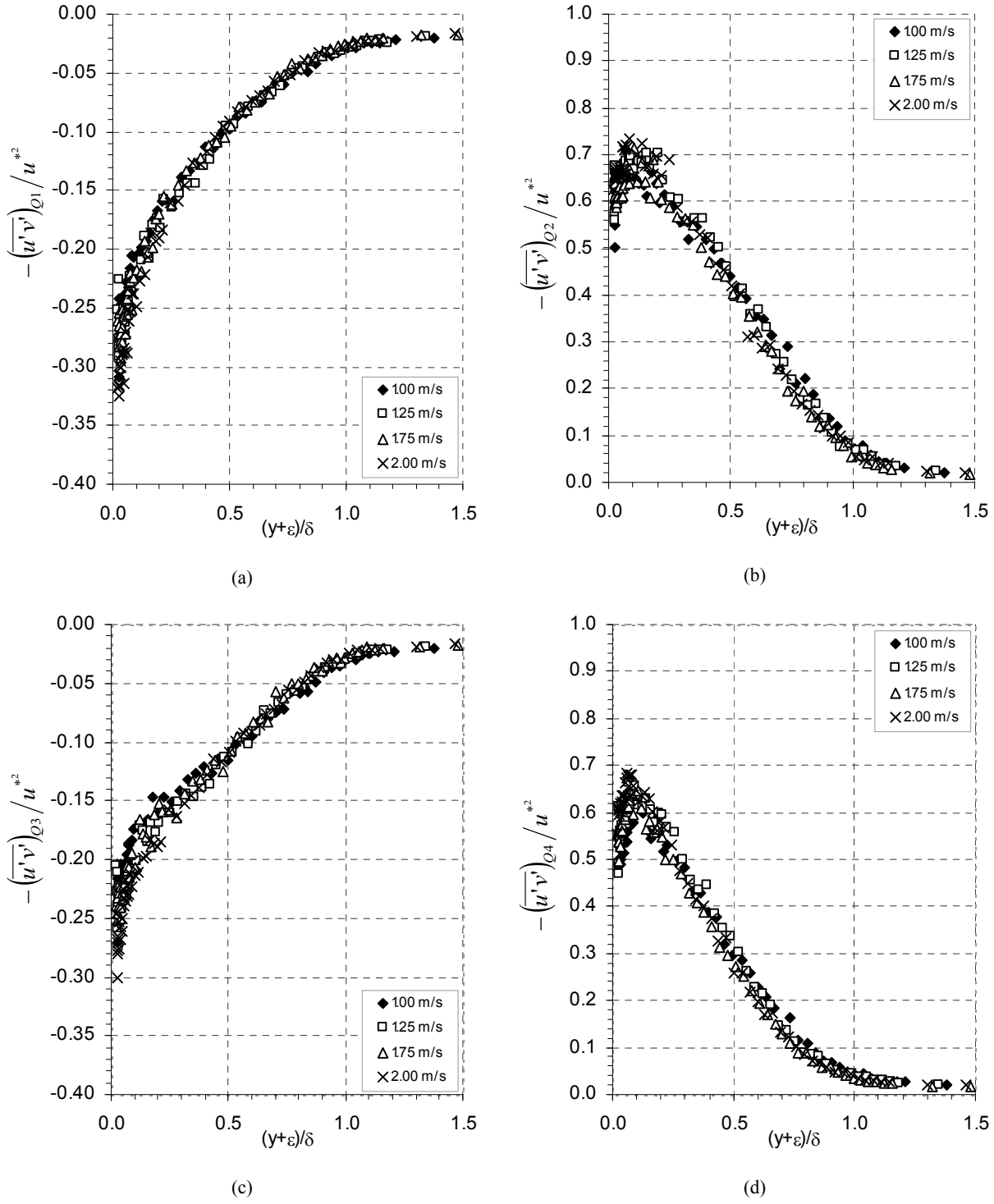

Figure A.56 SP Lab normalised Reynolds shear stress contributions with H = 0 at x = 850 mm: (a) Q1; (b) Q2; (c) Q3; (d) Q4

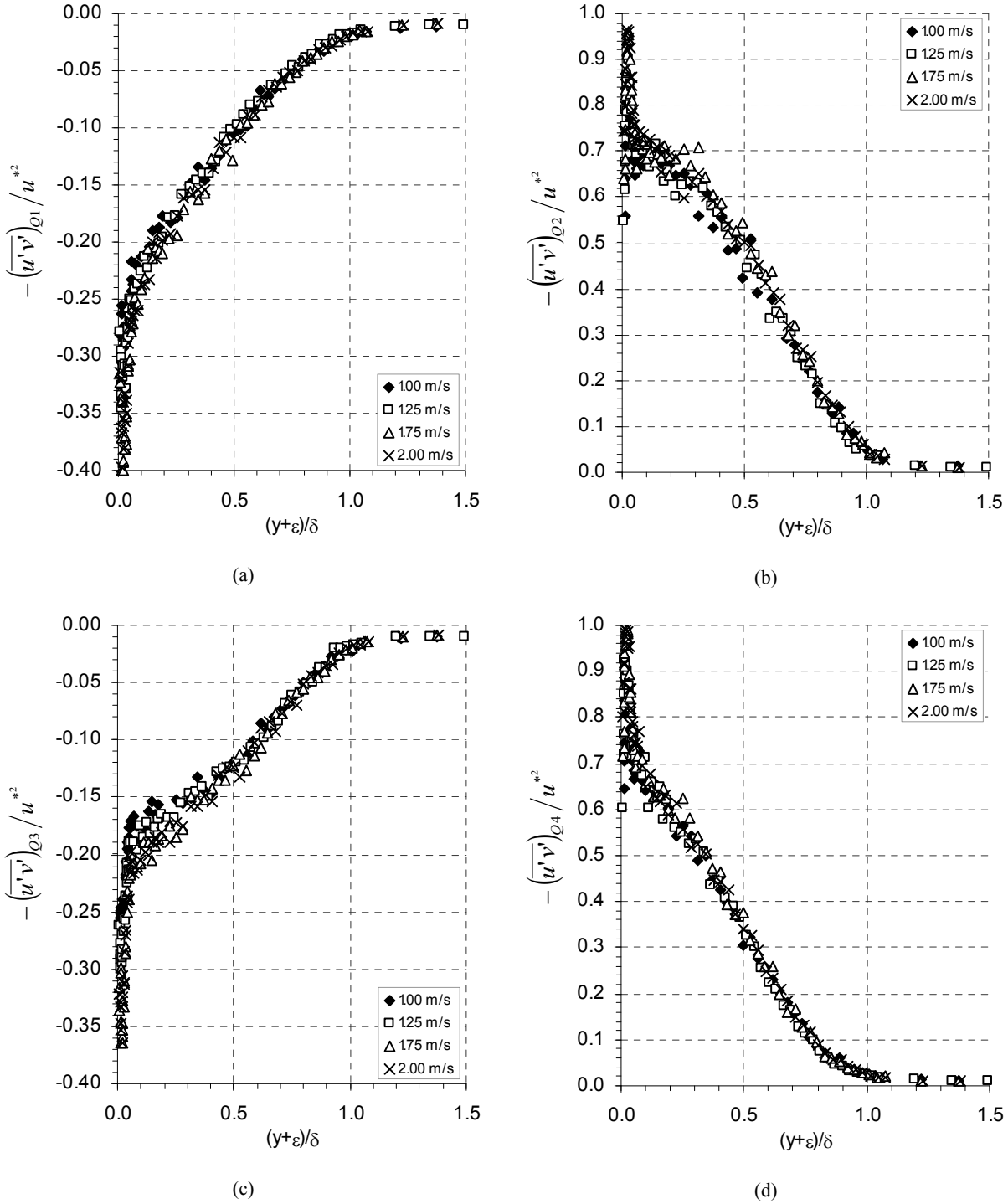

Figure A.57 RP Lab normalised Reynolds shear stress contributions with H = 0 at x = 850 mm: (a) Q1; (b) Q2; (c) Q3; (d) Q4

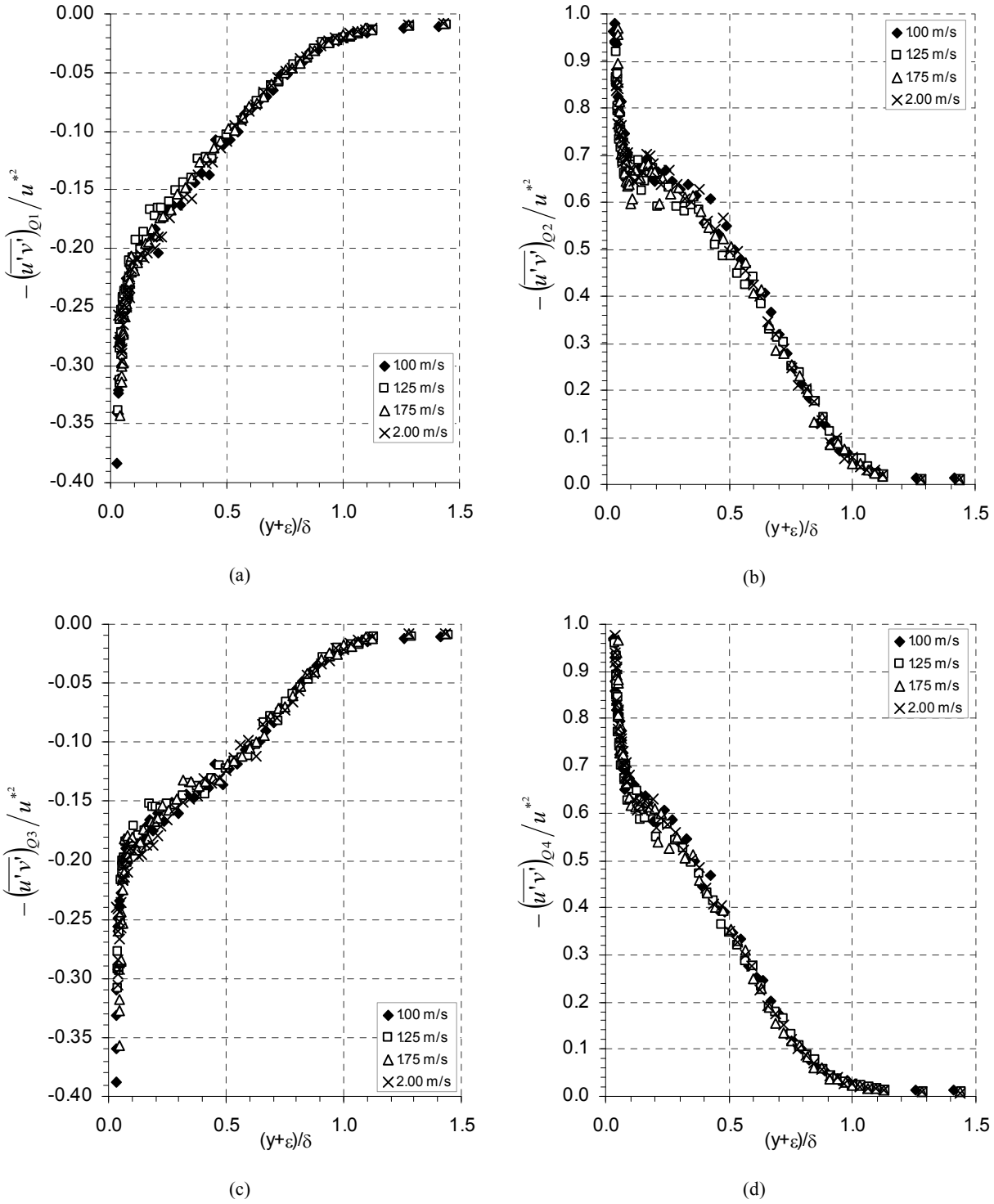

Figure A.58 RP2 F5 normalised Reynolds shear stress contributions with H = 0 at x = 850 mm: (a) Q1; (b) Q2; (c) Q3; (d) Q4

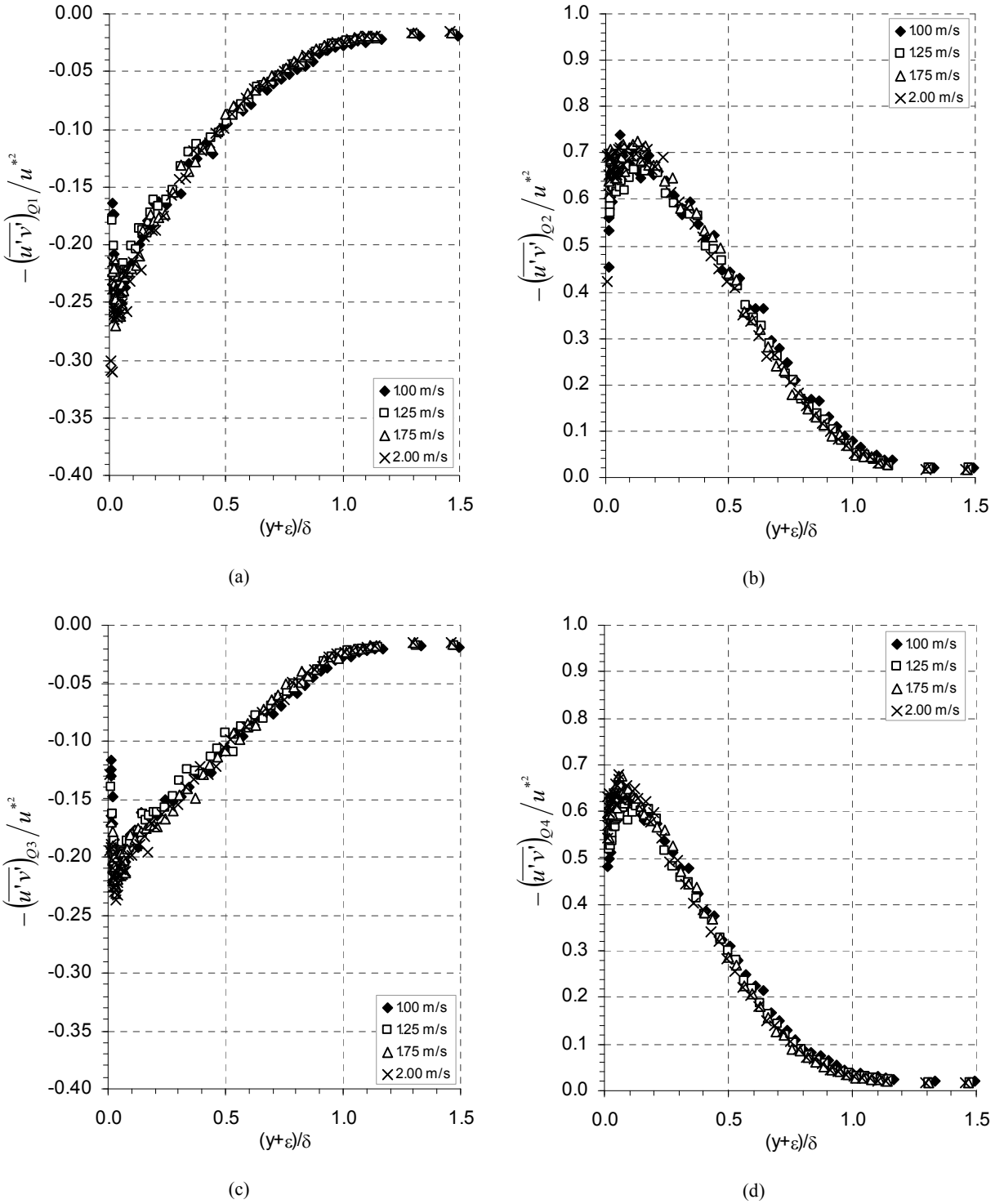

Figure A.59 SP1 F6 normalised Reynolds shear stress contributions with H = 0 at x = 850 mm: (a) Q1; (b) Q2; (c) Q3; (d) Q4

B HYDRO TASMANIA FIELD STUDY – TARRALEAH NO.1 CANAL CAPACITY

An investigation was undertaken by Hydro Tasmania between 2005 - 2007 to determine whether it was possible to refurbish Tarraleah No.1 Canal to restore the original design capacity of 25.5 m^3/s, or further upgrade the canal to increase the capacity beyond the original design capacity (Andrewartha 2005; Andrewartha et al. 2007). It was found by hydraulic modelling that the canal could be upgraded from its current capacity of approximately 21 m^3/s to a capacity of approximately 31 m^3/s by relining the canal to a smooth finish and applying a surface coating with favourable friction characteristics and resistance to biofilm growth, similar to the work completed at Liawenee (see Section 2.1.4.3) (Andrewartha 2005). The original model allowed for 338 mm freeboard, and ignored the Mossy Marsh Siphons, which are likely to be a limiting factor on the canal capacity. Andrewartha (2005) recommended that a testing program be undertaken to determine the maximum capacity of the siphons. Thus a study was undertaken to determine the maximum capacity of Tarraleah No.1 Canal, including the Mossy Marsh Siphons, under both clean and fouled conditions (Andrewartha et al. 2007).

B1 *Methodology*

Physical Testing

In order to determine the capacity of the Mossy Marsh Siphons, two tests were carried out. The first test (pre-clean) was undertaken on 5th - 6th April 2006. The entire canal and the siphons were cleaned on 22nd - 26th September 2006, as described in Section 2.1.4.2. The siphons were cleaned using a higher pressure water sprayer that was towed through them. The second test (post-clean) was undertaken on 12th - 13th October 2006.

The testing was undertaken for both the pre- and post-clean cases at nominal capacities of approximately 100%, 90%, 80% and 70%. The flow was allowed to pass through both siphons simultaneously, rather than isolating each siphon in turn. The minimum time period between adjusting the flow in Tarraleah No.1 Canal at Butlers Gorge and taking measurements at the Mossy Marsh Siphons was 2.5 hours to allow the flow to settle.

Freeboard readings were taken at nine locations in the canal using a tape measure from the top of the concrete walls. Gauge board readings were also taken where they were available. The flow in each siphon was measured using Panametrics ultrasonic flowmeters and the flow in the canal was gauged using two simultaneous measurements.

Hydraulic Model

A hydraulic model was used to model upgrade scenarios for Tarraleah No.1 Canal using HEC-RAS. HEC-RAS is a River Analysis System developed by the U.S. Army Corps of Engineers Hydrologic Engineering Centre. HEC-RAS was designed to perform one-dimensional hydraulic calculations for a full network of natural and constructed channels (U.S. Army Corps of Engineers). Steady flow water surface profiles are computed based on the solution of the one-dimensional energy equation. Energy losses are evaluated using Manning's equation. The momentum equation is utilised in situations where the water surface profile is rapidly varied, for example hydraulic jumps. The steady flow component is capable of modelling subcritical, supercritical, and mixed flow regime water surface profiles.

The original upstream and downstream models (from the Mossy Marsh Siphons) from Andrewartha (2005) were merged to form one continuous model, including the Mossy Marsh Siphons which were modelled as twin circular culverts. It was noted that there is a 0.3 m high 'hump' in the invert immediately downstream of the siphon outlet. The models were run both with and without this hump present to determine its influence on the water levels in the vicinity of the Mossy Marsh Siphon. The spillways were not modelled, as Tarraleah No.1 Canal is run with no spill allowed due to the condition of the foundation materials and the increased risk of landslide.

The inputs for the model are listed below:

- Survey data (taken as part of the study);
- Pre-clean flow, freeboard, and gauge board results (April 2006);
- Post-clean flow, freeboard, and gauge board results (September 2006);
- Minimum freeboard = 300 mm with areas of less freeboard to be highlighted. Note that freeboard is defined as the vertical distance from the water surface to the top of the open channel walls;
- Manning's n values: for fresh concrete n = 0.012, for painted and relined concrete n = 0.010 (based on results from Liawenee flume); and
- Flow regime – mixed (to identify areas of supercritical flow).

The model was run for several different scenarios. A calibration was conducted to determine the coefficients for the Mossy Marsh Siphons in both the cleaned and fouled states using results from the field tests. An upgrade model was also run to determine the capacity of the canal for several different upgrade options.

B2 Pre- and Post-Clean Test Results

Discharge

Table B.1 gives the discharge at Bridge 9 (see Figure 3.10) and the discharge through each siphon as measured by the Panametrics flowmeters. The readings from the Panametrics flowmeters were only used to obtain the percentage of the total discharge that flows through each siphon. It was determined that the left siphon carries approximately 47% of the flow, and the right siphon carries the remaining 53%. This could be due to a large tree branch on the trash rack of the left siphon, which could not be removed prior to the tests.

Table B.1 Discharge for Pre- and Post-Clean Tests

Nominal Capacity [%]	Bridge 9 (Flow Gauging) [m^3/s]		Siphon Discharge (Panametrics Flowmeters) [m^3/s]					
			Pre-Clean			Post-Clean		
	Pre-Clean	Post-Clean	Left Siphon	Right Siphon	Total	Left Siphon	Right Siphon	Total
100	20.61	21.37	10.67	11.55	22.22	9.61	10.78	20.39
90	19.14	19.74	9.85	10.86	20.71	8.88	9.97	18.84
80	17.10	17.85	8.93	9.78	18.71	8.13	9.13	17.26
70	15.72 *	16.09	7.97	8.92	16.90	7.15	8.21	15.36

* The discharge for the 70 % capacity pre-clean test was calculated based on the determined Manning's n and the recorded gauge height at Bridge 9.

Table B.2 and Table B.3 give data obtained from the flow gauging at Bridge 9 for the pre- and post-clean tests respectively. The area, wetted perimeter and discharge data were used to determine a representative Manning's n value for the canal in both the fouled (n = 0.0142) and clean (n = 0.0137) states using Manning's equation, as given by:

$$Q = \frac{1}{n} A R_H^{2/3} \sqrt{S_o} \qquad \textit{Equation B.1}$$

These Manning's n values were used in the hydraulic models. Note that the Manning's n values calculated are for the surface in the vicinity of Bridge 9. However, they have been adopted as representative values for the entire canal in the hydraulic models.

Table B.2 Pre-clean gauging results for Tarraleah No.1 Canal at Bridge 9

Nominal Capacity [%]	Gauge Height [m]	Measured Max. Depth of Flow [m]	Flow Cross-Sectional Area [m^2]	Mean Velocity [m/s]	Wetted Perimeter [m]	Discharge [m^3/s]	Hydraulic Radius [m]	Manning's n	Froude No.
100	1.680	1.610	10.04	2.08	9.35	20.87	1.075	0.0143	0.52
100	1.680	1.620	10.04	2.03	9.36	20.35	1.072	0.0146	0.51
90	1.600	1.550	9.44	2.03	9.12	19.21	1.036	0.0142	0.52
90	1.598	1.530	9.36	2.04	9.12	19.07	1.026	0.0141	0.53
80	1.507	1.450	8.67	2.00	8.85	17.30	0.980	0.0140	0.53
80	1.507	1.430	8.57	1.97	8.85	16.90	0.969	0.0141	0.53

Table B.3 Post-clean gauging results for Tarraleah No.1 Canal at Bridge 9

Nominal Capacity [%]	Gauge Height [m]	Measured Max. Depth of Flow [m]	Flow Cross-Sectional Area [m^2]	Mean Velocity [m/s]	Wetted Perimeter [m]	Discharge [m^3/s]	Hydraulic Radius [m]	Manning's n	Froude No.
100	1.578	1.660	10.24	2.11	9.62	21.58	1.064	0.0140	0.52
100	1.578	1.680	9.95	2.13	9.36	21.15	1.064	0.0139	0.52
90	1.512	1.550	9.40	2.09	9.12	19.65	1.031	0.0138	0.54
90	1.511	1.520	9.51	2.08	9.51	19.83	1.000	0.0136	0.54
80	1.461	1.450	8.62	2.05	8.73	17.67	0.988	0.0137	0.54
80	1.463	1.440	8.70	2.07	8.92	18.04	0.975	0.0134	0.55
70	1.404	1.380	8.04	2.00	8.62	16.05	0.933	0.0135	0.54
70	1.404	1.360	8.04	2.01	8.56	16.14	0.940	0.0135	0.55

Rating Curves

Rating curves were determined for all freeboard and gauge board measuring sites used during the pre- and post-clean testing. A sample rating curve is given in Figure B.1. The relationship between the freeboard and the discharge at Bridge 9 has been approximated using a linear relationship. The full set of rating curves, along with calculation tables, are given in Andrewartha *et al.* (2007). The pre-clean results should be used with caution, as the flow rate will vary according to the amount and type of biofilm present. Zero freeboard indicates that the canal will overtop. The model specification dictated that the minimum freeboard is 300 mm.

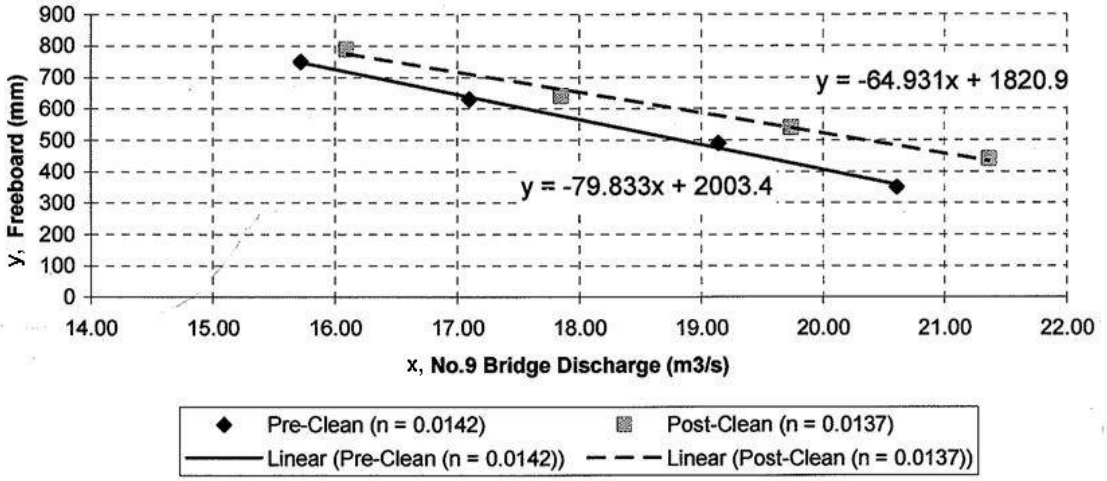

Figure B.1 Sample freeboard rating curve (325 m downstream of siphon outlet)

Gain from Cleaning

The gain from cleaning the open channel sections and the siphons, based on the nominal capacities, is approximately 3.4%. The pre- and post-clean tests were completed at nominal capacities, and are based on the operator's perception. Thus the 100% nominal capacity does not necessarily represent the maximum capacity of the canal.

Panel 22 is located approximately 325 m downstream of the outlet of the siphons, and is in an area of subsidence. This location is known to be an area of critical freeboard for Tarraleah No.1 Canal, and was thus chosen as the site for estimating the maximum capacity. For a minimum freeboard of 300 mm, the maximum capacity of the canal is 21.3 m^3/s in the fouled state and 23.4 m^3/s in the clean state. This corresponds to a 9.9% increase in capacity. These results must be viewed with some caution, as there may be other areas of critical freeboard in the canal where the freeboard was not measured or observed during the pre- and post-clean testing.

Measured Siphon Headloss

In order to determine the siphon headloss for the pre- and post-clean tests, the cleaning schedule must be considered. In between the pre- and post-clean tests, both the siphons and the open channel sections of Tarraleah No.1 Canal were cleaned. This particularly affects the water levels downstream of the siphon outlet, where the channel will be more efficient after cleaning due to the reduction in friction. Thus using the difference between the upstream and downstream water surface elevations to determine the total headloss for the pre- and post-clean test is inaccurate as two variables have effectively been changed – the siphon friction factor and the open channel

friction factor. If this method were to be used with any accuracy, only the siphons should have been cleaned between the pre- and post-clean tests. However, this was not practical due to the difficulties in securing outages for cleaning and maintenance purposes.

The water downstream of the siphons can be assumed to be free flowing, and will not have an impact on pipe operation. The water level for some distance upstream of the siphons is controlled by the siphons. The entrance loss coefficient should not change as the siphon inlets are well submerged; thus the difference in pre- and post-clean water level and the energy grade line upstream of the siphons indicate the improvements in headloss over the siphons due to cleaning.

The rating curve for the gauge board at the siphon inlet, given in Figure B.2, was used to determine the difference in water surface elevations for the pre- and post-clean tests at different flow rates, with the results given in Figure B.3. The relationship between the gauge board reading and the discharge at Bridge 9 was approximated by a linear curve. The energy grade line was then determined by adding the velocity head ($v^2/2g$) to the water surface elevations, as shown in Figure B.4.

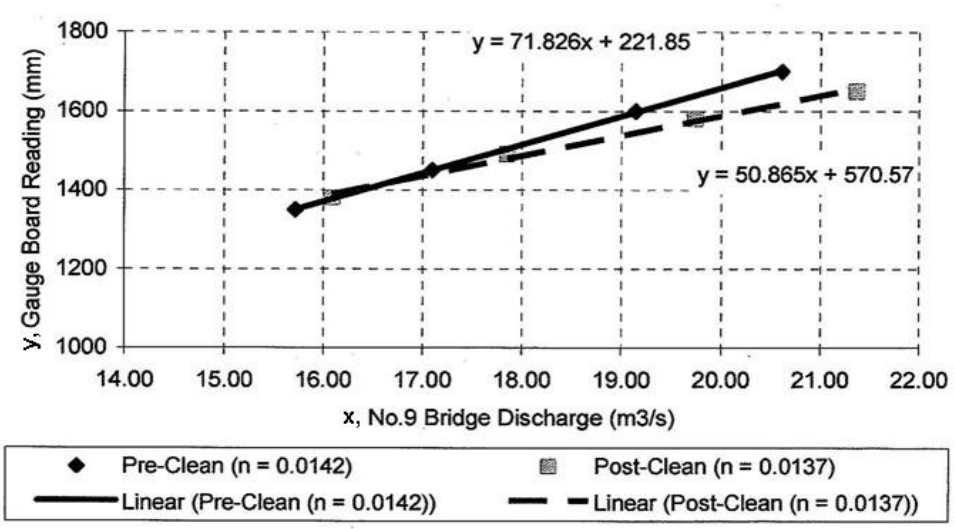

Figure B.2 Rating curve for the gauge board at the siphon inlet

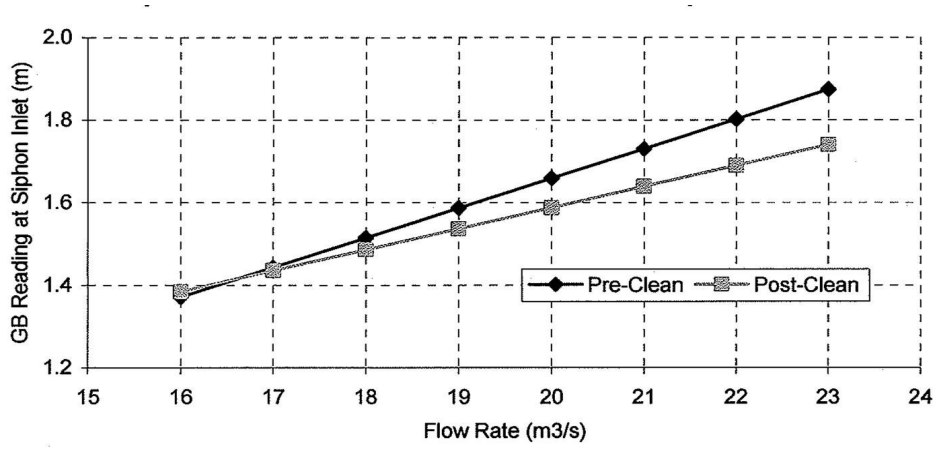

Figure B.3 Improvement in water surface elevations at the siphon inlet (GB = gauge board)

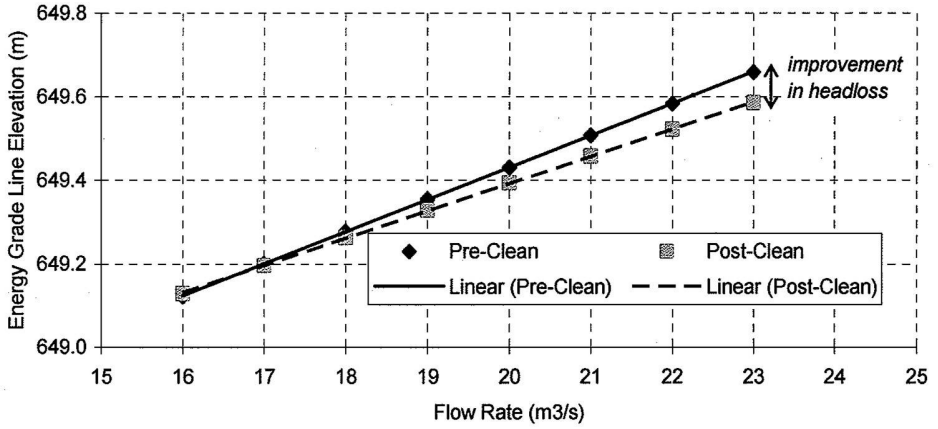

Figure B.4 Improvement in headloss (energy grade line elevation) at the siphon inlet

Figure B.3 shows that the water levels for the post-clean test are lower than for the pre-clean test, and this difference increases with flow rate. Figure B.4 demonstrates that there has been a reduction in the elevation of the energy grade line at the siphon inlet. This translates to an improvement in the friction factor for the siphons and an increase in capacity as a result of cleaning the siphons. This result is corroborated by video footage taken of the siphons after they were cleaned, which indicated that the majority of the coating was in very good condition, and an increase in capacity would be expected from the fouled to the clean condition.

The gauge board levels in Figure B.3 indicate that the improvement in capacity due to the cleaning of the siphons is in the order of 8% for a gauge board reading of 1.7 m. The results show that the cleaning of the Mossy Marsh Siphons was beneficial, as it improved the capacity of the siphons. However, a cost-benefit analysis should be undertaken to determine whether or not the cleaning should become a regular maintenance activity.

The measured headloss through the siphons is limited by the accuracy of the freeboard and gauge board readings. The water level varied considerably (± 100 mm) during the measuring periods, particularly in the region immediately downstream of the siphon due to wave action, as shown in Figure B.6. It is recommended that for all future pipeline headloss tests that the actual pressure in the pipeline be measured using pressure tappings and pressure transducers to improve the accuracy of the results, and to remove unknown variables such as the entry and exit loss coefficients.

Siphon Headloss Coefficients

Brett (1980) gives useful historical data for the friction characteristics of the Mossy Marsh Siphons. The highest recorded Manning's n for the siphons is given as n = 0.0148. After cleaning, the coefficients were found to be n = 0.0134 (No.1 Pipe) and n = 0.0116 (No.2 Pipe). Brett notes that the two steel pipes have quite different friction coefficients, which was observed in the current study where the two pipes were measured to carry different flow rates. However, due to the testing method employed in the current study, different friction coefficients for the two pipelines were unable to be determined.

Based on Brett's data, it is estimated that the n value for the siphons will be between 0.0135 and 0.0148 in the fouled state, and between 0.0112 and 0.0134 in the clean state. An entry loss coefficient of k_{entry} = 1.0 has been adopted due to the presence of the bend, the trash racks, and the extremely turbulent conditions at the inlet of the siphons. An exit loss coefficient of k_{exit} = 0.55 has been adopted for the outlet of the siphons.

The friction factor for the siphons cannot be accurately determined from the pre- and post-clean tests, for the same reasons that the headloss could not be determined based on the upstream and downstream water surface elevations. Other difficulties include the inability to differentiate between the friction loss coefficients for each siphon due to the testing method used, and the fact the friction coefficient varies with flow rate. Therefore a hydraulic model was employed to determine the maximum capacity of the siphons, as detailed in the following section.

B3 Hydraulic Model Results

Calibration Models

A calibration was undertaken to determine an appropriate friction factor for the Mossy Marsh Siphons under both clean and fouled conditions. This was done by comparing known water surface elevations from the pre- and post-clean tests with computed water surface elevations for

different friction factors for the siphons. The Manning's n values adopted for the open channel sections were computed from the Bridge 9 discharge gauging results.

The siphon friction factor does not impact the water levels downstream of the siphons, but does have a significant impact on the water levels upstream of the siphons. Thus a sensitivity analysis of the siphon friction factor was undertaken to determine its influence on water levels upstream of the siphons. It was found that for both the pre- and post- clean conditions the friction factor affects the upstream water level for high flows only. Below 80% nominal capacity (approximately 17 m^3/s) there was no effect on the upstream water levels by changing the friction factor for the siphons. The results indicated that there is a range of Manning's n values which could be applied to the siphons in the clean condition, thus making it difficult to assign a specific value. To overcome this issue, the upgrade scenarios were run for a full range of possible Manning's n values for the siphons in both the clean and fouled condition.

An example water surface profile in the vicinity of the siphons is given in Figure B.5. This particular water surface profile is for the post-clean calibration at 100% nominal capacity (21.4 m^3/s) with a siphon Manning's n of 0.0139. The 0.3 m hump in the invert at the siphon outlet is circled. The flow is borderline supercritical at the siphon outlet. This matches observations in the field where a large dip in the water surface profile was observed as the water shoots out of the siphon as illustrated in Figure B.6. It was also observed that periodic waves are formed after the flow exits the siphons, characteristic of an undular hydraulic jump, which continue for several hundred metres downstream of the siphon outlet. The effect of the hump in the invert at the siphon outlet is investigated in the following sections.

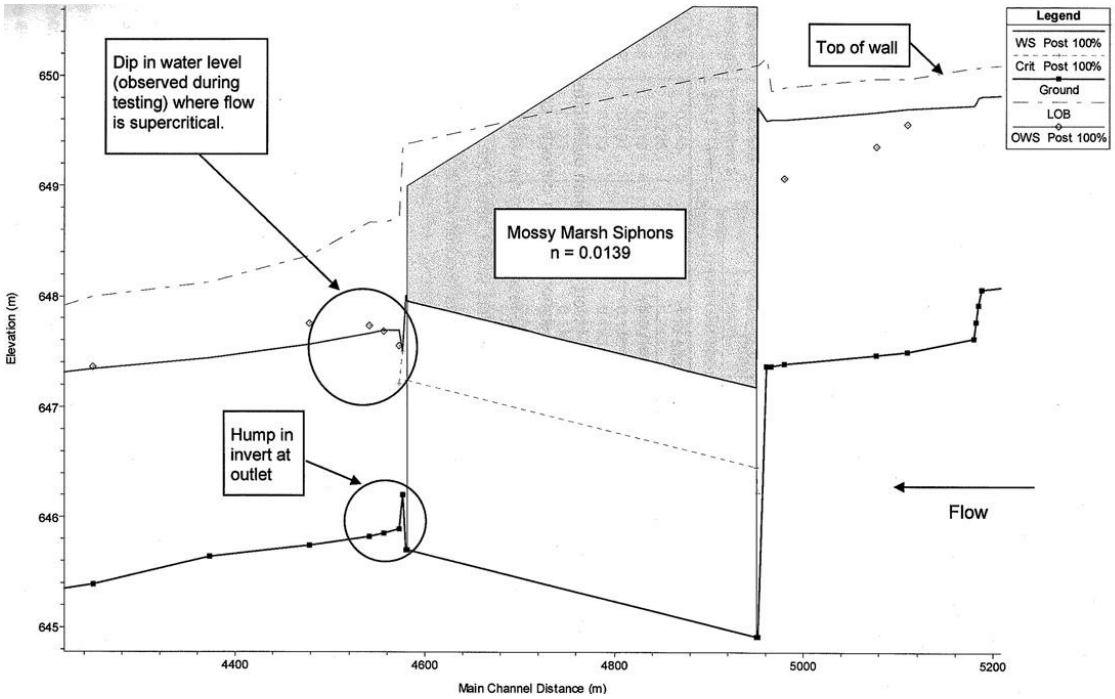

Figure B.5 Water levels for Mossy Marsh Siphons for the post-clean test at 100% capacity, 21.4 m^3/s (WS = water surface elevation, Crit = critical depth, LOB = wall height, OWS = observed water surface)

Figure B.6 Wave action at the siphon outlet (pre-clean test)

The pre- and post-clean calibration models were also run with the design flow rate of 25.5 m^3/s. It was found in both cases that Tarraleah No.1 Canal cannot pass the design flow in its current condition in either the clean or the fouled state, as the canal and flume sections would overtop

and the siphons would be unable to pass all of the flow. This result was expected, based on the current capacity restrictions observed by the operators, and is due to:

- The deterioration of the concrete lining in the open channel sections;
- Extensive biofouling in the open channel sections and some fouling in the siphons;
- Some deterioration of the internal lining of the Mossy Marsh Siphons (although it is generally in a very good condition); and
- Entry losses at the inlet to the Mossy Marsh Siphons.

Upgraded Canal Models

Three upgrade options were considered for Tarraleah No.1 Canal. Each option involves relining the open channel sections with a thin cementitious render to a smooth finish, and painting different sections with a protective surface coating with favourable friction characteristics and a resistance to the growth of biofouling, as specified in Table B.4. The siphons were modelled for a range of Manning's n values. The models were run with the canal geometry in existing configuration – i.e. with the 0.3 m hump in the invert at the siphon outlet present and removed.

Table B.4 Upgrade options for Tarraleah No.1 Canal

Option Number	Description
1	Paint walls and invert
2	Paint walls only
3	Paint invert only

Figure B.7 shows the water levels in the vicinity of the Mossy Marsh Siphons for a siphon Manning's n value of 0.012 at the design flow rate of 25.5 m^3/s. The flume section upstream of the siphon is overtopped, and there are freeboard issues up to 1 km upstream of the siphon inlet. Supercritical flow is evident at the siphon outlet, and is likely to cause wave action after it jumps to subcritical flow. Similar flow behaviour was found for all three upgrade options.

The supercritical flow and hydraulic jump at the siphon outlet are likely to cause freeboard issues for options 2 and 3 as the unprotected concrete surfaces deteriorate and become fouled, and will ultimately result in a forced reduction in capacity to avoid overtopping. The HEC-RAS model indicates that the siphons are not capable of carrying the design flow for any reasonable siphon Manning's n value due to localised overtopping upstream of the siphon inlet.

Further model runs found that if a freeboard of 300 mm is to be met then the capacity of the canal should be less than 24 m^3/s for all options and for all assumed Manning's n values for the siphons. Even if the canal was run with no freeboard immediately upstream of the siphon inlet, the siphons would only pass the design flow for low Manning's n values (below n = 0.0124, which is in the clean region given by Brett (1980)).

The models were then run for each upgrade option with the 0.3 m hump in the invert removed. The results indicate that if a freeboard of 300 mm is to be met, then the capacity of the canal would be less than the design capacity for all options and assumed Manning's n values for the siphons. Even if the canal were run with no freeboard immediately upstream of the siphon inlet, the siphons would only pass design flow for very low Manning's n values (below n = 0.0121, which is in the clean region given by Brett (1980)). Figure B.8 shows the water levels in the vicinity of the Mossy Marsh Siphons for a siphon Manning's n value of 0.012 at the design flow of 25.5 m^3/s, with the hump in the invert at the siphon outlet removed. The limited freeboard upstream of the siphon inlet is obvious.

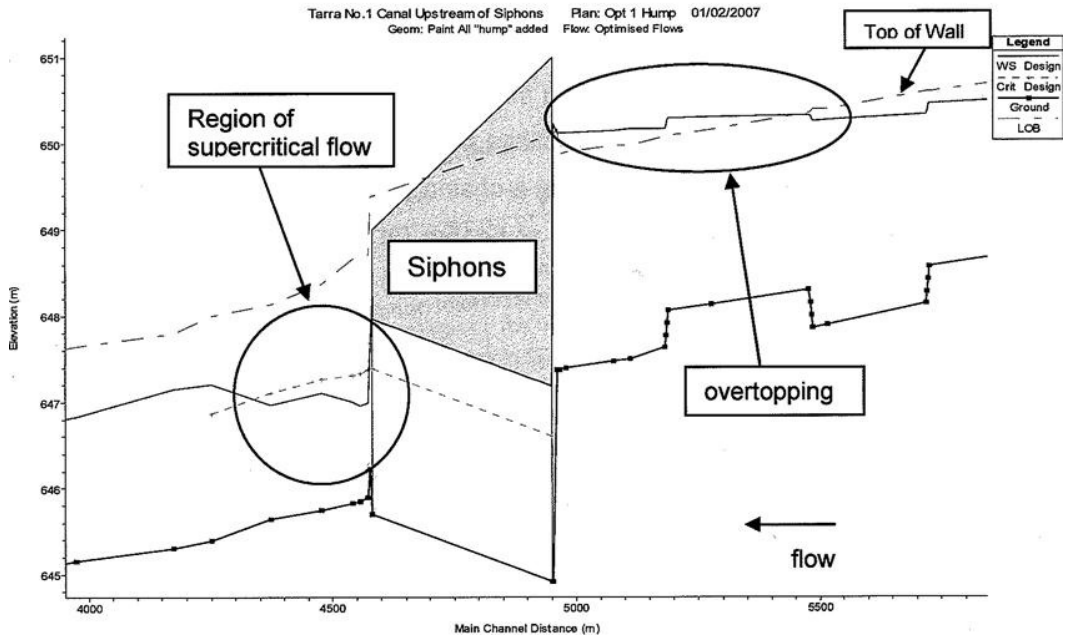

Figure B.7 Water levels in the vicinity of the siphons for option 1 (n = 0.012) in current geometrical configuration at the design flow rate of 25.5 m^3/s (WS = water surface, Crit = critical depth, LOB = wall height)

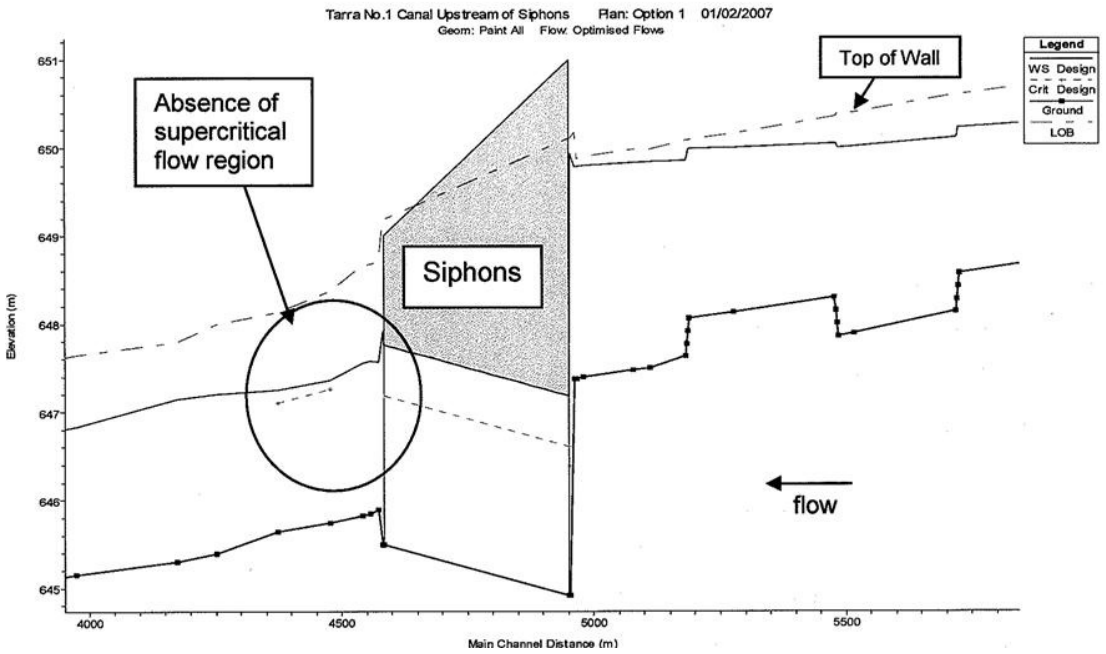

Figure B.8 Water levels in the vicinity of the siphons for option 1 (n = 0.012) with hump at siphon outlet removed at the design flow rate of 25.5 m^3/s

B4 Discussion of Hydraulic Model Results

It can be concluded from the above results that the Mossy Marsh Siphons are the principal constraint on the capacity of Tarraleah No.1 Canal. In the current configuration the capacity of the canal is less than 24 m^3/s for all three upgrade options. The Mossy Marsh Siphons affect the freeboard levels for a distance up to 1 km upstream of the siphon inlet.

The reduction in capacity of the siphons from the design capacity is probably due to losses at the siphon inlet, and some deterioration of the internal coating. Whilst the video footage taken just after the siphons were cleaned shows that the internal coating is in very good condition, there are some areas that could cause disturbances to the flow.

Even if the hump in the invert at the siphon outlet were to be removed, the Mossy Marsh Siphons would still be a constraint on the capacity of the canal. However, the hydraulic models indicate that the capacity would slightly increase, as illustrated by Figure B.7 and Figure B.8. The other significant improvement that would be made by removing the hump in the invert would be to remove the region of supercritical flow at the siphon outlet. This is clearly demonstrated in Figure B.8 for upgrade option 1, and similar results were found for options 2

and 3. The absence of the supercritical flow region should result in a reduced wave action downstream of the siphon outlet.

The model results also indicate that there may be some problems with the flow becoming supercritical through the transitions between canal and flume sections, which would need to be addressed if the canal and flume sections were to be upgraded. Apart from the freeboard issues in the 1 km section immediately upstream from the siphon inlet, there are no freeboard issues in the remainder of the canal for the design flow rate for any of the three upgrade options.

If the decision is made to upgrade the canal and the siphons, option 1 would be preferred in terms of durability of the concrete lining in the open channel sections. The protective surface coating will act as a barrier between the water and the cementitious render and will protect both the walls and the invert from the effects of frost attack, pure water leaching, and erosion. The smooth finish of the coating will also deter the growth of biofilms.

Any canal and flume upgrade works undertaken to increase the capacity are unlikely to achieve the desired increase unless work is also undertaken to improve the capacity of the Mossy Marsh Siphons.

B5 Conclusions

- The water level immediately upstream of the Mossy Marsh Siphon inlet is controlled by the friction coefficient for the siphons and the entry losses at flow rates > 17 m^3/s. At lower flow rates the water level is controlled only by the entry losses at the siphon inlet;

- The cleaning of Tarraleah No.1 Canal increased the capacity by 9.9%, based on a freeboard of 300 mm;

- With the siphons and canal cleaned Tarraleah No.1 Canal is not capable of passing the design flow rate of 25.5 m^3/s. The open channel sections would overtop due to the deteriorated condition of the concrete lining, and the siphons would be unable to pass the flow due to restrictions at the inlet and some defects in the internal coating;

- It is estimated that the maximum capacity of the siphons in their cleaned state is < 24 m^3/s with the open channel sections of the canal upgraded;

- The hump in the invert at the siphon outlet has the effect of raising the water levels immediately upstream of the siphon inlet and causing supercritical flow and wave action;

- If the hump was removed and the open channel sections upgraded, the capacity of Tarraleah No.1 Canal would be increased and the flow at the siphon outlet would cease to be supercritical. However, the minimum freeboard allowance of 300 mm would not be achievable within a 1 km length of canal upstream of the siphon inlet at the design flow of 25.5 m^3/s; and

- The capacity of Tarraleah No.1 Canal is constrained by the capacity of the Mossy Marsh Siphons, as shown by the hydraulic model results and historical observations. No benefit would be realised by upgrading the open channel sections of Tarraleah No.1 Canal to a capacity of 31 m^3/s as determined by Andrewartha (2005) unless the limited capacity of the Mossy Marsh Siphons were addressed.

B6 Recommendations

- Should the friction factor for each siphon be required in the future, each siphon should be isolated in turn and the pressure tapping rings on each siphon reinstated and attached to a pressure transducer on the upstream and downstream ends of the siphon to make the calculation of the friction losses easier and more accurate;

- The cleaning of the Mossy Marsh Siphons was beneficial, but a cost-benefit analysis should be undertaken to determine whether or not the cleaning should become a regular maintenance activity;

- The open channel sections of Tarraleah No.1 Canal should not be upgraded unless the limited capacity of the Mossy Marsh Siphons is addressed; and

- If the capacity of the canal is to be upgraded, an investigation should be undertaken to determine methods to reduce the entry losses concurrently with removing the hump in the invert at the siphon outlet, which were determined to be limiting factors on siphon capacity. The upgrade works may include improving the inlet alignment. Other possibilities include adding a third pipeline, replacing the siphons with a section of elevated flume, or raising the flume wall height in the sections with limited freeboard.

C MATLAB PROGRAMS

The Matlab m-files used in the data analysis (see Chapter 6) are provided on an accompanying compact disc.

For Bradshaws Method (Section 6.2.2):

- New_Bradshaws.m
- Origin_Correction.m
- polyintersect.m

For the Log Law Slope Method (Section 6.2.3):

- virtualorigin.m
- log_law_slope_method.m

For Perry and Li's Method (Section 6.2.4):

- Perry.m

For Hama's Method (Section 6.2.5):

- Hama.m

For the Total Stress Method (Section 6.2.6):

- Total_Stress.m

D PUBLICATIONS ARISING FROM THESIS

Several conference and journal papers were published during the course of this study, and in the months after the thesis was submitted for examination. They are listed below, and are provided on the accompanying compact disc.

Journal Publications

Andrewartha, J, Perkins, K, Sargison, J, Osborn, J, Walker, G, Henderson, A & Hallegraeff, G 2010, 'Drag force and surface roughness measurements on freshwater biofouled surfaces', *Biofouling,* vol. 26, no.4, pp. 487-496.

Andrewartha, J, Sargison, J & Perkins, K 2008, 'The influence of freshwater biofilms on drag in hydroelectric power schemes', *WSEAS Transactions on Fluid Mechanics: Special Issue: Sustainable Energy and Environmental Fluid Mechanics,* vol. 3, no. 3, pp. 201-206.

Conference Publications

Andrewartha, J, Sargison, J, Perkins, K, Walker, G & Henderson, A 2010, 'The turbulence structure of flows over rough surfaces and freshwater biofilms', *International Association of Hydraulic Engineering and Research (IAHR) Asia Pacific Division Congress,* University of Auckland, NZ.

Andrewartha, J & Cribbin, N 2009, "When the going gets rough, the rough stops flowing", *24th Biennial Conference of the Concrete Institute of Australia*, Sydney.

Andrewartha, J, Sargison, J, Henderson, A, Perkins, K & Walker, G 2008, 'The effect of freshwater biofilms on skin friction drag', *16th International Association of Hydraulic Engineering and Research International Symposium on Hydraulic Structures,* Nanjing, China, pp. 1940-1945.

Andrewartha, J, Sylvester, M, Sargison, J & Clarke, W 2008, 'The state of power: a Tasmanian perspective', *High-level International Forum on Water Resources and Hydropower,* China Institute of Water Resources and Hydropower Research, Beijing, China, pp 208-215.

Andrewartha, J, Sargison, J & Perkins, K 2007, 'The effect of *Gomphonema* and filamentous algae streamers on hydroelectric canal capacity and turbulent boundary layer structure', *16th Australasian Fluid Mechanics Conference,* Gold Coast, Australia, pp. 214-246.

Andrewartha, J & Cribbin, N 2006, "When the going gets rough, the rough stops flowing" Roughness issues in Hydro Tasmania water conveyance structures', paper presented to *12th Hydro Power Engineering Exchange*, 22-27 October, Tasmania.

Andrewartha, J, Sargison, J, Barton, A, Cribbin, N, Denne, A & Walker, G 2006, 'Roughness issues in Hydro Tasmania water conveyance structures', *Australasian Corrosion Association, Corrosion and Prevention Conference,* Hobart, Australia.